INFORMATION TO USERS

This manuscript has been reproduced from the microfilm master. UMI films the text directly from the original or copy submitted. Thus, some thesis and dissertation copies are in typewriter face, while others may be from any type of computer printer.

The quality of this reproduction is dependent upon the quality of the copy submitted. Broken or indistinct print, colored or poor quality illustrations and photographs, print bleedthrough, substandard margins, and improper alignment can adversely affect reproduction.

In the unlikely event that the author did not send UMI a complete manuscript and there are missing pages, these will be noted. Also, if unauthorized copyright material had to be removed, a note will indicate the deletion.

Oversize materials (e.g., maps, drawings, charts) are reproduced by sectioning the original, beginning at the upper left-hand corner and continuing from left to right in equal sections with small overlaps.

Photographs included in the original manuscript have been reproduced xerographically in this copy. Higher quality 6" x 9" black and white photographic prints are available for any photographs or illustrations appearing in this copy for an additional charge. Contact UMI directly to order.

ProQuest Information and Learning
300 North Zeeb Road, Ann Arbor, MI 48106-1346 USA
800-521-0600

Design and Synthesis of New Organomain Group Radicals

by

Greg William Patenaude
B.Sc., University of Guelph, 1996

A Dissertation Submitted in Partial Fulfillment of the
Requirements for the Degree of

DOCTOR OF PHILOSOPHY

in the Department of Chemistry

We accept this dissertation as conforming
to the required standard

Dr. R. G. Hicks, Supervisor (Department of Chemistry)

Dr. D. J. Berg, Departmental Member (Department of Chemistry)

Dr. P. Wan, Departmental Member (Department of Chemistry)

Dr. A. Gower, Outside Member (Department of Physics and Astronomy)

Dr. T. Chivers, External Examiner (Department of Chemistry, University of Calgary)

Supervisor: Dr. Robin G. Hicks

ABSTRACT

The goals of this thesis were to design and synthesize new stable radicals and to study their properties. The attempted synthesis of new stable thioaminyl, verdazyl, and dioxadiazinyl radicals is described. Successfully prepared radicals were characterized by spectroscopic methods.

The synthesis of new thioaminyl radicals and diradicals was attempted. Preparation of thioaminyl precursors, the sulfenamides, was accomplished with sulfenyl chlorides and amines. Oxidation with DDQ yielded radicals which decomposed back to the sulfenamides within 1–2 minutes. A bis(sulfenamide) was synthesized using a sulfenyl chloride and an appropriate bis(amine). The structure of the bis(sulfenamide) was confirmed by NMR spectroscopy and x-ray crystallography. Oxidation of the bis(sulfenamide) to the thioaminyl diradical was unsuccessful.

New phosphaverdazyl radicals were prepared and studied using EPR spectroscopy. The phosphaverdazyl precursors, the tetrazines, were prepared from the corresponding bis(hydrazides). The tetrazines were oxidized with benzoquinone to yield phosphaverdazyls. The phosphaverdazyls prepared do not share the same level of stability as the parent carbon-based verdazyls; they slowly decompose back to tetrazines. Incorporation of phosphorus into the verdazyl core has several effects on the properties of the radical relative to the parent verdazyl system. Through a combination of EPR and computational studies, it was concluded that the geometry of the verdazyl ring and the

electronic nature at phosphorus appear to be sensitive to the nature of the substituents attached to phosphorus. Exocyclic "spin-leakage" was observed for one phosphaverdazyl, which can be rationalized using a spiroconjugative mechanism. The phenomena of spiroconjugation was further explored through the synthesis of a phosphaverdazyl derivative attached to phosphazene in a spirocyclic manner.

Synthetic routes to the hitherto unknown dioxadiazinyl system were explored. An intermediate hydroxyamidoxime was synthesized and fully characterized. Cyclization reactions of the hydroxyamidoxime to putative dioxadiazines were carried out using aldehydes and a ketone. The cyclization products could not be unambiguously assigned. The cyclization products can be rationalized as the desired dioxadiazine or the 5-membered oxadiazolidine. One derivative was oxidized to a persistent radical, the EPR of which is consistent with a nitroxide structure.

Examiners:

Dr. R. G. Hicks, Supervisor (Department of Chemistry)

Dr. D. J. Berg, Departmental Member (Department of Chemistry)

Dr. P. Wan, Departmental Member (Department of Chemistry)

Dr. A. Gower, Outside Member (Department of Physics and Astronomy)

Dr. T. Chivers, External Examiner (Department of Chemistry, University of Calgary)

TABLE OF CONTENTS

List of Tables

List of Figures

List of Schemes

List of Abbreviations

a	hyperfine coupling constant
Å	angstroms
AFM	antiferromagnetic
Ar	aromatic
BTMA·Br_3	benzyltrimethylammonium tribromide
Bu	butyl
C	Curie constant
°C	degrees Celsius
CI	chemical ionization
cm	centimeter
CU	coupling unit
d	doublet (NMR descriptor)
dec	decompose
DC18C6	dicyclohexano-18-crown-6
DDQ	2,3-dichloro-5,6-dicyano-1,4-benzoquinone
DFT	density functional theory
DMF	dimethylformamide
DMSO	dimethylsulfoxide
DNA	deoxyribonucleic acid
DPPH	diphenylpicrylhydrazyl
EHMO	extended Hückel molecular orbital

EI	electron impact
ENDOR	electron nuclear double resonance
EPR	electron paramagnetic resonance
Et	ethyl
EtOAc	ethyl acetate
EtOH	ethanol
Et_3N	triethylamine
eV	electron volt
FAB	fast atom bombardment
FCU	ferromagnetic coupling unit
FM	ferromagnetic
g	g-factor
G	gauss
GHz	gigahertz
h	hour(s) or Planck's constant
H	magnetic field
HOMO	highest occupied molecular orbital
Hz	hertz
im	imidazole
I	intensity
IR	infrared
J	coupling constant
J	singlet-triplet energy gap

k	Boltzman constant
K	kelvin
kcal	kilocalorie
kJ	kilojoule
m	multiplet (NMR descriptor) or medium (IR descriptor)
M	molarity
Me	methyl
Mes	2,4,6-trimethylbenzene
Mes*	2,4,6-tri-*tert*-butylbenzene
mg	milligram
MHz	megahertz
min	minutes
M_I	nuclear spin state
mL	milliliters
mmol	millimole
*m*NBA	*meta*-nitrobenzyl alcohol
Mp	melting point
MQDM	*meta*-quinodimethane
M_s	magnetic spin state
MS	mass spectrometry
m/z	mass per charge
N	Avogadro's number
*n*BuLi	*n*-butyl lithium

NCS	*N*-chlorosuccinimide
nm	nanometer
NMR	nuclear magnetic resonance
[o]	oxidation
Ph	phenyl
ppm	parts per million
q	quartet
s	singlet (NMR descriptor) or strong (IR descriptor)
S	total spin
SOMO	singly occupied molecular orbital
t	triplet (NMR descriptor)
T	temperature
*t*Bu	tertiary butyl
THF	tetrahydrofuran
TLC	thin layer chromatography
TME	tetramethyleneethane
TMM	trimethylenemethane
UV	ultraviolet
vis	visible
zfs	zero field splitting
β	Bohr magneton
δ	parts per million
γ	magnetogyric ratio

μ_{eff}	effective magnetic moment
ν	frequency
λ_{max}	wavelength of lowest energy electronic absorption
χ	magnetic susceptibility

List of Numbered Compounds

1.1

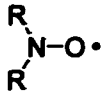

1.2

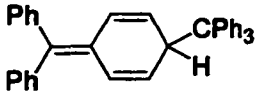

1.3

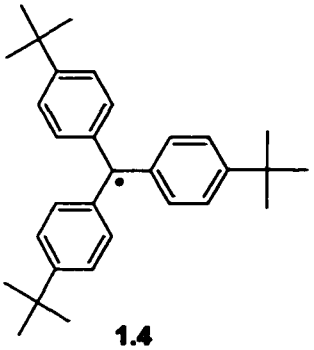

1.4

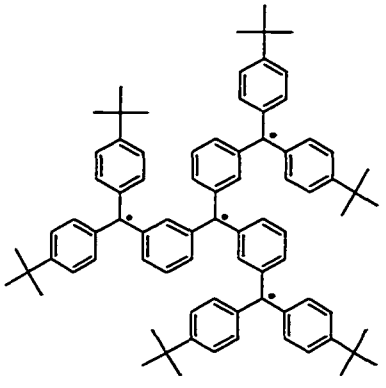

1.5

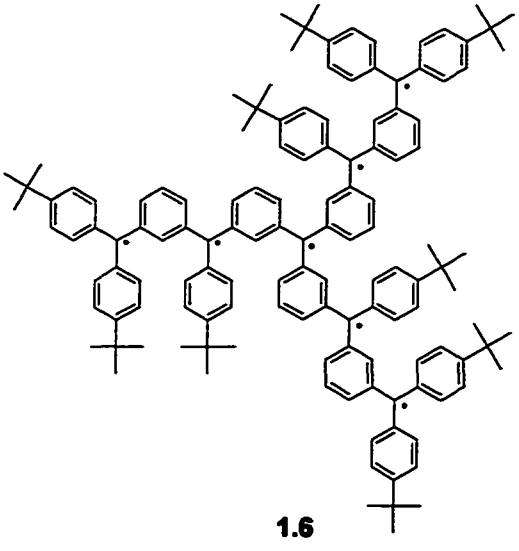

1.6

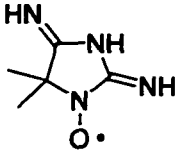

1.7

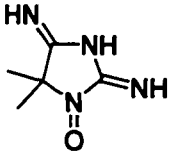

1.8

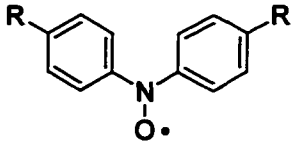

R = H or OMe

1.9

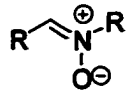

1.10

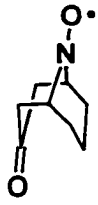

1.11

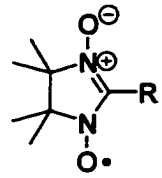

1.12

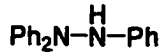

1.13

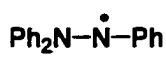

1.14

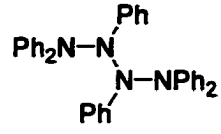

1.15

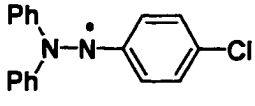

1.16

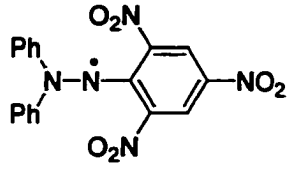

1.17

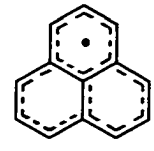

1.18

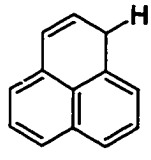

1.19

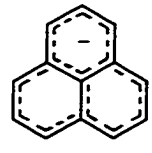

1.20

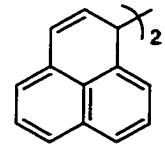

1.21

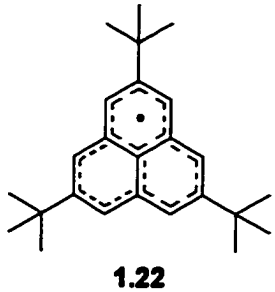

1.22

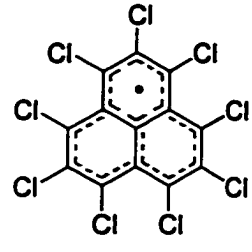

1.23

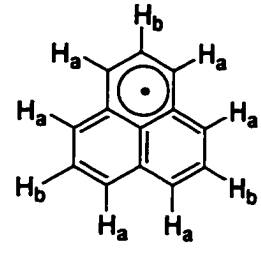

1.24

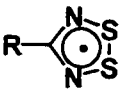

1.25

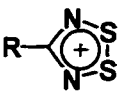

1.25a

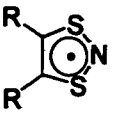

1.26

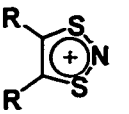

1.26a

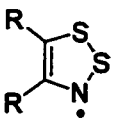

1.27

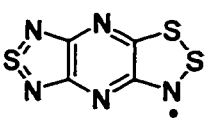

1.28

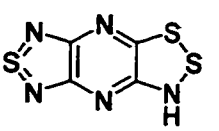

1.28a

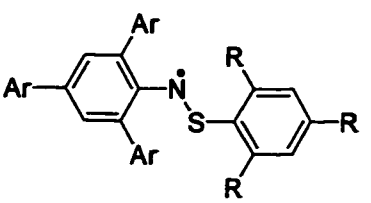

1.29

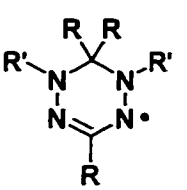

1.30

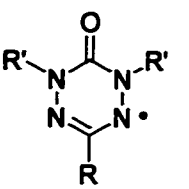

1.31

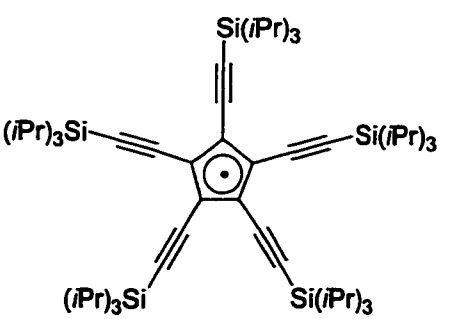

1.32

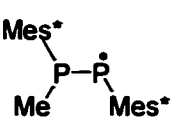

1.33

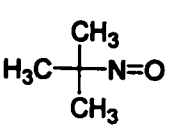

1.34

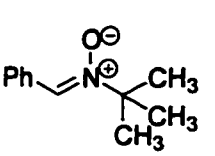

1.35

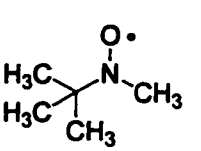

1.36

2.1

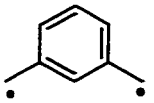

2.2

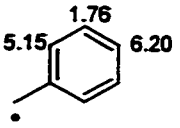

2.2a

2.3

2.4

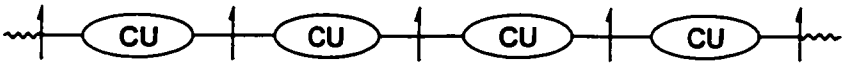

2.4a

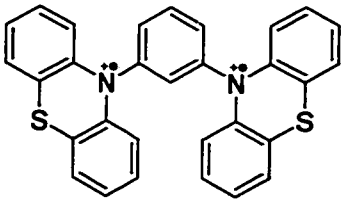

2.5

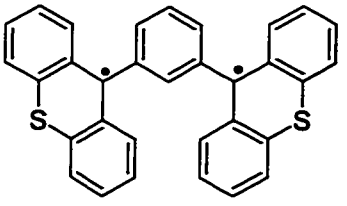

2.6

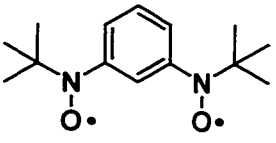

2.7

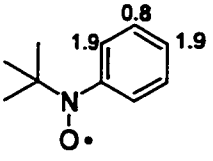

2.7a

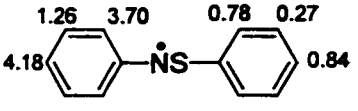

2.8

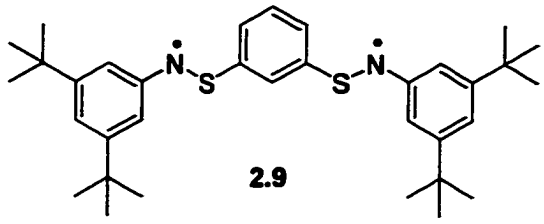

2.9

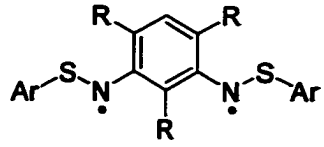

2.10

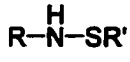

2.11

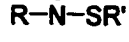

2.12

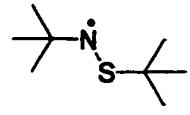

2.13

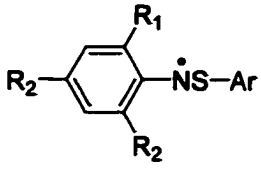

R_1 = Ph, *t*Bu, CN

R_2 = Ph, *t*Bu

2.14

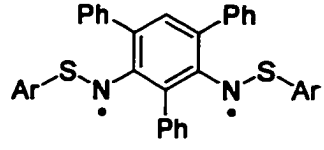

2.15

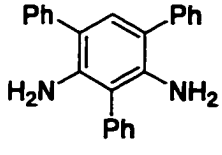

2.16

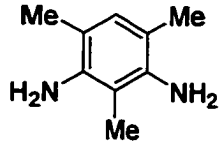

2.17

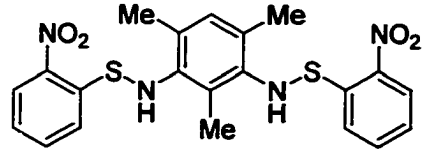

2.18

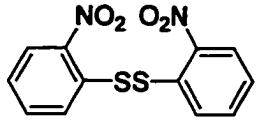

2.19

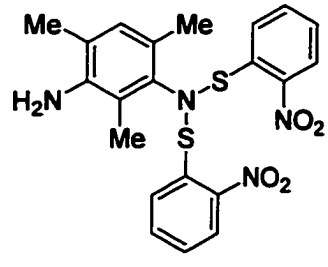

2.20

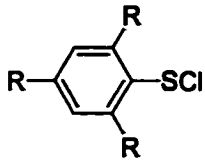

2.21

(a) R = Me
(b) R = ^{t}Bu

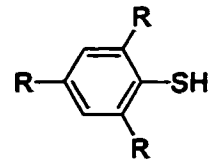

2.22

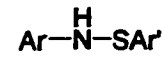

2.23

(a) Ar = Mes, Ar' = 4-$NO_2C_6H_4$
(b) Ar = Mes, Ar' = 2-$NO_2C_6H_4$
(c) Ar = 2,4,6-trichloroaniline, Ar' = 2-$NO_2C_6H_4$
(d) Ar = 4-MeC_6H_4, Ar' = Mes*
(e) Ar = Mes, Ar' = Mes*
(f) Ar = Mes, Ar' = Mes

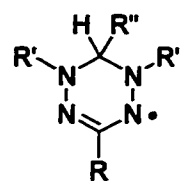

3.1

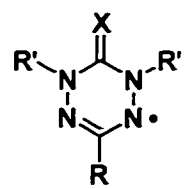

3.2

(a) X = O
(b) X = S

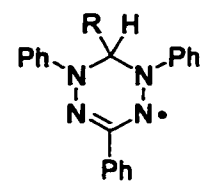

3.3

(a) R = H
(b) R = C_6H_5
(c) R = *p*-BrC_6H_4

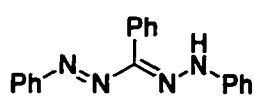

3.4

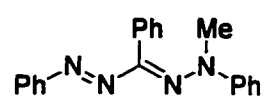

3.5

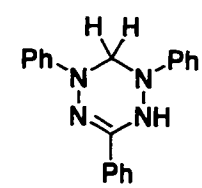

3.6

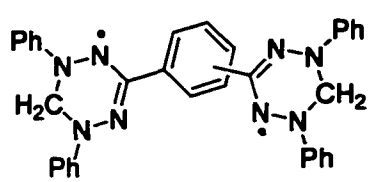

3.7 (a) = meta
(b) = para

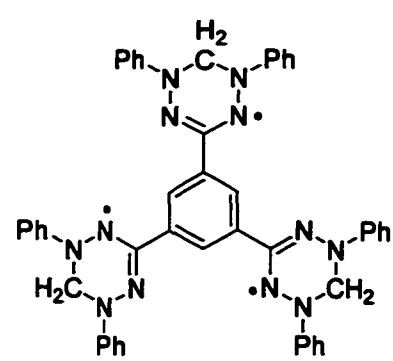

3.8

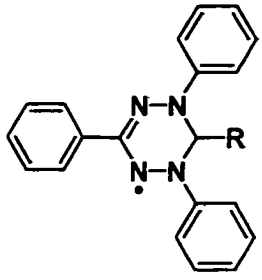

$R = C_nH_{2n+1}$
(n = 4-7, 9, 15)

3.9

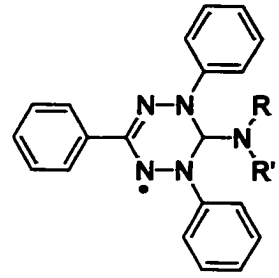

3.10

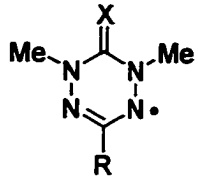

(a) X = O
(b) X = S

3.11

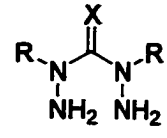

(a) X = O, R = Me
(b) X = S, R = Me
(c) X = O, R = CH_2Ph
(d) X = S, R = CH_2Ph

3.12

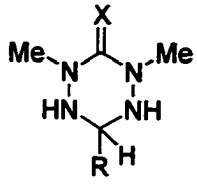

(a) X = O
(b) X = S

3.13

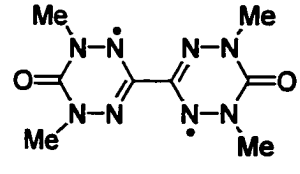

3.14

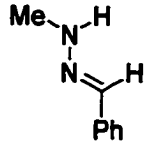

3.15

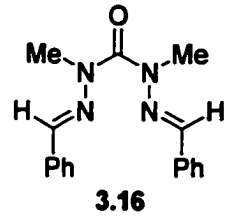

3.16

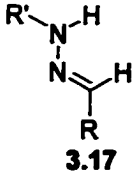

3.17

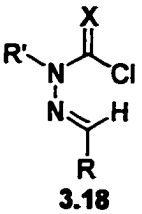

3.18

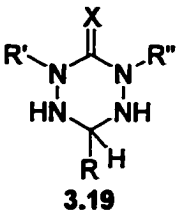

3.19

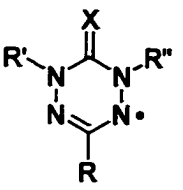

3.20

X = O, S
R = Ph, ^{t}Bu
R' = Ph, Me
R" = Ph

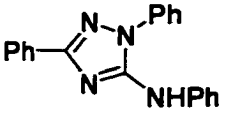

3.21

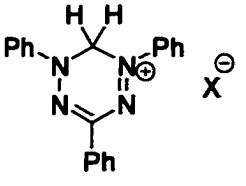

3.22

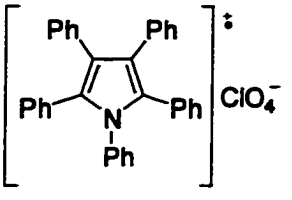

3.23

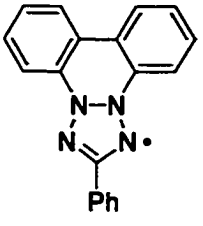

3.24

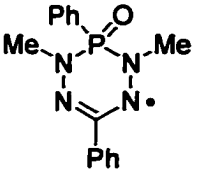

3.25

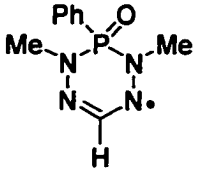

3.25a

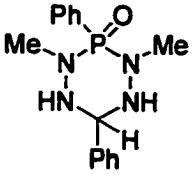

3.26

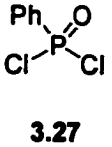

3.27

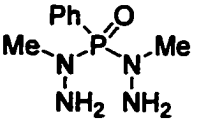

3.28

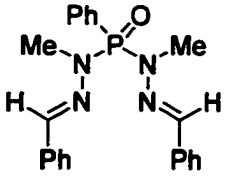

3.29

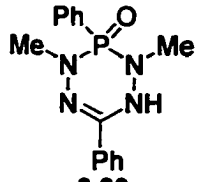

3.30

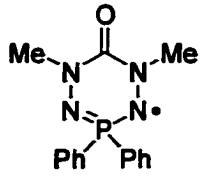

3.31

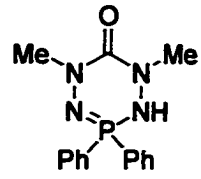

3.32

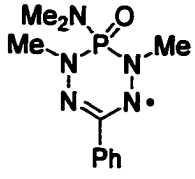

3.33

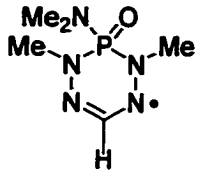

3.33a

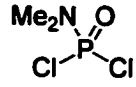

3.34

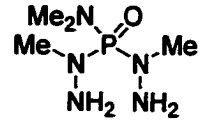

3.35

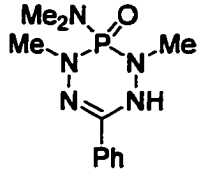

3.36

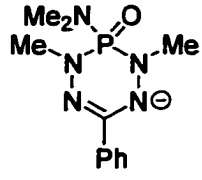

3.37

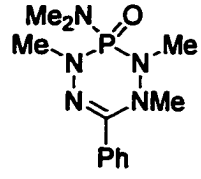

3.38

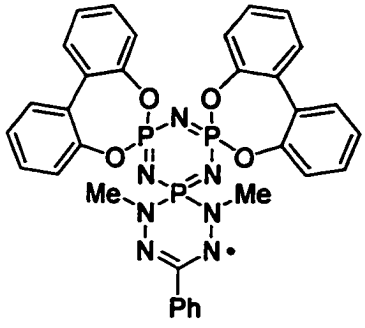

3.39

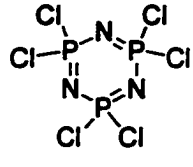

3.40

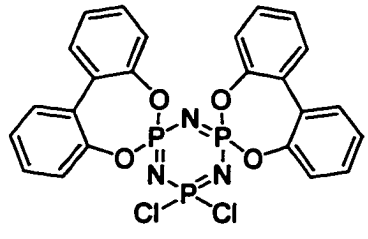

3.41

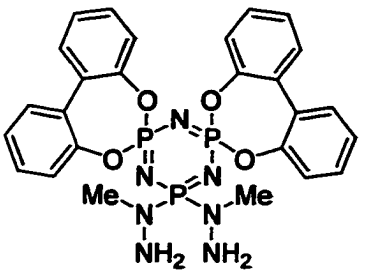

3.42

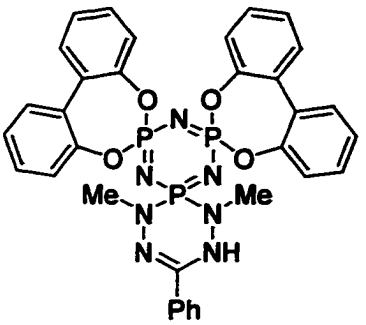

3.43

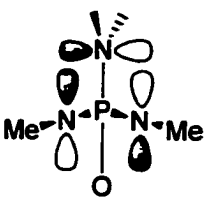

3.44

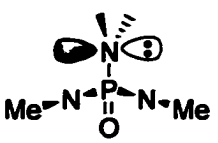

3.45

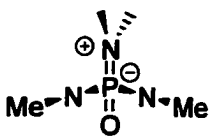

3.45a

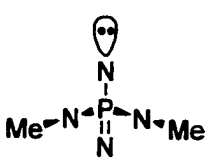

3.46

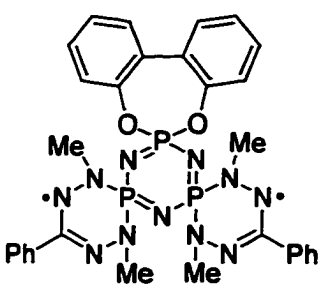

3.47

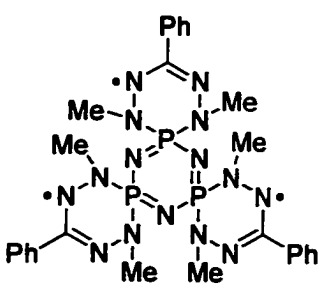

3.48

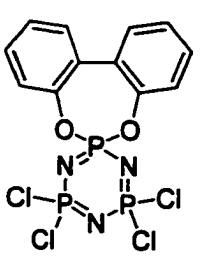

3.49

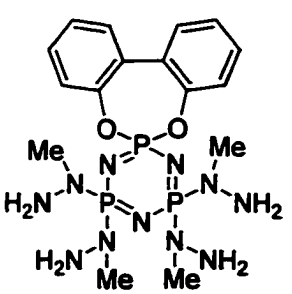

3.50

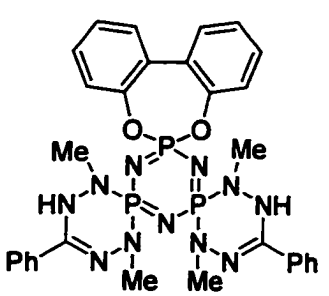

3.51

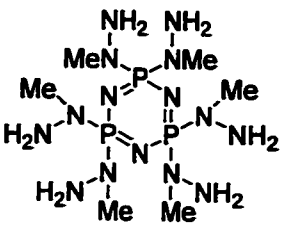

3.52

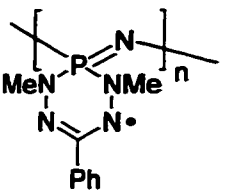

3.53

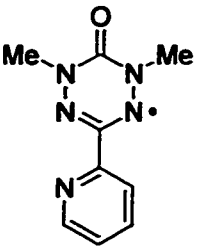

4.1

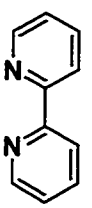

4.2

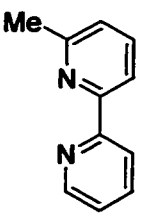

4.3

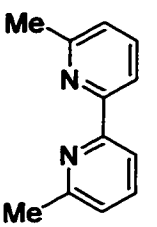

4.4

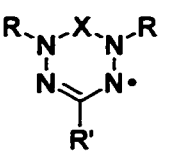

4.5

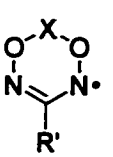

4.6

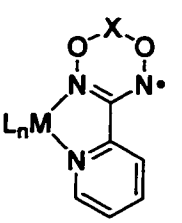

4.7

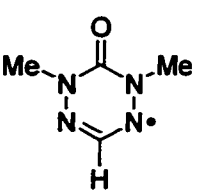

4.8

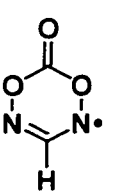

4.9

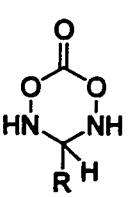

4.10

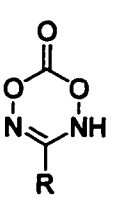

4.11

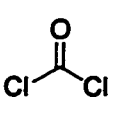

4.12

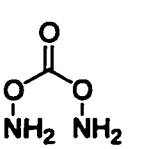

4.13

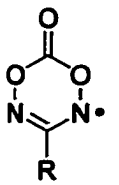

4.14

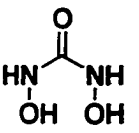

4.15

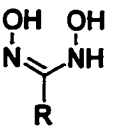

(a) R = Ph
(b) R = *p*-tolyl

4.16

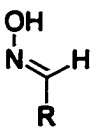

4.17

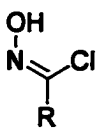

4.18

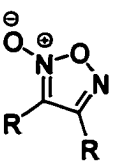

4.19

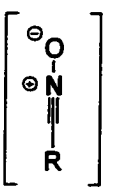

4.20

(a) R = Ph
(b) R = *p*-tolyl

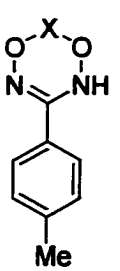

(a) C=O
X = (b) PhP(O)
(c) Me_2Si

4.21

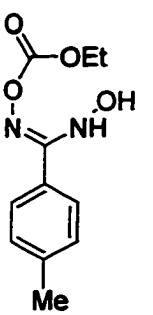

4.22

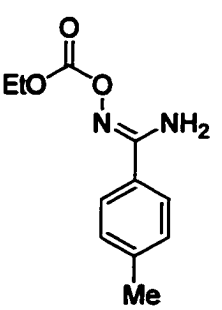

4.23

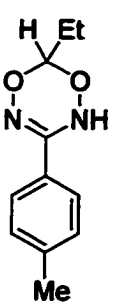

4.24a

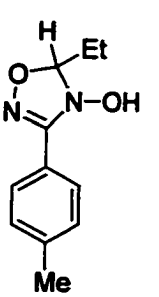

4.24b

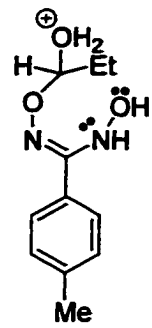

4.25a

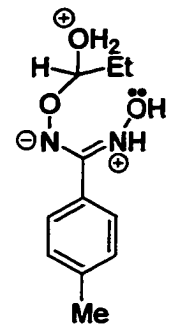

4.25b

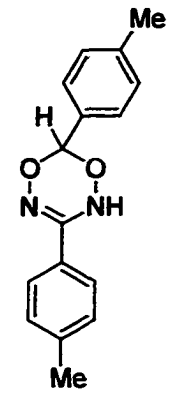

4.26a

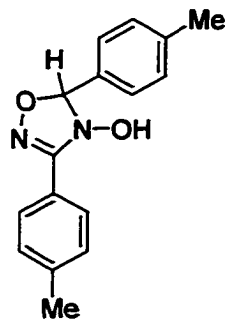

4.26b

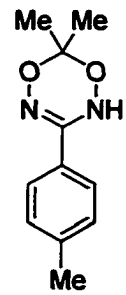

4.27a

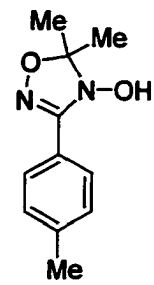

4.27b

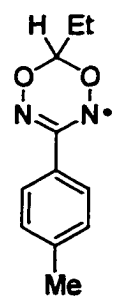

4.28

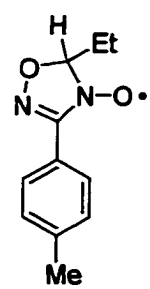

4.29

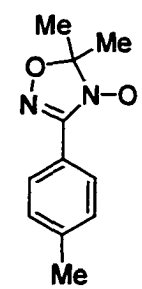

4.30

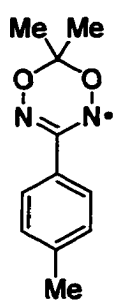

4.31

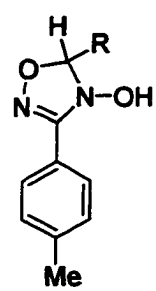

4.32

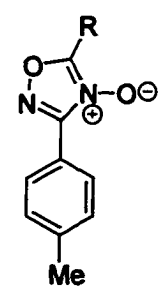

4.33

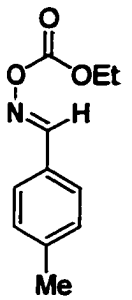

4.34

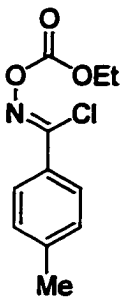

4.35

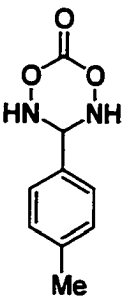

4.36

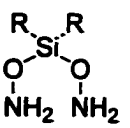

5.1

Acknowledgements

I would like to first express my appreciation to my supervisor Robin for all his patience, help, and guidance over the course of my degree and for (in his naiveté) taking me into his group. I would also like to thank the Hicks group members past and present: Hooper, Nodwell, Marty (Moonchild), Dan (Fonze), and Bryan (Bipy). A special thanks to Marty for all the non-chemistry discussions during the "Maiden Years" (or is that the "Wasted Years"). Many thanks to Todd for all the computer/thesis help (without which I would still be writing). Thanks to all grad students past and present for all their help over the years.

This thesis would not have been possible without the help of the (awesome) chemistry support staff: chem. office, Susanne, Carol, and Sandra; glassblowing shop, Sean Adams; mass spec. lab, Dave McGillivray; machine shop, Roy Bennett and Dick Robinson; NMR lab, Chris Greenwood; computer guru Bob Dean, and all at chem. stores. I would like to thank Dave Berg and Tom Fyles for their open door policy and Dave Berry for making teaching as tolerable as possible (whale watching was a nice bonus). Many thanks to John Richardson and Tosha Barclay for the x-ray structures, Andrew Ichimura for the ENDOR spectrum, and Lars Öhrström for the DFT calculations (better you than me). Finally, I must thank my girlfriend Melanie for...everything. Ti amo.

pour Man. et le Bonhomme

"Begin at the beginning, Master Li told me. Proceed
through the middle, continue to the end, and then stop.
That is what I shall do, and then, perhaps, a kind reader
will write and explain it to me"
-Number Ten Ox

Chapter 1

Introduction and Background

1.1 Organic Radicals

Radicals, molecules with unpaired electrons, are intriguing species because they contradict two fundamental concepts in chemistry – the valency rules of Kekulé[1,2] and the theory of the covalent bond of Lewis.[3] The valency rules state that elements form a distinct number of bonds. As shown in Figure 1.1, neutral radicals form one less bond than required for a particular element (i.e. they are subvalent). According to Lewis, electrons tend to "pair up" and form covalent bonds. Clearly, radicals are exceptions. It is this unique property of radicals that is the major driving force for their study.

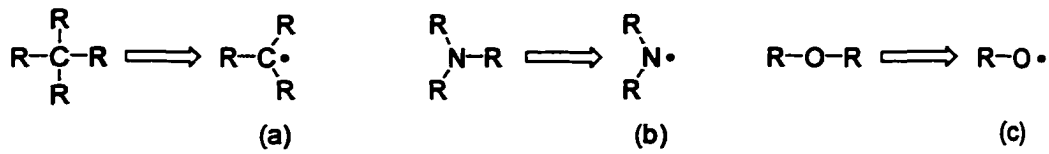

Figure 1.1. Carbon (a), nitrogen (b), and oxygen (c) radicals with reduced valency relative to their corresponding full valence analogues.

It was not until the turn of the twentieth century that a "stable" organic radical was synthesized. Since this landmark discovery, the number of new radicals and our knowledge of their properties have grown dramatically; radicals play a number of important roles in everyday life. Radical chemistry has important environmental consequences because the depletion of ozone in the stratosphere is known to occur through a series of radical reactions. In nature, the process of photosynthesis involves radicals. Radicals can be detrimental to biological systems because they destroy

biological structures such as membranes and DNA. Explosions, combustion and polymerization reactions also all involve radicals. This is a small part of a very large list of the many uses of radicals.

1.2 Stable Radicals

In general, most radicals are short-lived species with lifetimes of milliseconds or less. There are, however, classes of radicals that are much more long-lived and some that are indefinitely stable. These are referred to as "stable radicals". Although in the minority, the number of examples of stable radicals has grown dramatically since the turn of the twentieth century. Stable radicals are especially interesting because they offer the potential to answer many questions regarding the electronic structure, bonding, and reactivity of molecules. The remainder of this thesis is devoted to stable radicals.

Before proceeding, however, the term "stable" must be defined. This in itself is not a trivial matter because to date, there exists no unified description of what qualifies as "stable" in radical chemistry.[4] In the literature, the terms "stable" and "persistent" are often interchanged without careful consideration of the distinction between them. In order to define the stability of a radical, a time scale *and* the chemical environment must be specified. For example, a methyl radical can be stabilized almost indefinitely in a frozen argon matrix but at higher temperatures, the radical decomposes rapidly and irreversibly.[5] Many radicals are persistent and long-lived but not isolable in the solid state. In the context of this thesis, we define a stable radical as one which can be ideally isolated in the solid state. It is important to keep in mind that the term "persistent" is arbitrary and the distinction between persistent and reactive is dependent on the point of

view of the author. A "persistent" radical is defined herein as a radical with a sufficient lifetime to be examined by spectroscopic methods.

One of the most common decomposition pathways for radicals is dimerization. The thermodynamic driving force of these reactions is due to the large change in enthalpy from the formation of a carbon-carbon single bond (~350 kJ/mol). In order to stabilize these radicals the rate of dimerization must be suppressed. This kinetic stability can be achieved by attaching bulky groups around the radical. This is shown in Scheme 1.1. Two methyl radicals rapidly dimerize due to the favorable formation of the carbon-carbon bond in ethane. In contrast, triphenylmethyl radical **1.1** does not dimerize to form hexaphenylethane because of the bulky phenyl groups (but see later).

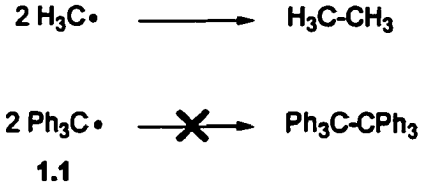

Scheme 1.1. Steric effects on the dimerization of methyl and triphenylmethyl radicals.

It is important to recognize that kinetic stability achieved through sterics does not necessarily translate to chemical stability. For example, although triphenylmethyl **1.1** does not dimerize to form hexaphenylethane, it readily reacts with atmospheric oxygen.

The stability of a radical is also aided by the delocalization of the unpaired electron. The more delocalized the unpaired electron is, the less likely it will react with itself (dimerization) or with another molecule. This can be illustrated by comparing the rates of dimerization of the methyl radical and the benzyl radical. The unpaired electron in the methyl radical is essentially localized on carbon and dimerizes to give ethane

($8.9x10^{-9}$ $M^{-1}sec^{-1}$).[6] In comparison, the unpaired electron in benzyl is more delocalized as can be represented by the four resonance pictures shown in Scheme 1.2. Because the unpaired electron is not as localized as in the methyl radical, the rate of dimerization of the benzyl radical is slower ($4.0x10^{-9}$ $M^{-1}sec^{-1}$).[6] This comparison assumes that steric effects are negligible in these radicals.

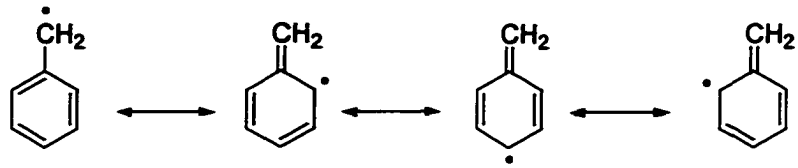

Scheme 1.2. Resonance structures of a benzyl radical.

The vast majority of "stable" radicals contain substantial spin density on heteroatoms rich in lone pairs. The inclusion of heteroatoms enhances the stability of radicals through the lone pair repulsions which disfavour dimerization. For example, the oxygen-oxygen bond (~180 kJ/mol) of peroxides is much weaker then a typical carbon-carbon single bond (~350 kJ/mol) due to the adjacent lone pairs repulsions on oxygen. In the case of nitroxide **1.2**, dimerization is extremely unfavourable because this would create a structure containing four consecutively bound heteroatoms rich in lone pairs (Scheme 1.3).

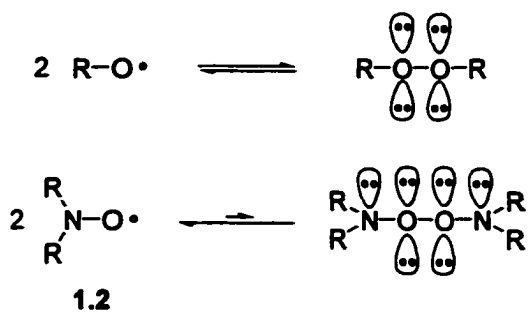

1.2

Scheme 1.3. Effect of lone pair repulsion on the dimerization of heteroatom based radicals.

The repulsion between lone pairs on adjacent atoms can help explain why small radicals such as oxygen and nitric oxide do not dimerize. There is no steric barrier to dimerization for these small molecules yet they are stable. Dimerization of these molecules would require four heteroatoms rich in lone pairs to be in close proximity.

1.3 A Survey of Stable/Persistent Radicals

1.3.1 Triarylmethyl Radicals

The first free radical, triphenylmethyl **1.1**, was discovered in 1900 by Gomberg.[7] While trying to prepare hexaphenylethane, Gomberg generated yellow solutions of triphenylmethyl **1.1**. In his landmark paper, Gomberg correctly surmised that he had made a molecule that contained trivalent carbon. Triphenylmethyl **1.1** was obtained by the reaction of triphenylmethyl chloride with a metal (typically silver, mercury, or zinc) in the absence of atmospheric oxygen as shown in Scheme 1.4.

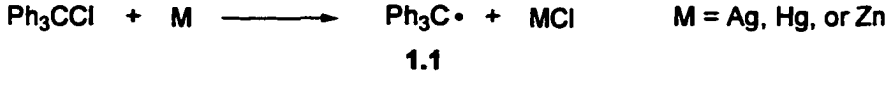

Scheme 1.4. Preparation of triphenylmethyl **1.1**.

According to the previous definition, triphenylmethyl is not "stable". The radical does persist indefinitely in dilute, deoxygenated solutions but in more concentrated solutions a σ-dimer forms. The structure of the dimer was a controversy which was not resolved until the late 1960's.[8] In 1968, the NMR spectrum showed unambiguously that the dimer was compound **1.3** and not hexaphenylethane (Scheme 1.5).

As new analytical techniques became available, researchers were able to study the distribution of the unpaired electron in triphenylmethyl. From the EPR spectrum of

triphenylmethyl, the unpaired electron is predominantly found on the methyl carbon ($a(^{13}C)$ = 22-26 G) and partially on the aromatic groups ($a(H_o)$ = 2.5-2.6, $a(H_m)$= 1.1, $a(H_p)$= 2.7-2.8 G). The spin density on the para carbons helps to explain the mode of dimerization. Thus the reactivity of triphenylmethyl is governed by both sterics and spin delocalization.

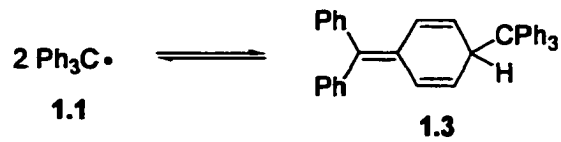

1.1 1.3

Scheme 1.5. Dimerization product of triphenylmethyl **1.1**.

This σ-dimerization can be prevented if the para positions are protected, for example radical **1.4**. Although still reactive towards atmospheric oxygen, radical **1.4** does not dimerize in solution.[9]

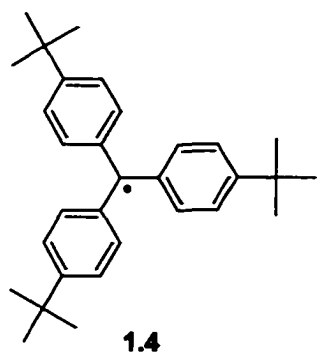

1.4

More than 100 years after their discovery, derivatives of triphenylmethyl continue to be a focus in radical chemistry. For example, Rajca *et al.* have developed polyradicals based on triphenylmethyl (e.g. **1.5** and **1.6**) and are studying their magnetic properties.[10,11]

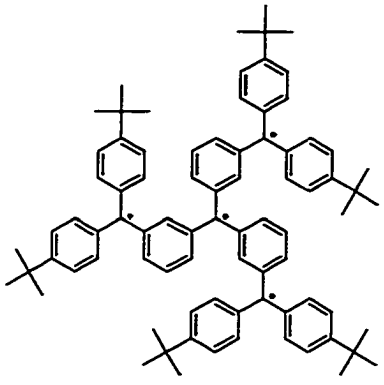

1.5

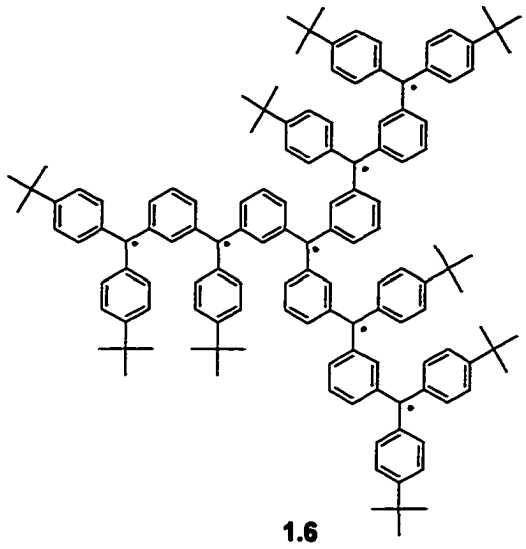

1.6

1.3.2 Nitroxide Radicals

Shortly after the discovery of triphenylmethyl **1.1**, Piloty and Schwerin prepared the first organic nitroxide **1.7**, although it was incorrectly formulated as **1.8**.[12,13] The synthesis of radical **1.7** was a milestone because it was the first organic neutral radical to be isolated.[14] In subsequent years, other groups prepared a number of diarylnitroxides, of which **1.9** are examples.[15-18] The nitroxide family is easily the most used and heavily studied class of radicals; hundreds of examples have been reported in the literature.[19,20] In general, nitroxides are stable and do not dimerize to give peroxides and many derivatives are isolable in the solid state.

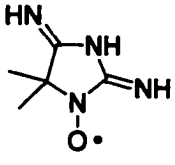

1.7

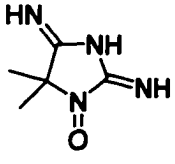

1.8

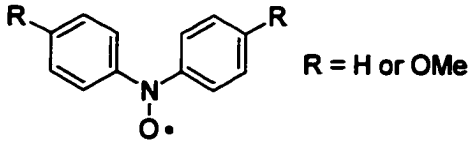

1.9

Nitroxides are most commonly prepared by the oxidation of *N,N*-disubstituted hydroxylamines with silver oxide or lead dioxide (Scheme 1.6).

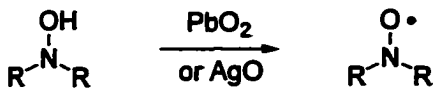

Scheme 1.6. General reaction for the preparation of nitroxides.

Although nitroxides do not undergo dimerization at oxygen (see **1.2**), some alkyl nitroxides can readily disproportionate to the corresponding nitrones **1.10** by loss of a hydrogen on a carbon α to the NO group (Scheme 1.7). For this reason, virtually all stable nitroxides have no α–hydrogens. However, under certain circumstances, disproportionation can be suppressed. For example, radical **1.11** is stable in the solid state because formation of the nitrone is prohibited by Bredt's rule.[21]

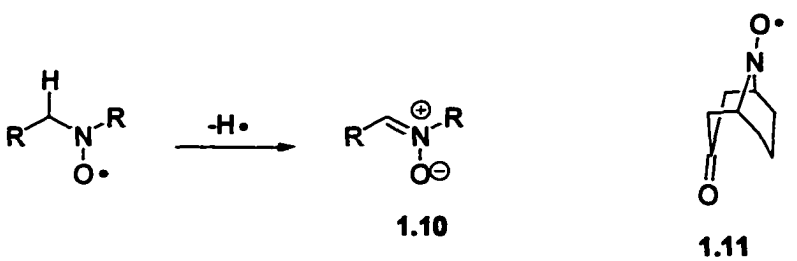

1.10 **1.11**

Scheme 1.7. Disproportionation of a nitroxide to nitrone **1.10**.

EPR spectra of nitroxides indicate that the unpaired electron is confined primarily to the nitrogen and oxygen atoms ($a(^{14}N)$ = 8–17 G). The relatively large coupling to nitrogen demonstrates the importance of the two resonance contributors shown in Figure 1.2.

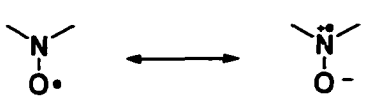

Figure 1.2. Important resonance contributors of nitroxide radicals.

Closely related to the nitroxides are the nitronyl nitroxides **1.12**, first prepared by Osiecki and Ullman in 1968 as shown in Scheme 1.8.[22,23] Like the nitroxides, nitronyl

nitroxides lacking α–hydrogens are stable, do not dimerize, and many derivatives can be isolated as monomeric species in the solid state. The unpaired electron in the nitronyl nitroxides are predominantly distributed about the two NO groups with $a(^{14}N)$ couplings in the range of 16.1-16.7 G.[24]

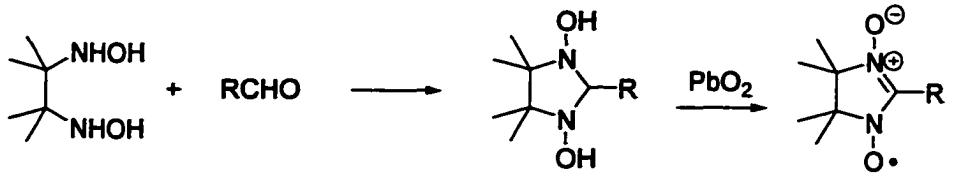

1.12

Scheme 1.8. Synthesis of nitronyl nitroxide **1.12**.

1.3.3 Hydrazyl Radicals

Goldschmidt and collaborators pioneered the work on hydrazyl radicals in the 1920s.[25] They observed that treatment of triphenylhydrazine **1.13** with lead dioxide produced blue solutions which quickly turned green then to a permanent red-brown. The reactive blue solution is due to hydrazyl radical **1.14** and the final product is the dimer, hexaphenyltetrazane **1.15** (Scheme 1.9).

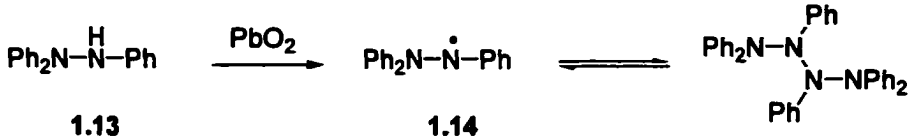

1.13 **1.14** **1.15**

Scheme 1.9. Preparation of hydrazyl **1.14**.

Goldschmidt also prepared aromatic hydrazyls **1.16** and **1.17**.[26,27] Compound **1.17**, 2,2-diphenyl-1-picrylhydrazyl (DPPH), is an exceptionally stable hydrazyl in that it shows no tendency to dimerize in the solid state or in solution, even at low temperatures.[28] DPPH

has been used extensively as a field standard in EPR spectroscopy.[14] It should be noted that although hydrazyl **1.17** is an exceptionally stable radical, in general hydrazyls do not enjoy this level of stability and are better described as persistent radicals. Similar to nitroxides, the unpaired electron in hydrazyl radicals is predominantly found on the nitrogen atoms. EPR spectra show that hyperfine coupling to the divalent nitrogen ($a(^{14}N)$ = 9.2–10.7 G) is slightly larger than that of the trivalent nitrogen atom ($a(^{14}N)$ = 7.0–7.9 G).[29]

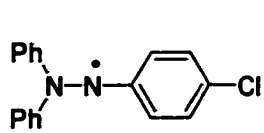

1.16

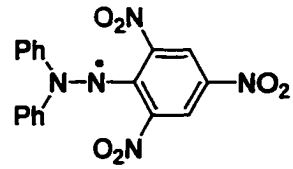

1.17

1.3.4 Phenalenyl Radicals

The phenalenyls **1.18** are a class of carbon-based radicals first prepared in the 1950s.[30,31] As shown in Scheme 1.10, phenalenyl **1.18** can be prepared by deprotonation of phenalene **1.19** followed by oxidation of the anion **1.20**. In solution, phenalenyl **1.18** is in equilibrium with a σ–dimer **1.21**. This σ–dimerization prevents the isolation of parent **1.18** as a monomeric species. Phenalenyl **1.18** and its derivatives represent rare examples of purely carbon-based radicals that are persistent despite the lack of steric protection.

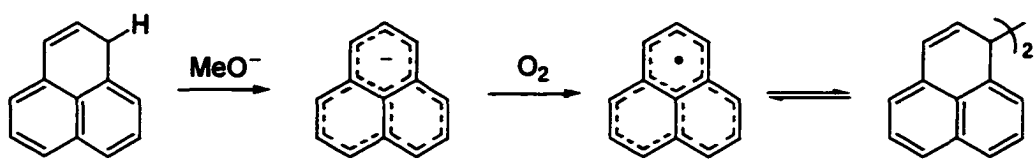

1.19 **1.20** **1.18** **1.21**

Scheme 1.10. Preparation of phenalenyl radical **1.18**.

The σ-dimerization can be prevented with the introduction of substituents around the periphery of the ring as shown in phenalenyl derivatives **1.22** and **1.23**.[9,32] In the solid state, radical **1.22** forms π–dimers from which the radical can be regenerated upon dissolution. Radical **1.23** does not show any tendency to associate in any way in solution or in the solid state.

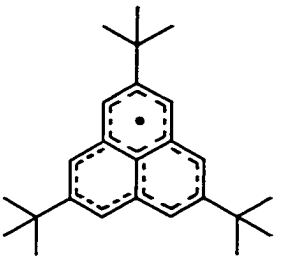

1.22

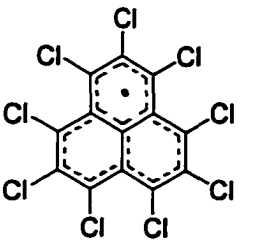

1.23

Analysis of the EPR spectra of phenalenyls indicates that the spin distribution is predominately found on the *peri*-carbons (**1.24**) with hyperfine coupling values of $a(H_a)$ = 7.3 G and $a(H_b)$ = 2.2 G.[33]

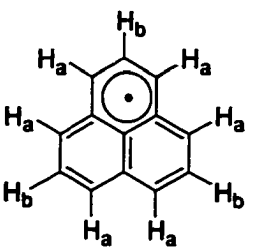

1.24

1.3.5 Heterocyclic SN Radicals

The dithiadiazolyls[34] (**1.25**), and the 1,3,2-dithiazolyls[35,36] (**1.26**) are stable, isolable classes of radicals based on CSN heterocyclic skeletons.

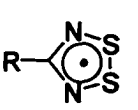

1.25

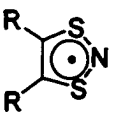

1.26

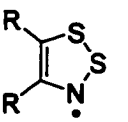

1.27

Dithiadiazolyls **1.25** and 1,3,2-dithiazolyls **1.26** are typically prepared by the reduction (Ph_3Sb) of the corresponding dithiadiazolium or dithiazolium salts, **1.25a** and **1.26a** respectively (Scheme 1.11).

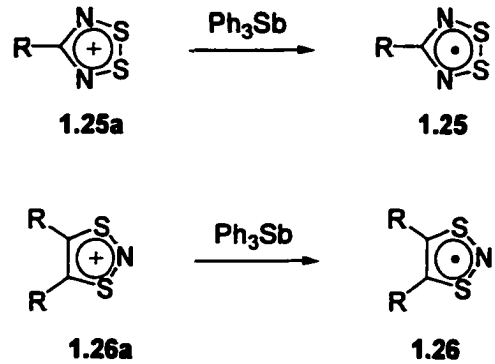

1.25a **1.25**

1.26a **1.26**

Scheme 1.11. Preparation of the dithiadiazolyls **1.25** and dithiazolyls **1.26**.

The isomeric counterpart to radicals **1.26** are the 1,2,3-dithiazolyls **1.27**. Although these radicals have been known for over twenty years,[37] the first isolable example, **1.28**, was only reported recently.[38] Radical **1.28** was prepared by the oxidation of **1.28a** with S_2Cl_2 as shown in Scheme 1.12. The spin distribution of the unpaired electron in radicals **1.25**, **1.26**, and **1.27** is predominantly found on the sulfur and nitrogen atoms.[36,38,39] For the dithiadiazolyls, $a(^{14}N)$ and $a(^{33}S)$ have values around 5.0 G and 6.3 G respectively. For the 1,3,2-dithiazolyls, $a(^{14}N)$ and $a(^{33}S)$ are found around 11 G and 4.0 G respectively. In the case of the 1,2,3-dithiazolyls, $a(^{14}N)$ is found in the range of 2.8–6.5 G.

In solution the dithiadiazolyls, 1,2,3- and 1,3,2-thiadiazolyls give strong EPR signals. In the solid state, however, some form monomeric radicals and others form cofacial π–dimers. These stable radicals are being actively studied as building blocks for molecular conductors.[38-42]

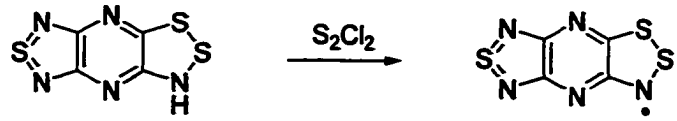

1.28a **1.28**

Scheme 1.12. Preparation of 1,2,3-dithiazolyl **1.28**.

1.3.6 Other Heteroatom-Based Radicals

Thioaminyls[43](**1.29**) and verdazyls[44,45] (**1.30** and **1.31**) are other classes of stable, isolable radicals. Both the thioaminyls and verdazyls will be discussed in more detail in Chapters 2 and 3 respectively.

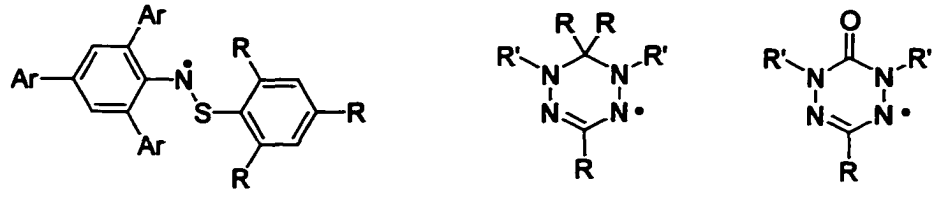

1.29 **1.30** **1.31**

1.4 Spectroscopic Study of Radicals

Electron Paramagnetic Resonance (EPR) is by far the most powerful technique to study paramagnetic molecules.[46] The theory behind EPR spectroscopy is in many ways analogous to that of NMR spectroscopy: both techniques involve the perturbation of nuclear spin states (NMR) or electronic spin states (EPR) by an external magnetic field.

In the absence of an applied magnetic field, the two spin states of an electron (M_s = ± ½) are degenerate. The degeneracy is removed when an electron is placed in a magnetic field similar to how nuclear spin states (M_I) of nuclei are split in NMR spectroscopy. For paramagnetic substances, the number of substates is given by the multiplicity, 2S + 1. Therefore, an electron placed in an external magnetic field can

either align with the field (M_s = -½) or against the field (M_s = ½) giving rise to two substates (Figure 1.3). This is known as the Zeeman effect. Absorption will occur if the resonance condition is satisfied according to:

$$\Delta E = h\nu = g\beta H$$

where h is Planck's constant, ν is the microwave frequency, and H is the applied magnetic field strength. The dimensionless term g is called the g-factor. For a free electron, g = 2.00232. The parameter β is the Bohr Magneton for the electron. Similar to the magnetogyric ratio γ in NMR, β determines the extent of splitting between the two spin states ($\Delta M_s = \pm ½$) of an electron in an external magnetic field. The absorption spectrum (Figure 1.3(a)) is typically presented as the first derivative (Figure 1.3(b)).

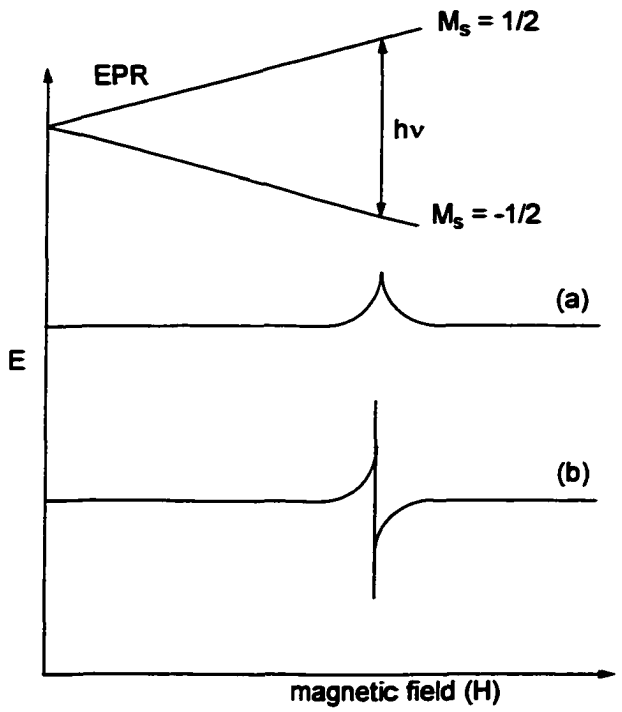

Figure 1.3. Zeeman Splitting of the two magnetic spin states of an electron (M_s), the corresponding absorption (a), and the first derivative of the absorption (b).

In EPR, the g-factor is analogous to the chemical shift in NMR spectroscopy. For most organic radicals, the value of g is usually close to the value for the free electron (g = 2.00232). Consequently, the g-value is of little diagnostic value in organic systems.

Of much greater use in EPR are the hyperfine splitting constants (*a*) which are analogous to coupling constants (*J*) in NMR. Hyperfine splitting arises because of small changes in the effective magnetic field strength experienced by the free electron caused by neighbouring magnetic nuclei. Thus, any magnetic nucleus ($I \neq 0$) can effect hyperfine splitting. The multiplicity of the EPR signal is then dependent on the number and the nuclear spin of the interacting nuclei. For n equivalent nuclei, the multiplicity observed is $2nI + 1$. For example, an unpaired electron coupled to one hydrogen nucleus gives rise to two transitions ($2(1)(\frac{1}{2}) + 1 = 2$). These are shown in Figure 1.4 as two-headed arrows. The corresponding absorption spectrum (Figure 1.4a) and the first derivative spectrum (Figure 1.4b) are shown below. Note that transitions only occur between substates when $\Delta M_s = \pm 1$ and $\Delta M_I = 0$. These are the selection rules for EPR spectroscopy. Hyperfine coupling values are useful because they can be related to nuclear–electron interactions, which in turn can be interpreted as a measure of the spin distribution in the radical.

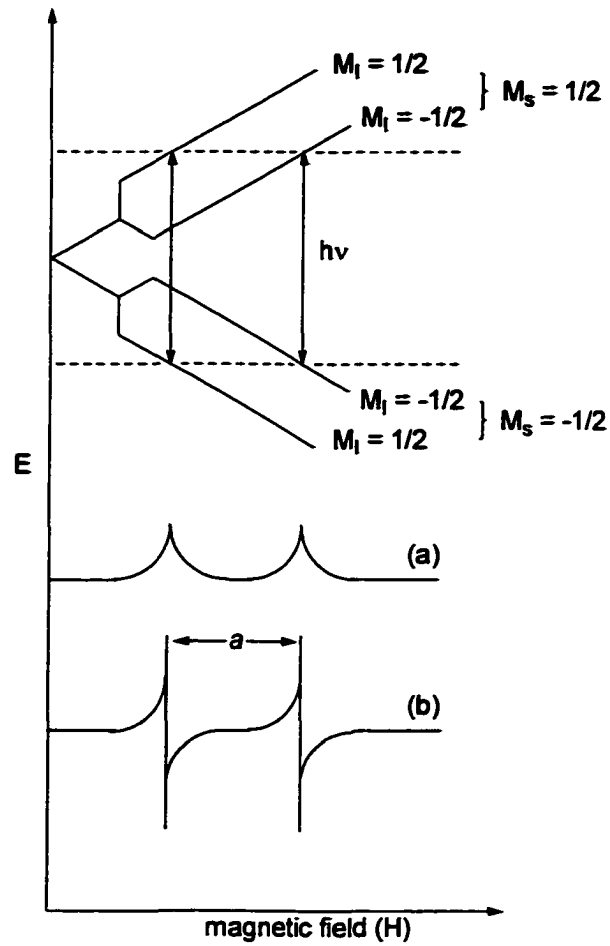

Figure 1.4. Splitting of the electron substates by a hydrogen nucleus.

1.5 Application and Uses of Stable Radicals

Why study stable radicals? This is a valid question which can be partly answered on the basis that radicals are inherently interesting molecules. Stable radicals are exceptions to one of the most fundamental assumptions about the electronic structure of molecules, that is, electrons prefer to "pair up" in orbitals. It is not surprising then that the discovery of new examples of stable radicals is still novel enough to warrant

publication. For example, **1.32** and **1.33** are radicals which were recently reported as novel species simply because they are stable.[47,48]

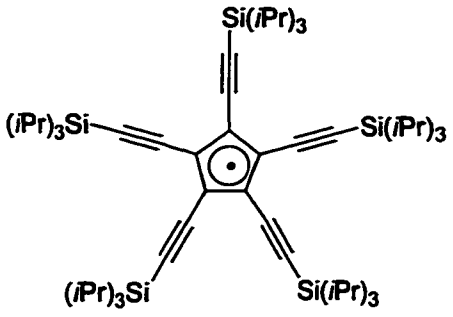

1.32

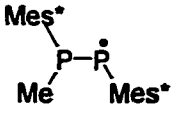

1.33

In addition to being of fundamental interest, radicals have been used in a variety of ways to synthesize new materials and to study existing complex molecules. Some of these applications, which rely on the stability of the radicals, are briefly discussed below.

1.5.1 Magnetic and Conducting Materials

From computers to household appliances, to motors and generators, magnets are an integral part of our society. Traditionally, magnets have been derived from inorganic solids (*e.g.* CrO_2), but more recently, efforts have been made towards magnets based solely on organic molecules.[49-51] The phenomenon of magnetism is dependent on the ferromagnetic alignment of a macroscopic amount of unpaired electrons, therefore, stable radicals are well suited as "building blocks" for molecular magnets. Nitroxides and nitronyl nitroxides have by far been most commonly used as molecular magnetic building blocks.[50] Although molecular magnets may never replace their traditional counterparts, they can offer new properties. Unlike traditional magnets, which are dense, brittle, intractable solids; molecular magnets have the potential to be lightweight, transparent,

and soluble.[52] These properties are well suited to the fabrication of electronic devices. Perhaps the most appealing aspect of molecular magnets is their processibility. Using established organic chemistry methodologies, the magnetic properties could be fine-tuned. The combination of magnetic properties with other electronic and/or optical properties is also appealing. These properties, which are not available with traditional magnets, may spawn new generations of electronic and optical devices.

Although ion radical conductors are well known, the idea of molecular conductors based on neutral radicals was first proposed by Haddon in 1975.[53] Haddon envisioned constructing molecular conductors using stable organic neutral radicals as the charge carriers. The radicals which have been predominately used as molecular conducting building blocks are the phenalenyl and thiazyl radicals.[38,54] The details behind the theory of molecular conductors is beyond the scope of this thesis, however, it is clear that stable organic radicals are required as building blocks.

1.5.2 Spin Trapping

The steady-state concentrations of reactive radicals are often too low to detect directly. Spin trapping is an experiment where a diamagnetic substance – the "spin trap" – is added to a solution of a reactive radical. The reactive radical reacts with the spin trap to form a new radical which is less reactive and often very stable. This allows indirect detection of the original reactive species. 2-methyl-2-nitrosopropane **1.34** and phenyl-*tert*-butyl nitrone **1.35** are two common spin traps.[55,56]

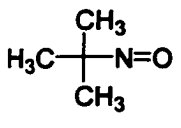

1.34

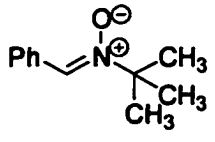

1.35

Reaction of either **1.34** or **1.35** with a radical produces a nitroxide radical. An example is shown in Scheme 1.13.

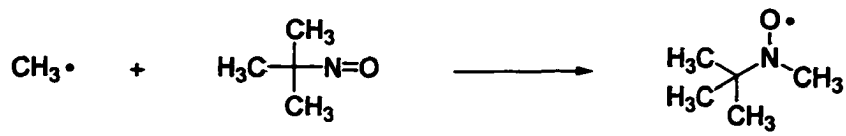

1.34 **1.36**

Scheme 1.13. Trapping of a methyl radical with **1.34** to form nitroxide **1.36.**

It is important to note that spin trapping allows only an indirect method at probing the original radical and therefore the amount of structural information gained is limited.

1.5.3 Spin Labeling

Spin labeling is a powerful technique used to study the structure of biological systems and the mechanism of biological reactions. The technique involves attaching a stable radical onto biologically important substances and analyzing the resulting EPR spectra. These spectra can yield valuable information about the environment around the label because the spectra are sensitive to the dynamic processes of the environment. Also, because the g-value and hyperfine splitting constants are dependent on the polarity of the solvent, the hydrophobic or hydrophilic nature of the environment around the label can be probed.[57]

Clearly, if a radical is to be used as a spin label, it must be stable under standard biological conditions. Therefore, it must be stable in aqueous solution, at pH 2-10, at high and low salt concentrations, and between temperatures of 20-70 °C. Also, the chemistry of the radical must be well understood. All these restrictions severely limit the

number of radicals that can be used as spin labels. Due to their robust nature and simple EPR spectra, nitroxides have been the most commonly used spin labels.

1.5.4 Living Free Radical Polymerization

One method for the preparation of polymers is free radical polymerization (Scheme 1.14). In this process a reactive radical attacks a monomer unit (in this example styrene) to form a new, longer chain radical. Subsequent addition of monomer to the newly formed radical lengthens the chain. This cycle is repeated to form the polymer. However, this technique is susceptible to side reactions such as hydrogen abstraction and radical coupling which leads to branching and premature chain termination. Consequently, free radical polymerization processes offer poor control of the molecular weight distribution. This is a significant disadvantage of radical polymerization because many applications require a high degree of molecular weight control.

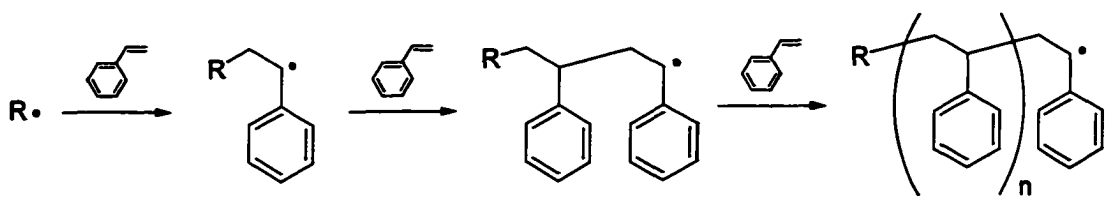

Scheme 1.14. Free radical polymerization of styrene.

Recently a new "living" free radical (LFR) polymerization process has been developed that permits the synthesis of polymers of high molecular weight and very narrow polydispersities.[58-60] The idea behind LFR polymerization is to add a stable radical to the free radical process to control the growth of the polymer. Thus, a nitroxide (or another stable radical) combines with the polymer to form a dormant intermediate (A

in Scheme 1.15). This intermediate is thermally labile and can be homolytically cleaved to give the nitroxide and the polymeric radical (**B**). Chain extension of the polymer with monomer then occurs to give the new, longer polymer (**C**). Subsequent recombination with the nitroxide gives the dormant, unreactive intermediate (**D**). The cycle of homolysis-monomer addition-recombination can then be repeated. The significance of this process is that the stable radical itself does not initiate the growth of extra polymer chains but does react at near diffusion-controlled rates with the carbon-centered radical. These features prevent branching and premature termination of the polymer and provide excellent molecular weight control for selected polymer systems. To date, virtually all LFR processes use nitroxides as the stable radical.

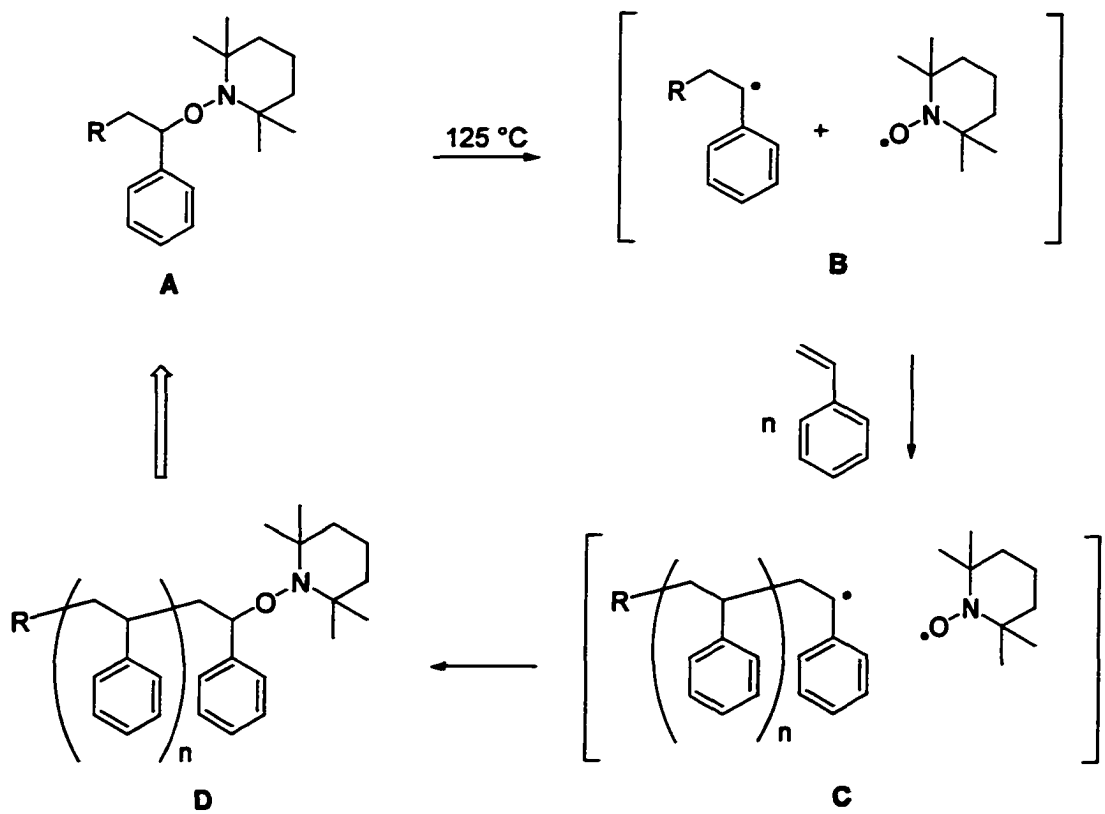

Scheme 1.15. Living free radical polymerization of styrene using a nitroxide radical.

1.6 Thesis objectives

As discussed above there are many reasons to study the chemistry of stable radicals. It is important to note that most classes of stable radicals were not made by design, but rather by accidental discovery. Considering their inherent interest and potential applications, it is surprising that very little research is aimed specifically at the *design* of new, stable radicals. Most applications make use of one class of radicals – the nitroxides, largely because of their excellent stability. However, it would be shortsighted to rely entirely on one class of radicals. Therefore, it would be desirable to be able to design new, stable radicals with properties tailored to specific applications.

The goals of this thesis are to explore the synthesis of new heteroatom-based stable radicals by design and to study structure/property relationships. Chapter 2 will present our attempts to synthesize thioaminyl triplet ground state diradicals. In Chapter 3, the synthesis, characterization, and properties of new phosphaverdazyls will be presented. Chapter 4 will present our results in the attempted synthesis of the unknown dioxadiazinyl radicals. In Chapter 5, general conclusions will be drawn followed by a brief outline of future goals.

Chapter 2

Synthetic Efforts Toward Thioaminyl Diradicals

2.1 Introduction

In Chapter 1, a brief history was given of the discovery and progress of stable free radicals. The factors governing stability were discussed as well as the structure and properties of some well known and new families of stable radicals. The spectroscopic technique EPR was introduced followed by some potential applications of these stable radicals.

In addition to the monoradicals, there exists a subset of radicals that have more than one unpaired electron. The presence of two or more unpaired electron raises some important questions that are not applicable to species with only one unpaired electron. For example, a fundamental question concerning diradicals is the way in which the two unpaired electrons interact with each other. When two unpaired electrons are in degenerate or near degenerate orbitals, they can exist in two possible spin states as shown in Figure 2.1. If the electrons are antiferromagnetically (AFM) coupled, the total spin S = 0 and the system is said to be in a low spin arrangement. If the electrons are ferromagnetically (FM) coupled, the total spin S = 1 and the system is said to be in a high spin arrangement. These are more commonly described as a singlet and triplet respectively (the multiplicity of the ground state is given by 2S + 1). For any diradical, either the singlet or triplet will be the ground state and the other will be an excited state. The energy difference between the singlet and triplet states is a measure of strength of the interaction between the two unpaired electrons and is represented by J.

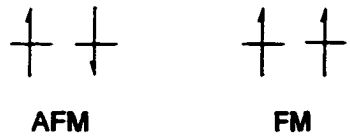

Figure 2.1. Possible spin states of a diradical.

A significant amount of research on diradicals has focused on systems in which the unpaired electrons are part of a π–conjugated system because it is these systems which tend to exhibit the strongest interactions between unpaired electrons. In these cases the ground state of a diradical can be rationalized by the nature of the two singly occupied molecular orbitals (SOMOs), which are commonly delocalized π–molecular orbitals.[61] If spin density is found on common atoms in these two orbitals, the SOMOs are said to be *coextensive*. In this case, the two unpaired electrons are able to remain spatially separated through a quantum mechanical *exchange interaction*, the existence of which requires the unpaired electrons to be ferromagnetically aligned. This exchange interaction minimizes the coulombic repulsion between the two electrons and stabilizes the triplet state. If spin density does not coincide on common atoms in the two orbitals, the SOMOs are said to be *disjoint*. In this case the conjugative π–system is not effective at mediating the exchange interaction. Consequently, the magnitude of J is much smaller and the ground state is much more difficult to predict.

To illustrate the relationship between diradical SOMOs and ground state preferences, three prototypical diradicals along with their SOMOs are shown in Figure 2.2. Both trimethylenemethane[62,63] (TMM, **2.1**) and *meta*-quinodimethane[64-68] (MQDM, **2.2**) are known to have triplet states in excess of 10 kcal/mol lower in energy than the singlet state. Their SOMOs are coextensive with spin density found on common atoms.

In the case of tetramethyleneethane (TME, **2.3**), the spin density of each SOMO is localized on different parts of the molecule; TME is therefore classified as a disjoint radical. TME is a ground state triplet, however, the energy difference between the singlet and triplet state is small at ~1 kcal/mol.[69,70]

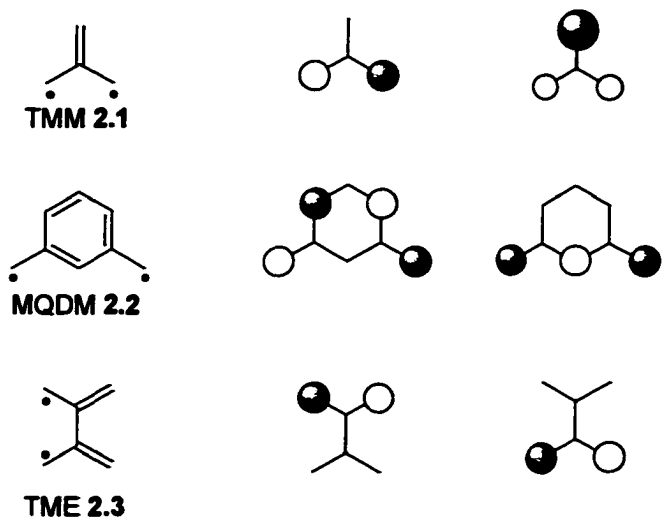

Figure 2.2. SOMOs of diradicals **2.1**, **2.2**, and **2.3**.

Longuet-Higgins has outlined a simple method for determining whether the SOMOs of *alternant* π–conjugated diradicals are disjoint or coextensive.[71] Alternant hydrocarbons are defined as molecules where each carbon atom can be marked "starred" or "unstarred" such that no starred or unstarred positions are adjacent (Figure 2.3). For such systems, if the number of starred atoms is greater than that of unstarred atoms, the triplet state is predicted to be the ground state. When the number of starred and unstarred atoms is equal, either the singlet or triplet can be the ground state. Applying this system on the above radicals, we would correctly predict TMM and MQDM as ground state triplets and TME as either a singlet or triplet ground state (This simple procedure does not reveal the forms of the SOMOs but only whether they are disjoint or coextensive).

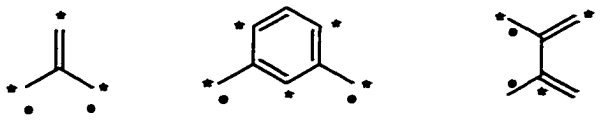

Figure 2.3. Coextensive (**2.1** and **2.2**) and disjoint (**2.3**) SOMOs for alternant hydrocarbons.

2.2 Characterization of Diradicals

2.2.1 EPR Spectroscopy

As discussed in Chapter 1, EPR spectroscopy is one of the most powerful tools to study radicals. The EPR spectra of diradicals, however, are generally more complicated than those of radicals. For any given diradical, there are three possible scenarios: a) when $J > 0$ and the triplet is the ground state, b) when $J < 0$ and the singlet is the ground state, and c) when $J = 0$ and the singlet and triplet states are degenerate. In the last case because the exchange energy is zero, the diradical effectively behaves as two non-interacting radicals. The EPR spectra of diradicals of this type consist of a superposition of the spectra of the individual isolated radicals. When $J < 0$, the singlet and triplet state are different in energy. For the singlet state, there is no EPR signal because $S = 0$. In the case of the triplet state of diradicals, the unpaired electrons are split into three substates as shown in Figure 2.4. There are two $\Delta M_s = \pm 1$ transitions which, because they are coincident, produce one signal. The scenario depicted in Figure 2.4 is true only when the three substates ($M_s = 0$ and $M_s = \pm 1$) are degenerate in the absence of an external magnetic field. Experimentally, this is rarely observed.

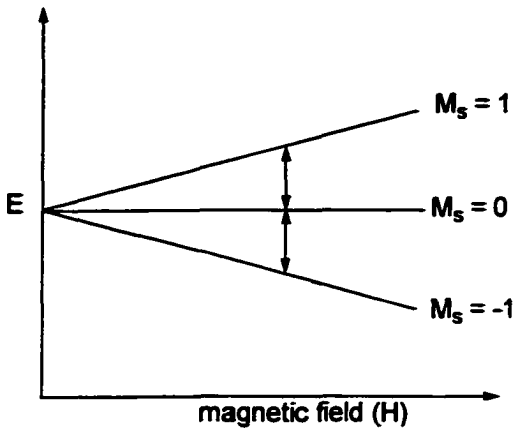

Figure 2.4. Schematic representation of the three substates produced when a triplet diradical is placed in a magnetic field (H).

Two unpaired electrons at zero magnetic field are often subject to spin-dipolar interactions which lifts the degeneracy of the substates. This phenomenon is known as Zero Field Splitting (zfs). Because the zfs has lifted the degeneracy of the substates, the two allowed $\Delta M_s = \pm 1$ transitions (solid arrows) are no longer coincident as shown in Figure 2.5. Note that the splitting pattern observed in Figure 2.5 occurs when the magnetic field is parallel to the z-axis.

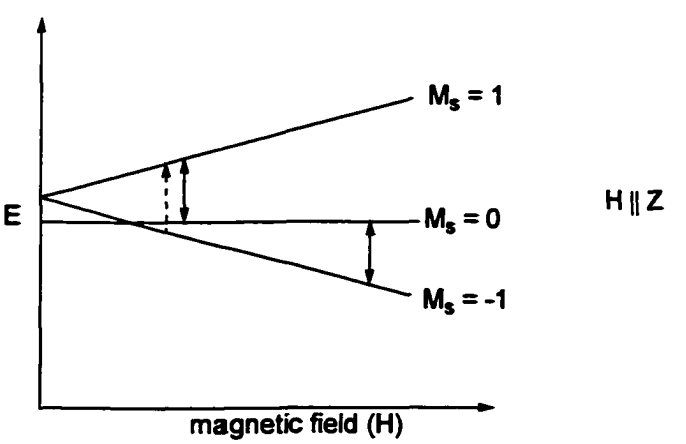

Figure 2.5. Zero Field Splitting of the triply degenerate substates of a diradical when the magnetic field is parallel to the z-axis.

When the magnetic field is perpendicular to the z-axis, the zfs pattern changes to that shown in Figure 2.6. The splitting patterns shown in Figure 2.5 and Figure 2.6 are for samples fixed in one direction (either parallel or perpendicular to the z-axis), and depending on the orientation, two signals are observed in each case. In randomly oriented samples, which are arranged at all possible angles to the magnetic field, four signals are typically observed.

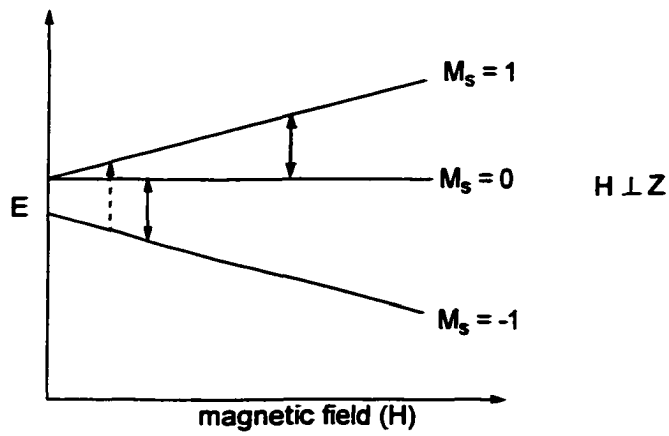

Figure 2.6. Zero Field Splitting of the triply degenerate substates of a diradical when the magnetic field is perpendicular to the z-axis.

One of the most diagnostic peaks of a triplet state diradical is the so-called "half-field" transition. For a system with three substates, the resonance condition is fulfilled not only for the two $\Delta M_s = \pm 1$ transitions, but also for a $\Delta M_s = \pm 2$ transition. These transitions are shown as dashed arrows in Figure 2.5 and Figure 2.6. As the name implies, this formally forbidden $\Delta M_s = \pm 2$ transition is usually found at a field half that of the $\Delta M_s = \pm 1$ transitions. It is important to note that the half-field $\Delta M_s = \pm 2$ transition merely identifies the *presence* of a triplet state. It does not distinguish between a triplet ground state or a low lying excited triplet state.

One method used to determine the ground electronic state of a diradical is to perform a Curie plot. According to the Curie Law:

$$I = C[\text{triplet}]/T$$

the intensity I of the half-field signal is inversely proportional to the temperature T. C is the Curie constant. The concentration of the triplet state can also be expressed as:

$$[\text{triplet}] = 3[\exp(J/RT)]/(1+3[\exp(J/RT)])$$

where the triplet state is dependent on the temperature and the size of the singlet-triplet gap (J). When either the singlet or triplet state is only slightly favoured (|J| is small), there is curvature to the I versus T plot which permits the determination of J. In practice, however, curvature of the plot is negligible below 70 K and the plot is essentially linear.[72] When the triplet state is strongly favoured (J is large and positive), the triplet state concentration is essentially constant over the experimental temperature range and the Curie plot will be linear. In the case where the singlet state is strongly favoured (J is large and negative), detection of an EPR signal below 70 K may be difficult due to a low population of the triplet state. When the singlet and triplet states are degenerate (J = 0), the Curie plot is also linear. Therefore, a linear Curie plot has two possible interpretations ($J \gg 0$ and $J = 0$) with entirely different meanings and is not always informative. This technique is optimum when |J| is small compared to kT.

2.2.2 Magnetic Susceptibility

Magnetic susceptibility is another useful technique to study paramagnetic substances provided the radical is sufficiently stable in the solid state. For a given diradical, the magnetic susceptibility is given by the Bleany-Bowers equation:

$$\chi = 2N\beta^2g^2/kT[3 + \exp(-J/kT)]$$

where χ is the magnetic susceptibility, N is Avogadro's number, g is the electronic g-factor, β is the Bohr Magneton of the electron, k is the Boltzman constant, T is the temperature and J is the magnitude of the singlet-triplet energy gap. J not only provides a measure of the strength of the exchange interaction, but the sign of J is indicative of whether the singlet or the triplet is the ground state. Thus, when $J < 0$, the singlet is the ground state and when $J > 0$, the triplet is the ground state.

2.3 High Spin Diradicals

Conceptually, the design of a diradical has been viewed as two radicals centres bridged by a coupling unit (CU) as shown as **2.4** in Figure 2.7.[73] Thus, depending on the coupling unit, the diradical may be a singlet or a triplet. For example, both TMM and MQDM can be viewed as two methyl radicals attached to the same end of an ethylene molecule or attached meta on a benzene ring respectively. As discussed in Chapter 1, magnetism is one major motivation behind the synthesis of new diradical species. Thus, diradicals **2.4** are potential models for polymeric magnetic materials as shown as **2.4a**.

2.4

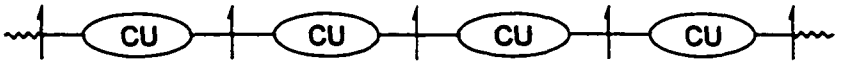

2.4a

Figure 2.7. Schematic representation of a generic diradical (**2.4**) and the corresponding polymer (**2.4a**).

However, for these hypothetical polymers to exhibit magnetic behaviour, the unpaired electrons must be ferromagnetically aligned. Therefore, the design of a diradical as outlined in Figure 2.7 is dependent on covalently attaching radicals to a coupling unit which will induce the unpaired electrons to align ferromagnetically.

Perhaps the best known ferromagnetic coupling unit (FCU) is *meta*-phenylene. It is not surprising then that many triplet state diradicals are based on the design of two radicals attached meta on a benzene ring.[74-78] Some examples are listed in Figure 2.8. All of these examples, however, are too reactive to have any practical use in materials.

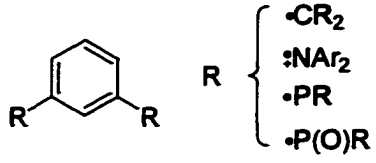

Figure 2.8. Examples of diradicals coupled by *meta*-phenylene.

Recent reports on the ground state of diradicals **2.5** and **2.6** provide exceptions to the general notion of *meta*-phenylene as a ferromagnetic coupling unit; both of these diradicals were found to be ground state singlets.[79,80] The reasons why radicals **2.5** and **2.6** are singlets are not known but it demonstrates that *meta*-phenylene is not a universal ferromagnetic coupling unit.

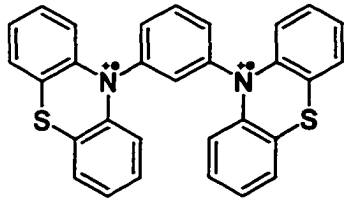

2.5

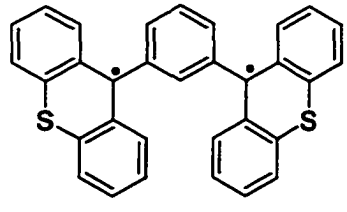

2.6

Nitroxide **2.7** is an example of a stable, triplet ground state diradical.[81] However, the triplet state of diradical **2.7** is only slightly favoured (~1 Kcal/mol) over the singlet state despite the use of the good high spin coupling unit *meta*-phenylene.

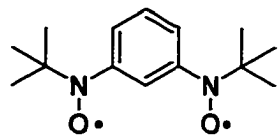

2.7

Rajca has proposed that for diradicals based on *meta*-phenylene, the magnitude of high-spin coupling between the unpaired electrons can be correlated with the strength of the hyperfine coupling to the aromatic protons in a model monoradical.[82] For example, shown in Figure 2.9 are diradicals **2.2** and **2.7** along with their corresponding monoradicals **2.2a** and **2.7a**. Monoradicals **2.2a** and **2.7a** are essentially diradicals **2.2** and **2.7** with one radical unit (CH_2• or *t*BuNO• respectively) replaced by a hydrogen atom. The hyperfine coupling values to the aromatic protons are given for the monoradicals. The relatively small hyperfine coupling values of nitroxide radical **2.7a** relative to those of benzyl radical **2.2a** correlates with relatively weak communication between the unpaired electrons of **2.7** (manifested as a small *J*).

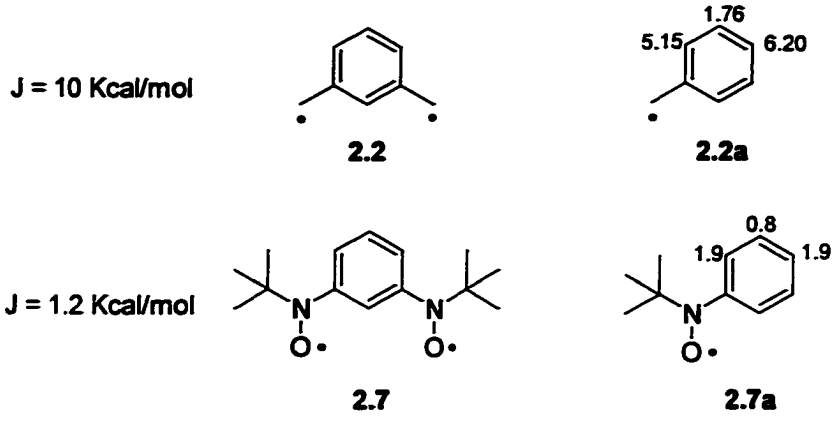

Figure 2.9. Proton hyperfine coupling values (Gauss) of model monoradicals of diradicals **2.2a** and **2.7a** and exchange coupling (J) for **2.2** and **2.7**.

Most known high-spin diradicals tend to fall in two categories: strongly coupled diradicals which are highly reactive species or stable diradicals which exhibit relatively weak interactions between the unpaired electrons. In the context of ferromagnetic building blocks, the ideal diradical would be stable and high-spin with a large J value. There is a family of radicals, the thioaminyl radicals, which meet these criteria. Thioaminyl radicals (for example **2.8**) are generally stable (see later) with some derivatives isolable as crystals.[83-86]

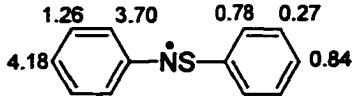

2.8

To make a thioaminyl diradical, a second radical centre could either be attached to the N-aryl or the S-aryl group of radical **2.8**. One example of a diradical linked at sulfur is known (**2.9**).[87] Unfortunately, the electronic ground state and the magnitude of J for diradical **2.9** is not known because these diradicals aggregate in solution. However, based on the relatively small proton hyperfine coupling values on the S-aryl ring of **2.8**,

this diradical is anticipated to have a relatively small J value. Conversely, the larger hyperfine values to the N-aryl group of **2.8** (comparable to that of benzyl radical **2.2a**) suggest that a more favourable approach would be to link two thioaminyl radicals to a ferromagnetic coupling unit at nitrogen. Therefore, putative diradical **2.10**, using Rajca's analysis, should be high-spin with a large J value and should also have good stability based on the known stability of thioaminyl radicals. The objective of this project is to synthesize and characterize stable, high-spin thioaminyl diradicals of general form **2.10**.

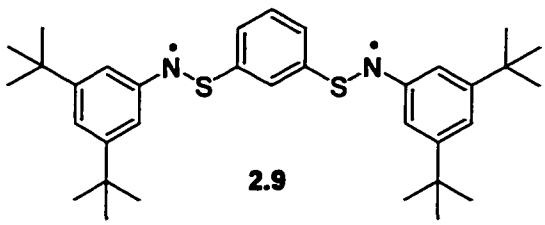

2.9

2.10

2.4 Thioaminyl Radicals

2.4.1 Synthesis

General synthetic routes to thioaminyl radicals have been established.[88-90] Two methods are outlined in Scheme 2.1. In both reactions, the key intermediate is sulfenamide **2.11**. In reaction A, the sulfenamide is prepared by the Ag^+ assisted reaction between an amine and a disulfide.[90,91] When aromatic disulfides are used, the sulfenamides are obtained in good yields (50-90%). The yields vary widely with alkyl disulfides (0-97%).

The more common method for the preparation of sulfenamides is the reaction of an amine with a sulfenyl chloride (reaction B). Typically, a sulfenyl chloride is added to two equivalents of an amine or to one equivalent of amine and an external base (Et_3N).

The yields of this reaction can vary widely depending on the starting sulfenyl chlorides.[84,89,92]

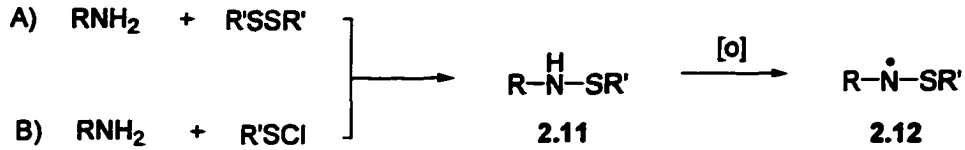

Scheme 2.1. General routes for the preparation of thioaminyl **2.12**.

The oxidation of sulfenamides **2.11** to thioaminyls **2.12** is generally performed by two methods: a) the photolysis of di-*t*-butylperoxide in degassed benzene in the presence of **2.11** and b) the oxidation of **2.11** in degassed benzene with PbO_2 and K_2CO_3.[43,89,92] The yields of the thioaminyls also vary widely depending on the substituents attached to the nitrogen and sulfur atoms.

2.4.2 Stability

The stability of the thioaminyl radicals is dependent on the substituents attached to the nitrogen and sulfur atoms. In general, alkyl substituted thioaminyl radicals are prone to dimerization. The exception is radical **2.13**. Thioaminyl **2.13** is exceptionally persistent in oxygen-free solvent and shows no tendency to dimerize, even at low temperatures.[93] In the presence of atmospheric oxygen, however, **2.13** rapidly decomposes.

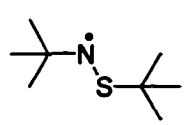

2.13

In contrast to the alkyl substituted thioaminyls, aryl substituted thioaminyl radicals are generally persistent, even in the presence of oxygen.[94-96] This added stability is attributed to the delocalization of the unpaired electron onto the aromatic ring.[89,93] Judicious substitution of the N-aryl group has led to the isolation of some stable thioaminyl radicals. For example, thioaminyls **2.14** were all isolated as radical crystals.[83,89,97] The large phenyl and *tert*-butyl groups protect the unpaired electron from hydrogen abstraction and dimerization.

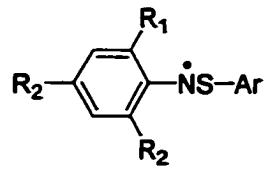

R_1 = Ph, *t*Bu, CN

R_2 = Ph, *t*Bu

2.14

In addition to the steric and aromatic delocalization factors, thioaminyl radicals are also stabilized by the conjugative delocalization of the unpaired electron from the nitrogen atom to the sulfur atom (Figure 2.10). This delocalization is also a stabilizing factor of other SN radicals discussed in Chapter 1.

Figure 2.10. Delocalization of the unpaired electron in SN radicals.

Although thioaminyl **2.14** are stable, isolable radicals, they immediately decompose in the presence of organic and inorganic acids. Therefore care must be taken to remove all traces of acids from the sulfenamide precursors and solvents.

The electronic nature of the substituents attached to the N-aryl and S-aryl groups also affect the general stability of the thioaminyls. Virtually all isolable thioaminyl radicals contain electron withdrawing groups attached to the S-aryl group. This

observation is explained on the basis that electron donating groups lead to the destabilization of the lone-pair rich sulfur-nitrogen bond.[89]

2.4.3 EPR Spectroscopy

Thioaminyl radicals typically give predominant three-line spectra with equal intensities of the three peaks. This is expected for an unpaired electron interacting with one nitrogen nucleus. For thioaminyl radicals, the a(N) values are found between 8.44-9.53 G. The peak widths are generally large due to numerous unresolved proton hyperfine splittings (a(H) < 1.5 G).

2.5 Results and Discussion

2.5.1 Attempted Synthesis of Thioaminyl Diradicals

Intermediate sulfenamides were prepared according to reaction B in Scheme 2.1. Our initial target was thioaminyl diradical **2.15**. Based on the known requirements for stability of thioaminyl monoradicals, we felt that the phenyl groups on the central benzene ring were needed in order to help stabilize the radical centres.

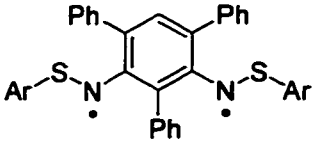

2.15

The synthesis of diradical **2.15** required 2,4,6-triphenyl-1,3-phenylenediamine **2.16**. Diamine **2.16** was prepared according to the literature.[98] The synthesis is outlined in Scheme 2.2.

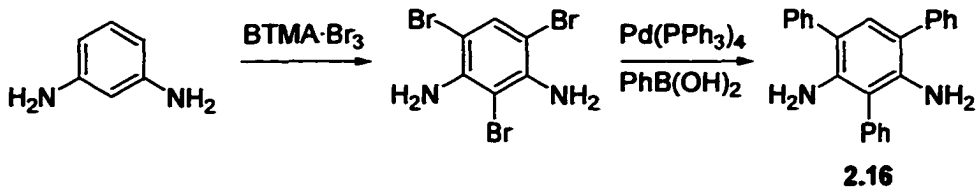

2.16

Scheme 2.2. Synthesis of 2,4,6-triphenyl-1,3-phenylenediamine **2.16**.

Unfortunately, reaction of diamine **2.16** with aromatic sulfenyl chlorides (2-$NO_2C_6H_4SCl$ and 4-$NO_2C_6H_4SCl$) failed to produce the corresponding bis(sulfenamides). In all reactions, a large number of products were observed by chromatography and ^1H NMR. Aromatic disulfides, from the reduction of the sulfenyl chlorides, were the only isolated and identified reaction products. It is possible diamine **2.16** was oxidized to a number of unidentifiable compounds.

In light of the difficulties using **2.16**, commercially available 2,4,6-trimethyl-1,3-phenylenediamine **2.17** was used. Under the standard conditions from the literature (ether, -42 °C, Et_3N), reaction of diamine **2.17** with 2-nitrobenzenesulfenyl chloride did not produce bis(sulfenamide) **2.18**. Typical products isolated were disulfide **2.19** and diamine **2.20**, both of which were identified by their ^1H NMR spectra. After numerous changes to the reaction conditions, we were finally able to prepare bis(sulfenamide) **2.18**. Thus, an acetonitrile solution of 2-nitrobenzenesulfenyl chloride was added to diamine **2.17** and 2,4,6-trimethylpyridine in acetonitrile at 0 °C (Scheme 2.3). The product precipitated as a yellow/orange solid in good yield (81 %). ^1H NMR spectroscopy revealed that the precipitated product was essentially pure. The two NH protons gave one sharp singlet at 4.8 ppm in the ^1H NMR spectrum and the expected aromatic resonances were also observed. The IR spectrum of **2.18** contained a strong peak at 3303 cm^{-1} due to the NH stretch.

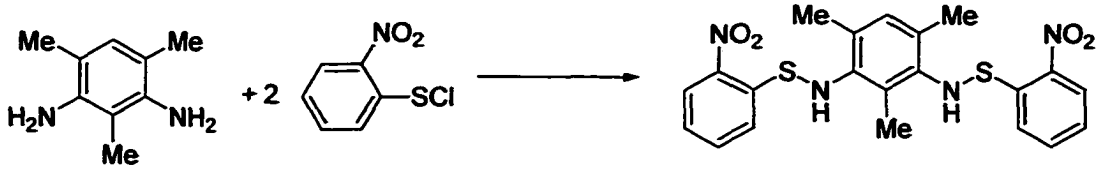

2.17 2.18

Scheme 2.3. Synthesis of bis(sulfenamide) **2.18**.

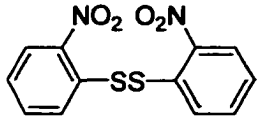

2.19

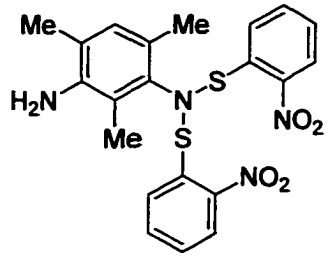

2.20

Crystals of **2.18** were studied by X-ray crystallography by Dr. Tosha M. Barclay, University of Mississippi. The crystal structure of bis(sulfenamide) **2.18** is presented in Figure 2.11 and a partial list of bond angles and bond lengths are presented in Table 2.1. The molecule resides on a mirror plane rendering both halves of the molecule crystallographically equivalent. The torsion angle between the two substituents about the N-S bond is 130.5°. The S–aryl rings form a dihedral angle of 163.7° with the central aromatic ring.

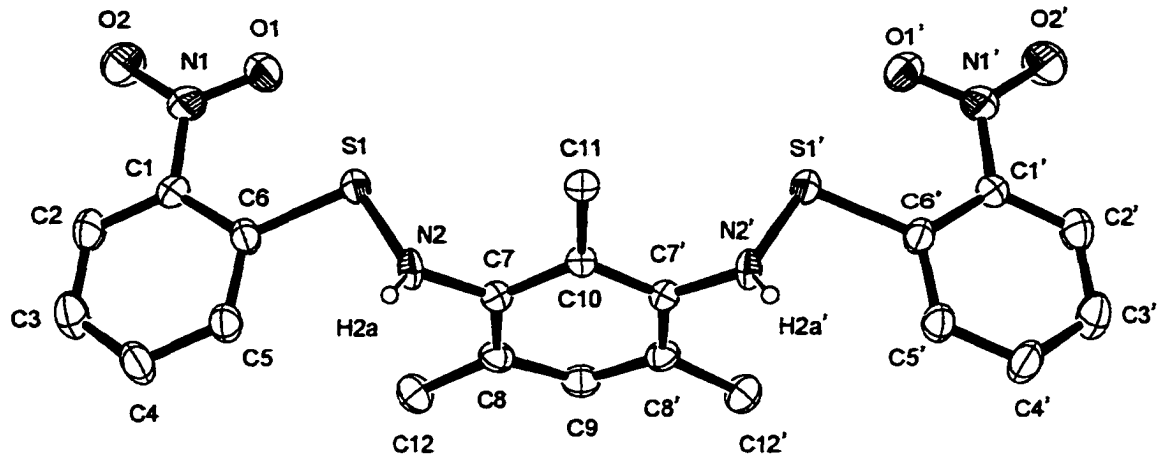

Figure 2.11. X-ray crystal structure of bis(sulfenamide) **2.18**. Hydrogen atoms removed for clarity.

Table 2.1. Selected bond lengths (Å) and bond angles (°) for bis(sulfenamide) **2.18**.

Atoms	Distance	Atoms	Distance
S(1)-N(2)	1.683(4)	N(2)-C(7)	1.439(5)
S(1)-C(6)	1.772(4)	C(8)-C(12)	1.502(6)
N(1)-C(1)	1.429(6)	C(10)-C(11)	1.490(8)

Atoms	Angle	Atom	Angle
N(2)-S(1)-C(6)	101.2(2)	C(5)-C(6)-S(1)	121.3(3)
O(1)-N(1)-O(2)	121.8(5)	C(1)-C(6)-S(1)	122.2(3)
O(1)-N(1)-C(1)	118.8(4)	C(8)-C(7)-C(10)	121.7(4)
O(2)-N(1)-C(1)	119.5(4)	C(8)-C(7)-N(2)	119.1(4)
C(7)-N(2)-S(1)	117.3(3)	C(10)-C(7)-N(2)	119.1(4)
C(2)-C(1)-C(6)	121.8(5)	C(9)-C(8)-C(7)	117.6(4)
C(2)-C(1)-N(1)	117.6(4)	C(9)-C(8)-C(12)	119.6(5)
C(6)-C(1)-N(1)	120.5(4)	C(7)-C(8)-C(12)	122.8(4)
C(5)-C(6)-C(1)	116.5(4)	C(7)-C(10)-C(11)	121.3(3)

It was unclear whether the mesityl group would provide enough stability for the radical centres of **2.18** but we anticipated that it would provide enough stability to acquire an EPR spectrum. The results, however, were unexpected and surprising. Bis(sulfenamide) **2.18** was resistant to all attempts at oxidation. PbO_2, chloranil, and DDQ were all ineffective. At this time, it is still unclear why **2.18** is so resistant to oxidation.

2.5.2 Synthesis of Thioaminyl Radicals

With the inability to oxidize **2.18**, we decided to prepare derivatives of the mono(sulfenamides) and examine their oxidation reactions in the hopes that these derivatives may shed some light on the inability to oxidize bis(sulfenamide) **2.18**.

The sulfenamides were all prepared according to reaction B from Scheme 2.1. The aromatic amines as well as 2- and 4-nitrobenzenesulfenyl chlorides were all commercially available. MesSCl (**2.21a**) and Mes*SCl (**2.21b**) were prepared from the corresponding thiols (**2.22a-b**). The thiols were prepared according to literature procedures.[99,100] Thus, a thiol solution was added to a solution of NCS in CH_2Cl_2 (Scheme 2.4). This reaction is essentially quantitative and the sulfenyl chlorides were used without purification.

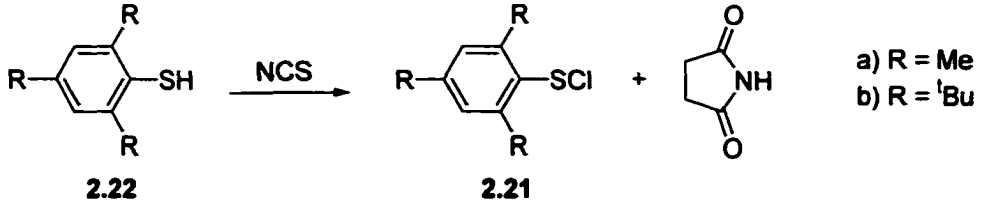

2.22 **2.21**

Scheme 2.4. Preparation of sulfenyl chlorides **2.21a-b**.

Thus, for sulfenamides **2.23**, an ether solution of the sulfenyl chloride was added dropwise to a cold ether solution of an aromatic amine and an external base. The crude residues were chromatographed to give the corresponding sulfenamides. Listed in Table 2.2 are the reagents and yields for the sulfenamide derivatives prepared.

Table 2.2. Reagents and yields for the synthesis of sulfenamides **2.23a-f**.

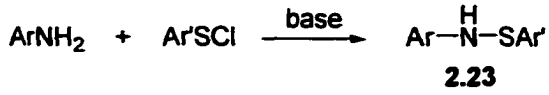

2.23

Compound	Ar[a]	Ar'[b]	Base	Yield (%)
2.23a	Mes	4-$NO_2C_6H_4$	Et_3N	35[c]
2.23b	Mes	2-$NO_2C_6H_4$	2,4,6-trimethyl-pyridine	78[c]
2.23c	2,4,6-trichloro-aniline	2-$NO_2C_6H_4$	2,4,6-trimethyl-pyridine	51
2.23d	4-MeC_6H_4	Mes*	toluidine	32[c]
2.23e	Mes	Mes*	2,4,6-trimethyl-aniline	10
2.23f	Mes	Mes	2,4,6-trimethyl-aniline	25

[a]Mes = 2,4,6-trimethylphenyl. [b]Mes* = 2,4,6-tri-*tert*-butylphenyl. [c]Yields based on recrystallized products.

In addition to the aromatic protons, the ^1H NMR spectra of the sulfenamides are characterized by a diagnostic NH resonance. These peaks are typically sharp and appear in the 3.5-5.5 ppm range. The sulfenamides are also typified by an NH stretch in the IR spectra between 3300-3400 cm^{-1}. Mass spectrometry and/or elemental analysis were consistent for the proposed structures of sulfenamides **2.23a-f**.

The oxidation of sulfenamides **2.23a-f** using literature procedures (PbO_2, AgO) did not produce the corresponding thioaminyl radicals. Alternatively, oxidation with DDQ produced intensely coloured solutions which decomposed within minutes back to the corresponding sulfenamide and other unidentifiable products. It appears that substituents smaller than a phenyl group do not provide enough steric protection for the radical.

2.6 Conclusions

We were successful in preparing bis(sulfenamide) **2.18**. The synthesis is sensitive to the nature of the solvent and base used. The dependence on the external base was also observed for some of the mono(sulfenamides) **2.23**. Oxidation of **2.18** with homogeneous and heterogeneous oxidants was unsuccessful. The oxidation of sulfenamides **2.23** was performed using DDQ, however, the radicals quickly decomposed back to the sulfenamides. It is clear that the Mes group attached to the nitrogen atom is not sterically large enough to protect the radical centre. For reasons unknown, bis(sulfenamide) **2.18** cannot be oxidized to the thioaminyl diradical. Therefore, we were unfortunately not able to test our hypothesis that thioaminyl diradicals of the form **2.10** should be strongly coupled, high-spin molecules.

2.7 Experimental

General Experimental.

Unless otherwise indicated, all reactions were carried out under an Argon atmosphere using standard Schlenk techniques. Glassware was oven dried at 125 °C for

24 h prior to each reaction. THF and diethylether were distilled from Na/benzophenone before each use. Toluene, benzene, hexanes, methylene chloride, acetonitrile, and triethylamine were distilled from CaH_2 before each use. All reagents were used as received, with the following exception: benzoquinone was recrystallized from 100% ethanol.

All ^{1}H and ^{13}C NMR spectra were recorded on a Bruker AC300 instrument (300 MHz for ^{1}H, 75.47 MHz for ^{13}C), unless otherwise noted. ^{31}P NMR spectra were recorded on a Bruker AMX360 instrument (145.78 MHz). ^{1}H and ^{13}C NMR spectra were referenced to the central solvent line, relative to tetramethylsilane. ^{31}P NMR spectra are proton decoupled and are referenced relative to 85% H_3PO_4. UV-vis spectra were recorded on a Varian Cary 5 instrument. Elemental analyses were performed by Canadian Microanalytical Services, New Westminister, B.C. EPR spectra were carried out on a Bruker EMX instrument at 9.51 GHz. IR spectra were recorded on a Perkin Elmer Spectrum One FT-IR spectrometer. Mass spectra were recorded on a Finnigan 3300 or a Kratos Concept H spectrometer using chemical ionization or electron impact (70 eV) sources. Melting points were taken on a Gallenkamp melting point apparatus and are uncorrected.

Attempted Synthesis of Bis(sulfenamide) 2.15 (Ar = 4-NO_2-C_6H_4)

2,4,6-Triphenyl-1,3-phenylenediamine **2.16** (0.126 g, 0.375 mmol) and 2,4,6-trimethylpyridine (0.224 mL, 1.69 mmol) were dissolved in 8 mL acetonitrile and cooled to 0 °C. A solution of 4-nitrobenzenesulfenyl chloride (0.160 g, 0.844 mmol) in 8 mL acetonitrile was cooled to 0 °C was slowly added over a 5 min period. After the addition

was complete, the reaction mixture turned a dark brown. After stirring for 16 h, the solution was concentrated to a brown solid. ^{1}H NMR of the crude solid revealed the solid consisted mostly of bis(4-nitrophenyl) disulfide.

Synthesis of *N,N'*-Bis[(2-nitrophenyl)thio]-2,4,6-trimethyl-1,3-phenylenediamine (2.18)

2,4,6-Trimethyl-1,3-phenylenediamine **2.17** (0.125 g, 0.832 mmol) and 2,4,6-trimethylpyridine (0.448 mL, 3.39 mmol) were dissolved in 8 mL acetonitrile and cooled to 0 °C. A solution of 2-nitrobenzenesulfenyl chloride (0.319 g, 1.682 mmol) in 8 mL acetonitrile cooled to 0 °C was slowly added via syringe over a five minute period. An orange precipitate immediately formed. After stirring for 1.5 h, the yellow/orange precipitate was filtered and dried *in vacuo*. The product was recrystallized from acetonitrile to give yellow crystals, yield 310 mg (81.7 %). ^{1}H (CD_2Cl_2): δ 8.40 (dd, 2H, J = 8.1 Hz, 1.5 Hz), 8.30 (dd, 2H, J = 8.1 Hz, 1.5 Hz), 7.73 (dt, 2H, J = 7.7 Hz, 1.5 Hz), 7.32 (dt, 2H, J = 8.6 Hz, 1.5 Hz), 6.88 (s, 1H), 4.80 (s, 2H), 2.26 (s, 6H), 2.16 ppm (s, 3H). ^{13}C ($CDCl_3$): δ 144.6, 142.0, 141.4, 133.9, 130.7, 127.4, 125.7, 125.0, 124.7, 18.3, 13.8 ppm. IR (KBr): 3303 (s), 1593 (s), 1566 (s), 1513 (s), 1462 (s), 1447 (s), 1377 (s), 1334 (s), 1302 (s), 1237 (s), 1173 (w), 1153 (w), 1099 (s), 1055 (m), 1039 (m), 1013 (w), 973 (w), 901 (w), 851 (s), 791 (s), 735 (s), 684 (w), 657 (w) cm^{-1}. Mp: 210-212 °C Anal. Calcd for $C_{21}H_{20}N_4O_4S_2$: C, 55.25; H, 4.42; N, 12.27; S, 14.05. Found: C, 55.34; H, 4.64; N, 12.17; S, 15.68.

Attempted synthesis of *N,N'*-Bis[(2-nitrophenyl)thio]-2,4,6-trimethyl-1,3-phenylenediamine (2.18)

2,4,6-Trimethyl-1,3-phenylenediamine **2.17** (0.301 g, 2.00 mmol) and Et_3N (0.65 mL, 4.68 mmol) were dissolved in 30 mL ether and cooled to -42 °C. A solution of 2-nitrobenzenesulfenyl chloride (0.799 g, 4.21 mmol) in 20 mL ether cooled to 0 °C was slowly added dropwise. After 1 h, the red solution was gravity filtered and the filtrate concentrated to a red semi-solid. The crude product was passed through an alumina column (benzene) which yielded a red oil. The product was crystallized from hexane/benzene (1:6) to give orange crystals. ^{1}H NMR confirmed that the product isolated was compound **2.20** and not bis(sulfenamide) **2.18**. ^{1}H ($CDCl_3$): δ 8.24 (d, 2H, J = 8.1 Hz), 7.83 (d, 2H, J = 8.1 Hz), 7.53 (t, 2H, J = 7.7 Hz), 7.29 (t, 2H, J = 7.7 Hz), 6.81 (s, 1H), 3.55 (s, 2H), 2.48 (s, 3H), 2.39 (s, 3H), 2.12 ppm (s, 3H).

Synthesis of 2,4,6-Tri-*tert*-butylbenzenesulfenyl chloride (2.21b)

A solution of NCS (0.483 g, 3.61 mmol) in 20 mL CH_2Cl_2 was added dropwise to a solution of 2,4,6-tri-*tert*-butylbenzenethiol **2.22b**[100] (1.002 g, 3.60 mmol) in 20 mL CH_2Cl_2 over 40 min. The solution was allowed to stir for 16 h. The orange solution was concentrated under vacuum to give an orange solid. The solid was redissolved in hexane and the white precipitate was filtered. The orange solution was concentrated to an orange solid. The product was used without further purification. ^{1}H NMR ($CDCl_3$): δ 7.42 (s, 2H), 1.61 (s, 18H), 1.22 ppm (s, 9H).

Synthesis of *N*-[(4-Nitrophenyl)thio]-2,4,6-trimethylphenylaniline (2.23a)

2,4,6-Trimethylaniline (0.685g, 5.06 mmol) and triethylamine (1.38 mL, 9.88 mmol) were dissolved in 30mL of ether and cooled to 0 °C. A solution of 4-

nitrobenzenesulfenyl chloride (1.005 g, 5.30 mmol) in 20mL ether was added dropwise over a ten minute period. A yellow precipitate quickly formed. After stirring for 2h, the green solution was filtered *in vacuo* and the filtrate concentrated *in vacuo* to give an orange solid. Recrystallization from hexanes afforded as small yellow prisms, yield 508 mg (34.7%). ^{1}H NMR ($CDCl_3$): δ 8.18 (d, 2H, J = 8.8 Hz), 7.52 (d, 2H, J = 8.8 Hz), 6.83 (s, 2H), 4.82 (s, 1H), 2.22 ppm (s, 9H). ^{13}C NMR ($CDCl_3$): δ 152.3, 145.3, 140.2, 134.1, 131.3, 129.8, 123.9, 122.5, 20.6, 18.7 ppm. IR (KBr): 3344 (m), 1594 (w), 1577 (s), 1510 (s), 1479 (m), 1336 (s), 1213 (m), 1110 (w), 1083 (m), 851 (s), 742 (s), 683 (w) cm^{-1}. Mp: 87-89 °C Anal. Calcd for $C_{15}H_{16}N_2O_2S$: C, 62.47; H, 5.59; N, 9.71. Found: C, 62.45, 5.61, 9.67.

Synthesis of *N*-[(2-Nitrophenyl)thio]-2,4,6-trimethylaniline (2.23b)

2,4,6-Trimethylaniline (0.499g, 3.69 mmol) and 2,4,6-trimethylpyridine (0.998 mL, 7.56 mmol) were dissolved in 40mL of ether in a 100mL flask and cooled to 0 °C. A solution of 2-nitrobenzenesulfenyl chloride (0.702 g, 3.70 mmol) in 20mL ether was added dropwise over a fifteen minute period. The solution quickly turned orange and a yellow precipitate formed. After stirring for 1h, the orange solution was filtered *in vacuo*, the precipitate washed with 2x 5mL ether and the orange/red filtrate concentrated *in vacuo* to yield an orange oil. The crude oil was purified by chromatography on alumina (benzene) to give the product as an orange solid. Recrystallization from hexanes afforded the product as red crystals, yield 832 mg (78%). ^{1}H NMR (CD_2Cl_2): δ 8.42 (dd, 1H, J = 8.1 Hz, 1.5 Hz), 8.31 (dd, 1H, J = 8.1 Hz, 1.5 Hz), 7.74 (dt, 1H, J = 7.7 Hz, 1.5 Hz), 7.33 (t, 1H, J = 7.7 Hz), 6.84 (s, 2H), 4.76 (s, 1H), 2.25 (s, 6H), 2.23 ppm (s, 3H).

^{13}C NMR ($CDCl_3$): δ 145.1, 142.0, 139.8, 133.8, 133.5, 131.1, 129.8, 125.6, 125.0, 124.6, 20.6, 18.6 ppm. IR (KBr): 3344 (m), 1593 (s), 1564 (s), 1508 (s), 1480 (s), 1446 (m), 1333 (s), 1304 (s), 1249 (w), 1214 (s), 1152 (m), 1097 (m), 1057 (w), 1038 (m), 851 (s), 786 (m), 734 (s) cm^{-1}. Mp: 111-113 °C. Anal. Calcd for $C_{15}H_{16}N_2O_2S$: C, 62.47; H, 5.59; N, 9.71. Found: C, 62.73; H, 5.65; N, 9.68.

Synthesis of *N*-[(2-Nitrophenyl)thio]-2,4,6-trichloroaniline (2.23c)

A solution of 2-nitrobenzenesulfenyl chloride (0.996 g, 5.25 mmol) in 15 mL ether was added dropwise to a solution of 2,4,6-trichloroaniline (1.008 g, 5.12 mmol) and 2,4,6-trimethylpyridine (0.7 mL, 5.30 mmol) in 30 mL ether at 0° C. The solution was stirred for 16 h after which the solution was gravity filtered and the filtrate concentrated in vacuo to an orange solid, yield 916 mg (51.0%). The crude product was chromatographed on silica gel (hexanes/CH_2Cl_2) to give the product as a yellow solid. The product was recrystallized from 100% ethanol to give yellow flakes. ^1H NMR ($CDCl_3$): δ 8.30-8.25 (m, 2H), 7.71-7.66 (m, 1H), 7.34-7.29 (m, 3H), 5.53 ppm (s, 1H). ^{13}C NMR ($CDCl_3$): δ 143.8, 142.1, 138.7, 133.9, 128.9, 128.7, 128.5, 125.6, 125.4, 125.2 ppm. IR (KBr): 3327 (m), 3099 (w), 3071 (w), 1595 (m), 1566 (m), 1554 (m), 1504 (s), 1442 (s), 1415 (s), 1369 (m), 1359 (m), 1335 (m), 1309 (s), 1261 (m), 1237 (w), 1189 (w), 1172 (w), 1155 (w), 1140 (w), 1124 (w), 1106 (w), 1059 (w), 1041 (w), 887 (w), 864 (w), 850 (m), 795 (w), 785 (w), 736 (s), 717 (w), 706 (w), 661 (w), 596 (w), 565 (w), 546 (w), 490(w) cm^{-1}. Mp: 127-129 °C (dec). Anal. Calcd for $C_{12}H_7Cl_3N_2O_2S$: C, 41.23; H, 2.02; N, 8.01. Found: C, 41.04; H, 2.05; N, 8.09. MS (FAB, *m*NBA): m/z 349 (M + 1).

Synthesis of *N*-[(2,4,6-Tri-*tert*-butylphenyl)thio]-4-methylaniline (2.23d)

A solution of **2.21b** (1.13 g, 3.6 mmol) in 30 mL ether was added dropwise to a solution of p-toluidine (0.782 g, 7.3 mmol) in 40 mL ether at 0° C. A white precipitate quickly formed in the brown solution. The reaction mixture was stirred for 16 h after which the toluidine hydrochloride salt was filtered. The filtrate was concentrated in vacuo to give a green solid. The solid residue was recrystallized from 100% ethanol to give the product as amber blocks, yield 886 mg (31.6 %). ^{1}H NMR ($CDCl_3$): δ 7.37 (s, 2H), 6.90 (d, 2H, J = 8.1 Hz), 6.62 (d, 2H, J = 8.1 Hz), 4.28 (s, 1H), 2.21 (s, 3H), 1.52 (s, 18H), 1.30 ppm (s, 9H). ^{13}C NMR ($CDCl_3$): δ 155.1, 150.9, 144.1, 133.9, 130.4, 129.2, 122.9, 119.1, 38.3, 35.1, 33.1, 31.3, 20.6 ppm. IR (KBr): 3344 (m), 2957 (s), 2911 (m), 2866 (m), 1612 (m), 1592 (m), 1551 (w), 1537 (w), 1508 (s), 1476 (w), 1463 (w), 1426 (w), 1409 (w), 1391 (m), 1359 (m), 1278 (m), 1258 (w), 1242 (w), 1227 (m), 1214 (m), 1176 (w), 1133 (w), 1114 (w), 904 (w), 880 (m), 870 (m), 813 (m), 763 (w), 654 (w), 638 (w), 497 (m) cm^{-1}. Mp 98-100° C. Anal. Calcd for $C_{25}H_{37}NS$: C, 78.27; H, 9.72; N, 3.65. Found: C, 77.89; H, 9.44; N, 3.55. MS (CI methane): m/z 384 (M + 1, 100%), 412 (M + 29, 14 %), 424 (M + 41, 1%).

Synthesis of *N*-[(2,4,6-Tri-*tert*-butylphenyl)thio]-2,4,6-trimethylaniline (2.23e)

A solution of **2.21b** (0.407 g, 1.30 mmol) in 7.5 mL ether was added dropwise to a solution 2,4,6-trimethylaniline (0.354 g, 2.62 mmol) in 7 mL ether. A yellow precipitate quickly formed. The reaction was stirred for 16 h after which the solution was gravity filtered and the filtrate concentrated in vacuo to a yellow semi-solid. The solid residue was chromatographed on basic alumina (activity III, hexanes) to give the product

as white flakes, yield 110 mg (10.2%). ^{1}H NMR ($CDCl_3$): δ 7.30 (s, 2H), 6.62 (s, 2H), 3.55 (s, 1H), 2.15 (s, 3H), 1.66 (br s, 6H), 1.36 (s, 18H), 1.30 ppm (s, 9H). ^{13}C NMR ($CDCl_3$): δ 155.7, 151.2, 141.3, 136.3, 133.3, 133.0, 128.6, 122.5, 38.0, 35.1, 33.2, 31.4, 20.7, 17.6 ppm. IR (KBr): 3373 (m), 2957 (s), 2911 (m), 2866 (m), 1589 (m), 1546 (w), 1529 (w), 1479 (m), 1462 (m), 1406 (w), 1391 (w), 1377 (w), 1361 (m), 1255 (w), 1244 (w), 1218 (m), 1154 (w), 1134 (w), 1038 (w), 1011 (w), 924 (w), 906 (w), 878 (w), 853 (m), 759 (m), 653 (w), 605 (w), 587 (w), 577 (w), 566 (w), 513 (w), 490 (w), 472 (w) cm^{-1}. Mp: 118-119° C. Anal. Calcd for $C_{27}H_{41}NS$: C, 78.77; H, 10.04; N, 3.40. Found: C, 78.58; H, 10.13; N, 3.46. MS (CI, methane): m/z 412 (M + 1, 100%), 440 (M + 29, 6%), 452 (M + 41, 1%).

Synthesis of *N*-[(2,4,6-Trimethylphenyl)thio]-2,4,6-trimethylaniline (2.23f)

A solution of **2.21a** (369 mg, 1.98 mmol) in 7 mL ether was added dropwise to a solution of 2,4,6-trimethylaniline (544 mg, 4.0 mmol) in 10 mL ether at 0 °C. A yellow precipitate quickly formed. The reaction was stirred for 16 h after which the solution was filtered and the brown filtrate was concentrated in vacuo to a brown solid. The solid residue was chromatographed on basic alumina (activity III, hexanes) to give the product as a pale yellow solid, yield 141 mg (25%). ^{1}H NMR ($CDCl_3$): δ 6.82 (s, 2H), 6.69 (s, 2H), 4.40 (s, 1H), 2.30 (s, 6H), 2.23 (s, 3H), 2.19 (s, 3H), 2.02 ppm (s, 6H). ^{13}C NMR ($CDCl_3$): δ 143.2, 141.9, 139.9, 133.6, 133.1, 131.8, 129.0, 128.8, 21.4, 21.1, 20.7, 17.8, ppm. IR (KBr): 3344 (m), 3008 (m), 2974 (m), 2945 (m), 2911 (m), 2848 (m), 2729 (w), 1599 (m), 1480 (s), 1460 (m), 1434 (m), 1373 (m), 1297 (w), 1268 (w), 1246 (w), 1217 (s), 1150 (w), 1031 (w), 1011 (w), 959 (w), 936 (w), 849 (w), 777 (w), 726 (w), 715 (w),

626 (w), 590 (w), 578 (w), 554 (m), 537 (w), 498 (w), 473 (w) cm^{-1}. Mp: 78-79° C. Anal. Calcd for $C_{18}H_{23}NS$: C, 75.74; H, 8.12; N, 4.91. Found: C, 75.67; H, 8.38; N, 4.74. MS (CI, methane): m/z 286 (M + 1, 100%).

Attempted oxidation of bis(sulfenamide) 2.18 and sulfenamides 2.23

A mixture of bis(sulfenamide) (100 mg)/sulfenamide (200 mg) and K_2CO_3 (1.0 g) in 20 mL benzene was stirred for 1 min. To this solution was added 0.8-1.0 g of PbO_2 and the resulting solution was stirred for an additional 5 min. No colour changes were observed.

Attempted Oxidation of 2.18 with DDQ

A solution of **2.18** (50 mg, 0.109 mmol) and K_2CO_3 (100 mg) in 20 mL benzene was stirred for 1 min. To this yellow solution was added DDQ (12 mg, 0.055 mmol) and the resulting solution was stirred for an additional 5 min. No colour change was observed.

Oxidation of sulfenamides 2.23 with DDQ

A mixture of sulfenamide (50 mg) and K_2CO_3 in 15 mL benzene was stirred for 1 min. To this yellow solution was added DDQ (20 mg). The solution quickly turned an intense green. Within minutes, the colour quickly began to fade. After 5 min the solution had faded to a yellow colour. The yellow solution was concentrated to a yellow solid. ^1H NMR analysis of the solid confirmed it as the starting sulfenamide.

Chapter 3

Phosphaverdazyl Radicals

3.1 Introduction

Verdazyls are a class of stable organic radicals that were discovered in the early 1960s. These initial derivatives (**3.1**) consist of 6-membered heterocyclic rings comprising four nitrogens, an sp^2-hybridized carbon in the 3 position, and an sp^3 carbon in the 6 position. Approximately 20 years later verdazyls with a slightly different structure (**3.2**) were discovered – the main difference being that position 6 is either a carbonyl group (**3.2a**) or a thiocarbonyl group (**3.2b**).

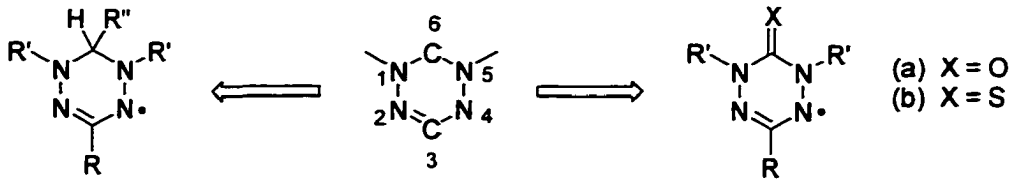

3.1 **3.2**

These radicals display excellent stability and many derivatives have been isolated in pure state. Yet, in spite of these properties, most research into verdazyls has been confined to their synthesis and basic characterization. Various groups have studied the effects on the verdazyl properties by changing the R and R' substituents, but little work has focused on any fundamental changes to the verdazyl skeletal core. This chapter describes the synthesis and characterization of phosphorus-based heteroverdazyls - the 'phosphaverdazyls' - and discusses the physical and electronic properties of these new radicals.

3.2 Verdazyl Radicals

3.2.1 Synthesis

In 1963, Kuhn and Trischmann fortuitously discovered the first examples of verdazyl radicals (**3.3a-c**) while attempting to alkylate formazans.[44] These radicals were isolated in the solid state.

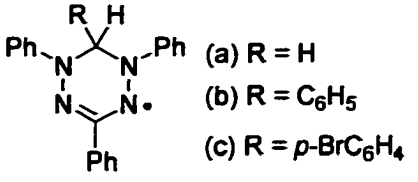

3.3

1,3,5-Triphenylformazan **3.4** was alkylated with methyl iodide (or dimethylsulfate) to give N-alkylformazan **3.5**, which cyclized to the corresponding tetrazine **3.6**. Atmospheric oxygen dehydrogenated the tetrazine to yield triphenylverdazyl **3.3a** (Scheme 3.1).

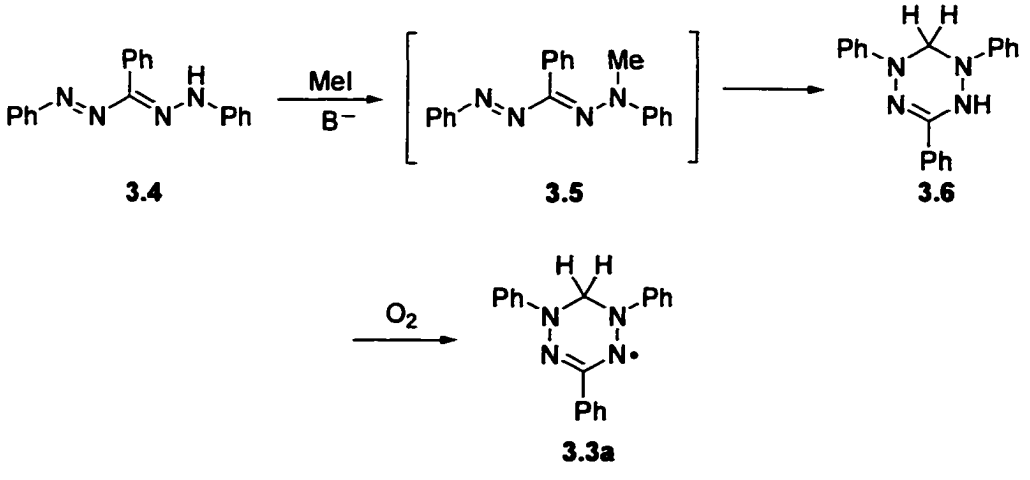

3.4 **3.5** **3.6**

3.3a

Scheme 3.1. Synthesis of verdazyl **3.3a**.

This synthetic methodology has proven to be general and has been used to prepare a wide range of verdazyls of general structure **3.1** (R' = substituted aromatic). This

methodology has also been used to prepare biverdazyls **3.7** and triverdazyl **3.8** using the appropriate bis- or tris-formazans.[101,102]

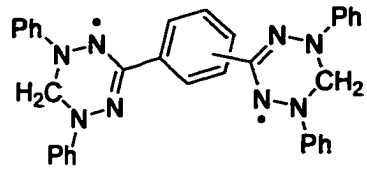

3.7 (a) = meta (b) = para

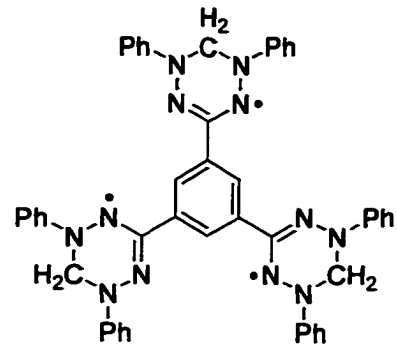

3.8

Typical yields of the reaction depicted in Scheme 3.1 are variable and often low (< 20%). Katritzky *et al.*[103] have improved on this synthetic method and made a series of 6-(*n*-alkyl)verdazyls **3.9** in improved yields (58-77%). The use of a crown ether (DC18C6) as a solid-liquid phase-transfer catalyst allowed them to use less reactive alkyl bromides in a 1:1 molar ratio with the starting formazan (Scheme 3.2). Using a similar methodology, they also prepared a series of new 6-*N*,*N*-dialkylaminoverdazyls (**3.10**) in moderate yields (43-69%).

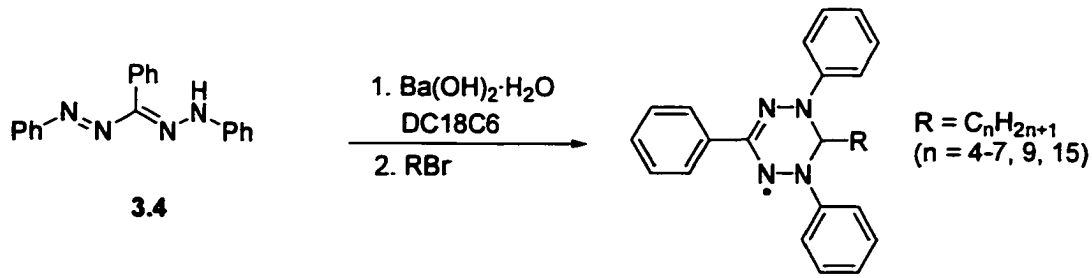

3.4 **3.9**

Scheme 3.2. Synthesis of 6-(n-alkyl)verdazyls **3.9** from formazan **3.4**.

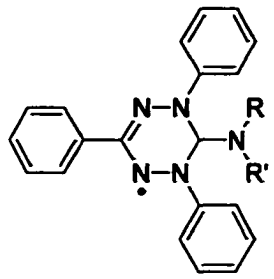

3.10

In 1980, Neugebauer *et al.* reported the first synthesis of the 6-oxoverdazyls and 6-thioxoverdazyls **3.11**.[45] The synthetic approach to these radicals differs from that of radicals **3.3**. Reaction of 2,4-dimethylcarbohydrazide or 2,4-dimethylthiocarbohydrazide (**3.12a** or **3.12b**) with aldehydes yields tetrazanes **3.13**. Subsequent dehydrogenation (Ag_2O, $K_3Fe(CN)_6$ or PbO_2) gives 6-oxoverdazyls **3.11** (Scheme 3.3). These 6-oxoverdazyls are isolable in the crystalline state as pure monomeric radicals.

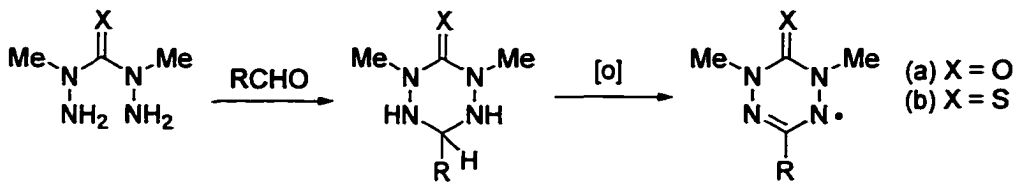

3.12 **3.13** **3.11**

Scheme 3.3. Synthesis of 6-Oxo and 6-Thioxoverdazyls.

The synthetic methodology of Scheme 3.3 has been applied to many derivatives of **3.2a** (R' = CH_3, CH_2Ph; R = H, alkyl, aryl) as well as verdazyl diradicals such as **3.14**.[45]

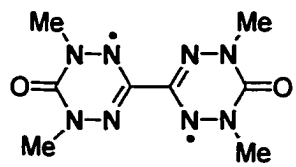

3.14

The key intermediate for the synthesis of the 6-oxoverdazyls is bis(hydrazide) **3.12**. The synthesis of this reagent was first reported by Raphaelian *et al.* (Scheme 3.4).[104] Initially,

it was believed that protection of methylhydrazine was necessary to ensure that the substituted nitrogen would attack phosgene. This was accomplished with benzaldehyde to form hydrazone **3.15**, which was subsequently treated with phosgene to give Schiff base **3.16**. Deprotection of **3.16** with aqueous acid afforded **3.12a**.

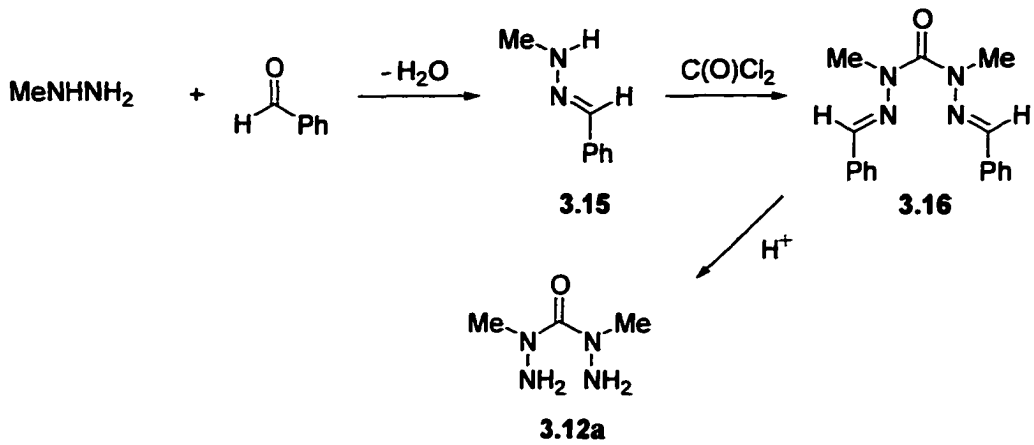

Scheme 3.4. Initial synthesis of bis(hydrazide) **3.12a**.

Neugebauer later found that the protection/deprotection sequence was unnecessary if the phosgene/methylhydrazine reaction was carried out at low temperature.[105] Thus, a solution of phosgene or thiophosgene was slowly added to a cold solution of the appropriate alkylhydrazine to yield bis(hydrazide) **3.12** and hydrazine hydrochloride salt as a byproduct (Scheme 3.5).

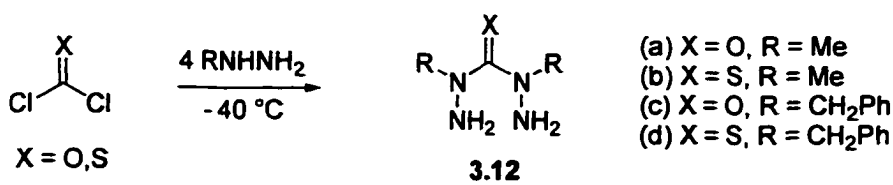

Scheme 3.5. Synthesis bis(hydrazides) **3.12**.

Up to this point, all bis(hydrazides) made were limited to derivatives with N-alkyl substituents. In 1993, Neugebauer devised a synthetic methodology for the 6-oxo and 6-

thioxoverdazyls which incorporated aromatic groups in positions 1 and 5.[106] Phosgene or thiophosgene was carefully reacted with hydrazones **3.17** to give carbamoyl chlorides **3.18**. Reaction of **3.18** with arylhydrazines gave saturated tetrazanes **3.19**. The tetrazanes were then oxidized to give the verdazyls **3.20** (Scheme 3.6).

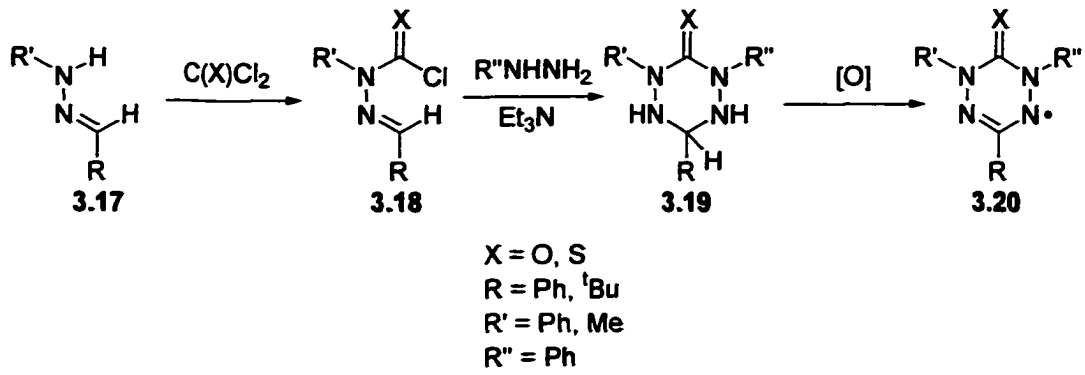

Scheme 3.6. Alternative synthesis of 6-oxo and 6-thioxoverdazyls.

3.2.2 EPR Spectra

The EPR spectra of verdazyls **3.1** typically consist of nine broad lines. This is consistent with the unpaired electron interacting with four nearly equivalent nitrogen atoms. Hyperfine coupling to all nitrogen atoms ($a(^{14}N)$) falls between 5-6 Gauss; coupling to the two-coordinate nitrogens is slightly higher than that of the three-coordinate nitrogens.[107] The broad nature of the lines arises from many small couplings (<<1 G) to aromatic protons. From this EPR data the verdazyl radical can be represented as four resonance forms shown in Scheme 3.7.

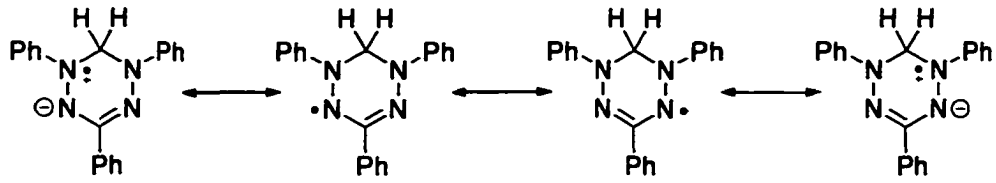

Scheme 3.7. The four canonical forms of verdazyls.

The resonance structures parallel the results of simple molecular orbital calculations.[108] The Singly Occupied Molecular Orbital (SOMO) shown in Figure 3.1 shows that the electron density resides primarily on the four nitrogens in a delocalized orbital of π symmetry.

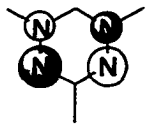

Figure 3.1. The π SOMO of verdazyl **3.3a**.

In the case of *N,N'*-dimethyl-6-oxo and 6-thioxoverdazyls **3.11**, the EPR spectra are more complicated than those of radicals **3.3a**. The typical broad nine line pattern is split by an additional six methyl protons with hyperfine coupling of 5.30 Gauss. This coupling is comparable to that of $a(N_{1,5})$ and $a(N_{2,4})$ at 6.50 and 5.30 Gauss respectively.[45]

3.2.3 Structures of Verdazyls

In 1973, Williams published the crystal structure of 2,4,6-triphenylverdazyl **3.3a**.[109] The verdazyl ring was found to be non-planar with the methylene group in position 6 puckered from the plane of the ring by 0.59Å (Figure 3.2a). The bond lengths between N2-C3 and N4-C3 are almost identical (1.337Å and 1.338Å respectively). The N1-N2 and N4-N5 bond lengths are 1.348 Å and 1.353 Å respectively.

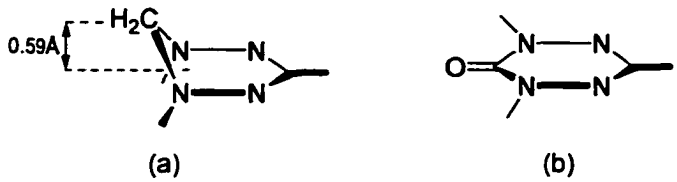

Figure 3.2. Schematic structures of the methylene (a) and carbonyl (b) bridged verdazyls.

In contrast, X-ray crystal structures of 6-oxoverdazyl derivatives indicate that the entire six membered ring is planar (Figure 3.2b).[106,110] The driving force for planarity likely arises from π–orbital overlap between the heterocyclic π system and the carbonyl π* orbital – an amide-type resonance (Scheme 3.8). In the case of the methylene bridged verdazyls (Figure 3.2a), there is no such interaction and therefore the ring system puckers.

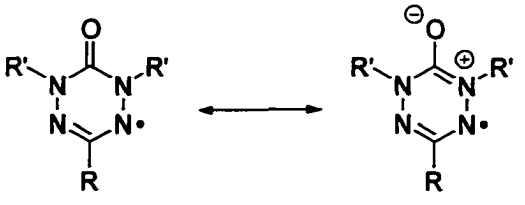

Scheme 3.8. Amide-type resonance of 6-oxoverdazyl **3.2a**.

3.2.4 Stability

The ability to isolate derivatives of radicals **3.3a** and **3.11** as single crystals attests to their stability. In general, the verdazyls are isolable in the solid state. They are also generally stable in dilute solutions for a minimum period of several weeks. However, in saturated solutions, the radicals are sometimes subject to disproportionation reactions.[111] For example, Neugebauer observed that refluxing a saturated benzene solution of verdazyl **3.3a** for one day yielded tetrazine **3.6** and triazole **3.21** (Scheme 3.9).

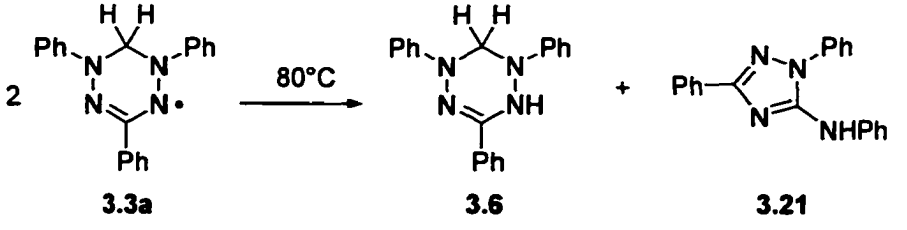

3.3a **3.6** **3.21**

Scheme 3.9. Disproportionation reaction of 1,3,5-triphenylverdazyl **3.3a**.

When treated with mineral acids, verdazyl **3.3a** reversibly disproportionate to form the coloured verdazylium ion **3.22** and tetrazine **3.6**. In air, the tetrazines are easily oxidized back to the radical (Scheme 3.10).

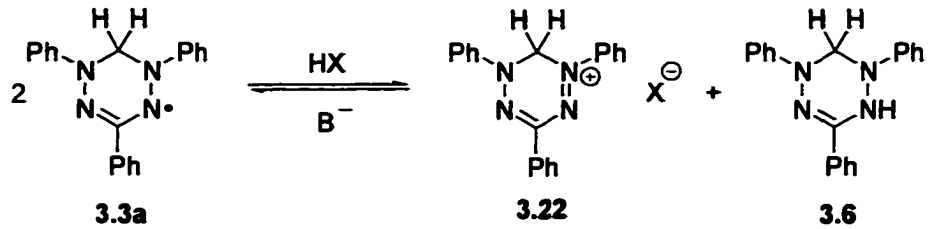

3.3a **3.22** **3.6**

Scheme 3.10. Disproportionation of verdazyl **3.3a** in acid.

The general stability of verdazyls is in sharp contrast to radicals **3.23** and **3.24** which decompose in air or when treated with acids respectively.[44]

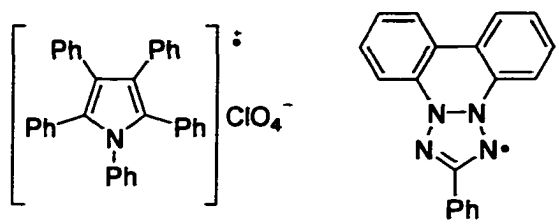

3.23 **3.24**

3.3 Heteroverdazyls

To date, almost all modifications of verdazyls have been carried out exclusively on the ring substituents R and R'. As was mentioned in the introduction of this chapter, we were interested in making structural changes to the ring skeleton itself and determining the chemical and physical consequences of these skeletal atom substitutions. As depicted in Figure 3.3, replacement of carbon(s) 3 and/or 6 with a heteroatom (X/Y) would give the so-called heteroverdazyls. The rationale behind altering the C3 and/or C6 atoms of the verdazyl skeleton (as apposed to any of the four nitrogen atoms) is related to general factors governing radical stability: as discussed in Chapter 1, most stable radicals contain

spin density predominately on nitrogen and oxygen atoms and the spin density of verdazyl radicals is known to reside primarily on the four nitrogen atoms. Therefore, we wanted to alter the verdazyl ring without having a drastic effect on the stability of the verdazyl system.

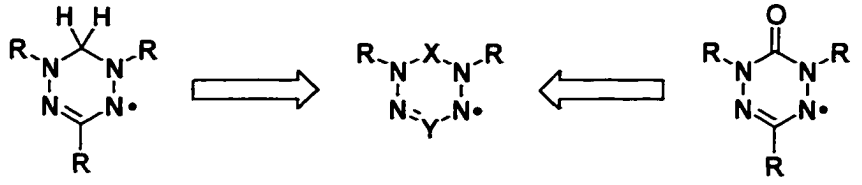

Figure 3.3. Heteroatom substitution at carbons 3 and 6 of the verdazyl backbone.

Phosphorus was chosen as the heteroatom to incorporate for several reasons. Firstly, the starting materials are easily made and/or commercially available (*vide infra*). Secondly, the phosphorus nucleus (S = ½; 100% abundant) provides another probe for NMR and EPR characterization. In the latter case, the phosphorus nucleus may help determine the spin distribution in these radicals. Finally, there are a few reports on phosphaverdazyls that merit further studies. The first phosphaverdazyl (**3.25**) was reported by Kornuta *et al.* in 1978.[112] Although radical **3.25** was synthesized, its characterization was incomplete. A 27 line EPR spectrum was reported without any mention of hyperfine coupling constants. The remainder of this chapter describes the synthesis and characterization of several phosphaverdazyl radicals.

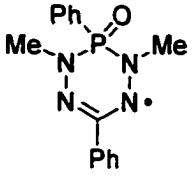

3.25

3.4 Synthesis of Phosphaverdazyls.

The synthesis of 6-oxo and 6-thioxoverdazyls is well established (Scheme 3.3). Therefore, it was desirable to use a similar methodology for the synthesis of the phosphaverdazyls. The attempted synthesis of tetrazane **3.26** is shown in Scheme 3.11.

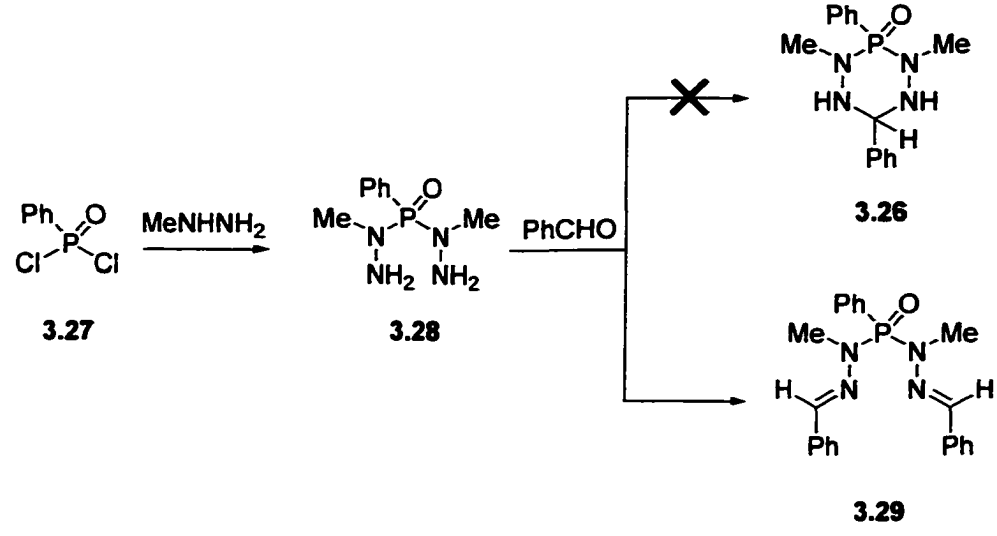

Scheme 3.11. Attempted synthesis of tetrazane **3.26**.

Phenylphosphonic acid dichloride **3.27** was reacted with excess methylhydrazine to give bis(hydrazide) **3.28** in a modified version of the literature synthesis.[113] However, the reaction of **3.28** with benzaldehyde gave the bis(imine) **3.29** and not the desired tetrazane **3.26**. Based on a modified procedure reported by Kornuta *et al.*,[112,114] bis(hydrazide) **3.28** was cyclized to tetrazine **3.30** using trimethylorthobenzoate (Scheme 3.12). Red solutions of radical **3.25** were generated by quantitative deprotonation of **3.30** with NaH followed by oxidation with tetrabutylammonium periodate.[115] In the solid state, verdazyl **3.25** is indefinitely stable if stored at –30 °C. In solution, however, the radical decomposes within 1 to 2 weeks. Treatment of the radical with ascorbic acid regenerates tetrazine **3.30** in near quantitative yield.

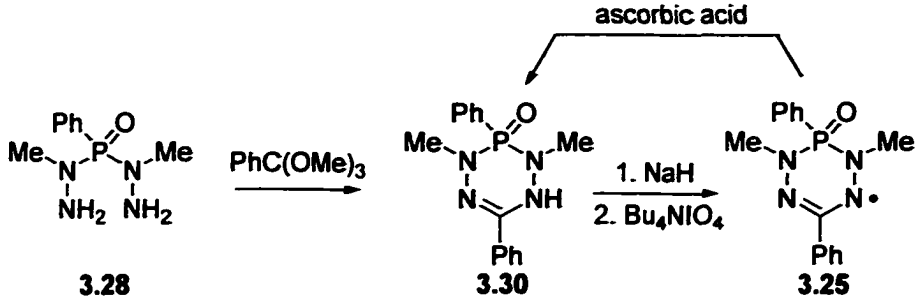

Scheme 3.12. Synthesis of radical **3.25** via tetrazine **3.30**.

The ^{1}H NMR of bis(hydrazide) **3.28** was characterized by two resonances in addition to the multiplet from the phenyl group. The N-Me protons appear at 2.89 ppm as a doublet with a J_{PH} of 9.1 Hz and the NH_2 protons appear as a broad singlet at 3.60 ppm. The ^{31}P $\{^{1}H\}$ NMR, **3.28** consists of a sharp singlet at 31 ppm. Tetrazine **3.30** gives three characteristic peaks in the ^{1}H NMR. The protons of the two N-Me groups give rise to two distinct doublets at 3.23 ppm and 2.87 ppm with J_{PH} of 6.0 and 10.3 Hz respectively. The NH proton appears as a doublet at 6.3 ppm with a J_{PH} of 8.7 Hz. Tetrazine **3.30** is characterized by a sharp singlet at 12.8 ppm in the ^{31}P $\{^{1}H\}$ NMR. The chemical shifts and coupling constants of bishydrazide **3.28** and tetrazine **3.30** are characteristic for these families of compounds.

Crystals of **3.30** were studied by X-ray crystallography by Dr. John F. Richardson, University of Louisville. The crystal structure of tetrazine **3.30** is presented in Figure 3.4 and a partial list of bond lengths and bond angles are presented in Table 3.1.

Table 3.1. Selected bond lengths (Å) and bond angles (°) for the structure of tetrazine **3.30**.

Atoms	Distance	Atoms	Distance
C(1)-N(3)	1.294(3)	P-O	1.480(2)
C(1)-N(2)	1.378(4)	P-N(4)	1.654(2)
C(1)-C(2)	1.476(4)	P-N(1)	1.671(2)
C(8)-N(1)	1.458(4)	N(1)-N(2)	1.424(3)
C(9)-N(4)	1.460(3)	N(3)-N(4)	1.401(3)
C(10)-P	1.789(3)		

Atoms	Angle	Atoms	Angle
N(3)-C(1)-N(2)	122.0(3)	N(2)-N(1)-C(8)	114.9(2)
N(3)-C(1)-C(2)	117.3(3)	N(2)-N(1)-P	108.1(2)
N(2)-C(1)-C(2)	120.7(3)	C(8)-N(1)-P	118.8(2)
O-P-N(4)	115.4(1)	C(1)-N(2)-N(1)	116.8(2)
O-P-N(1)	112.8(1)	C(1)-N(3)-N(4)	116.3(2)
O-P-C(10)	111.0(1)	N(3)-N(4)-C(9)	112.5(2)
N(4)-P-N(1)	101.4(1)	N(3)-N(4)-P	125.8(2)
N(4)-P-C(10)	107.4(1)	C(9)-N(4)-P	120.7(2)
N(1)-P-C(10)	108.2(1)		

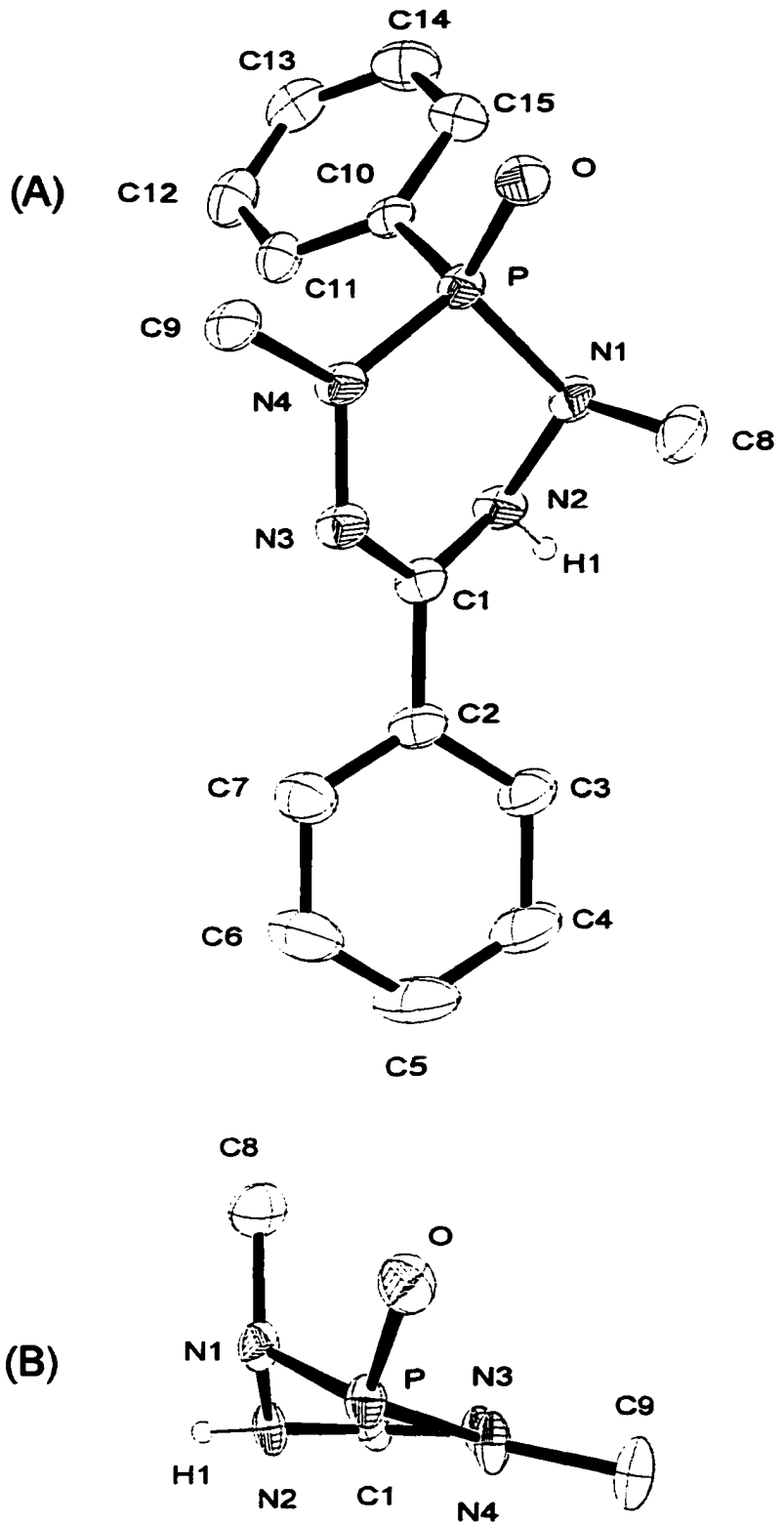

Figure 3.4. X-ray crystal structure of tetrazine **3.30** (A) and edge-on view looking down the phosphorus atom (B). Hydrogen atoms removed for clarity.

One feature of the molecular structure in Figure 3.4 is the non-planarity of the verdazyl ring. One of the N-Me groups (N4 and C9) is in the plane of the verdazyl ring (defined by atoms C9-N4-N3-C1-N2) and the other N-Me group (N1 and C8) is almost perpendicular to this plane. Assuming a similar conformation is adopted in solution, this structure provides an explanation for the distinct chemical shifts and J_{PH} differences between the two N-Me groups.

The long-lived nature of radical **3.25** permitted its study by EPR spectroscopy. The experimental and simulated EPR spectra of phosphaverdazyl **3.25** are shown in Figure 3.5.

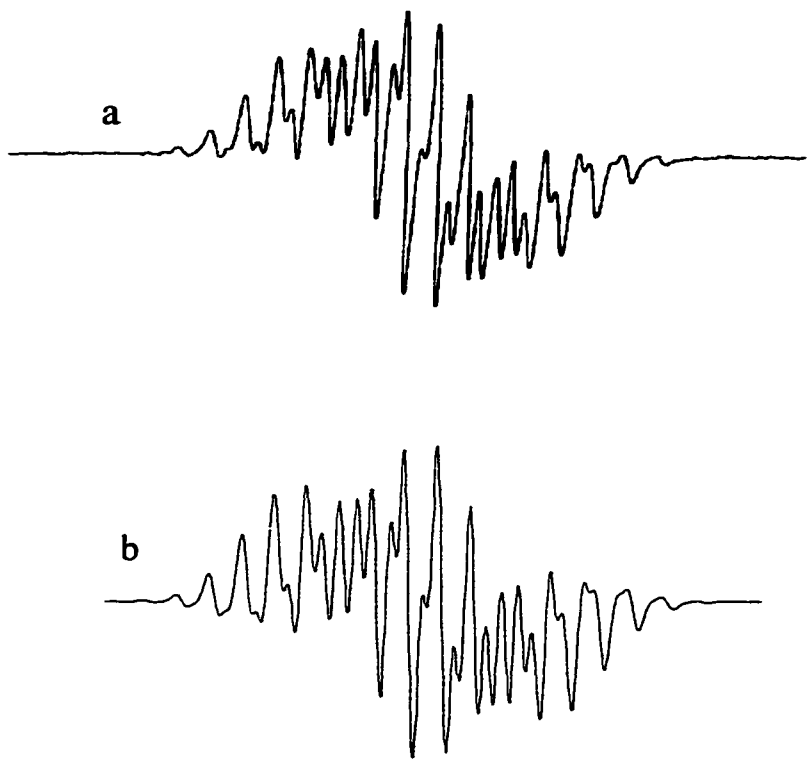

Figure 3.5. Experimental (a) and simulated (b) EPR spectra of phosphaverdazyl **3.25**. Sweep width of the experimental spectrum is 100 G.

The best simulation of the experimental spectrum was produced using coupling to two 2-coordinate nitrogens (6.4 G), two 3-coordinate nitrogens (4.4 G), six methyl protons (4.6 G), and one phosphorus nucleus (5.2 G). The hyperfine coupling constants of the 2-coordinate nitrogen, 3-coordinate nitrogen, and N-Me protons are characteristic for the phosphaverdazyls (vide infra), and are fairly close to the hyperfine coupling constants for the 1,5-dimethyl-6-oxoverdazyls **3.2a**.

Dr. Richard Hooper, a postdoctoral fellow in our group, also explored the introduction of phosphorus into the other end of the ring. 3-Phosphaverdazyl **3.31** was prepared according to Scheme 3.13.[115]

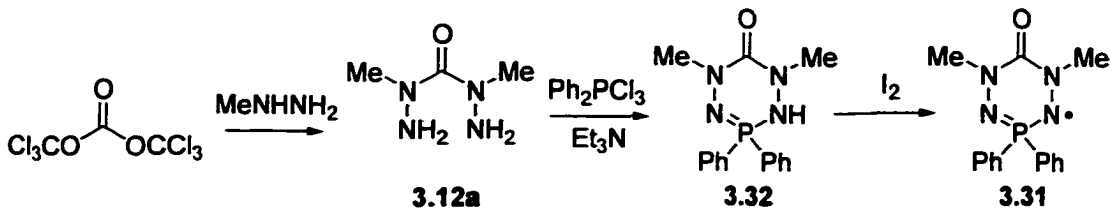

Scheme 3.13. Synthesis of 3-phosphaverdazyl **3.31**.

Bis(hydrazide) **3.12a** was prepared by a different reaction than described in the literature (Scheme 3.5). Thus, triphosgene and not phosgene, was added to a cold solution of methylhydrazine to afford **3.12a**. Triphosgene was used in place of phosgene because it is a solid and can be measured out safely and stoichiometrically. When bis(hydrazide) **3.12a** was reacted with Ph_2PCl_3 in the presence of triethylamine, tetrazine **3.32** was isolated. Treatment of a benzene solution of **3.32** with iodine generated radical **3.31**. Similar to radical **3.25**, radical **3.31** is stable in the solid state if stored at –30 °C but decomposes within 1 to 2 days in solution.

In the ^{1}H NMR of tetrazine **3.32**, the N-Me protons appear as singlets at 3.0 and 2.8 ppm. Coupling to the ^{31}P nucleus was not observed. The NH proton appears as a doublet at 6.0 ppm with a J_{PH} of 19 Hz.

The experimental and simulated EPR spectra for phosphaverdazyl **3.31** are shown in Figure 3.6. In radical **3.31**, the unpaired electron is coupled to the 2-coordinate and 3-coordinate nitrogen atoms with constants of 6.4 G and 5.3 G, respectively. Coupling to the N-Me protons and phosphorus was found to be 5.4 G and 0.2 G, respectively.

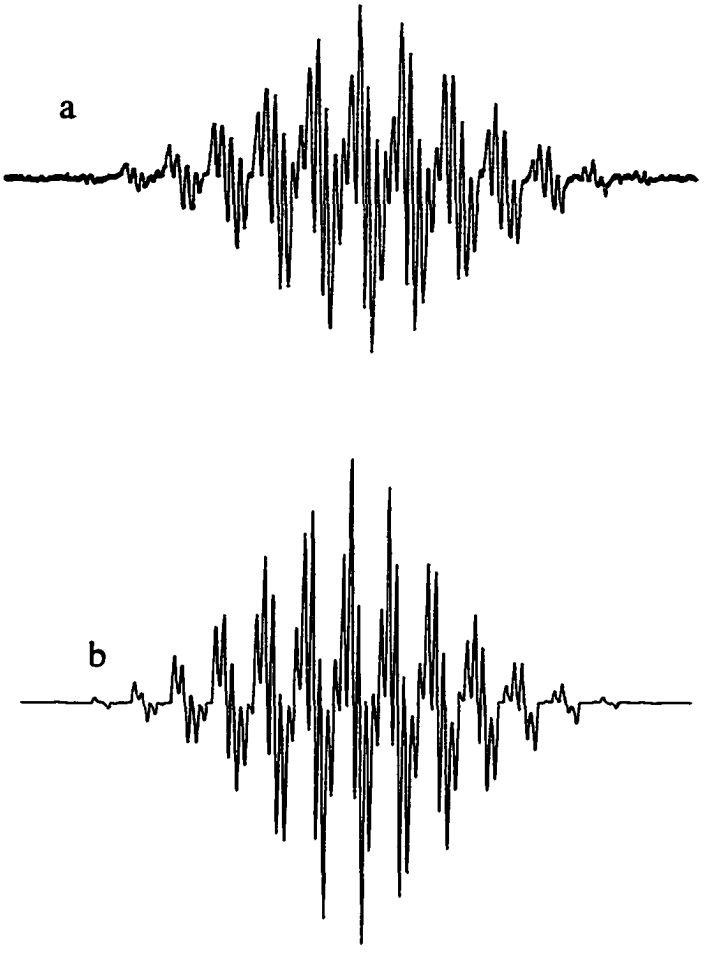

Figure 3.6. Experimental (a) and simulated (b) EPR spectra of phosphaverdazyl **3.31**. Sweep width of the experimental spectrum is 100 G.

The relatively large coupling at phosphorus for phosphaverdazyl **3.25** as well as its qualitatively better stability compared to **3.31** prompted studies on other 6-substituted phosphaverdazyls. A phosphaverdazyl with a P-dimethylamino group (**3.33**) was targeted for two reasons: (1) to study the effects (if any) of altering the phosphorus substituent on the verdazyl properties, and (2) to study a derivative with a substituent with a spin-active nucleus directly onto phosphorus – this may permit assessment of how much spin density "leaks" from phosphorus onto the substituent. The synthesis of **3.33** is outlined in Scheme 3.14.

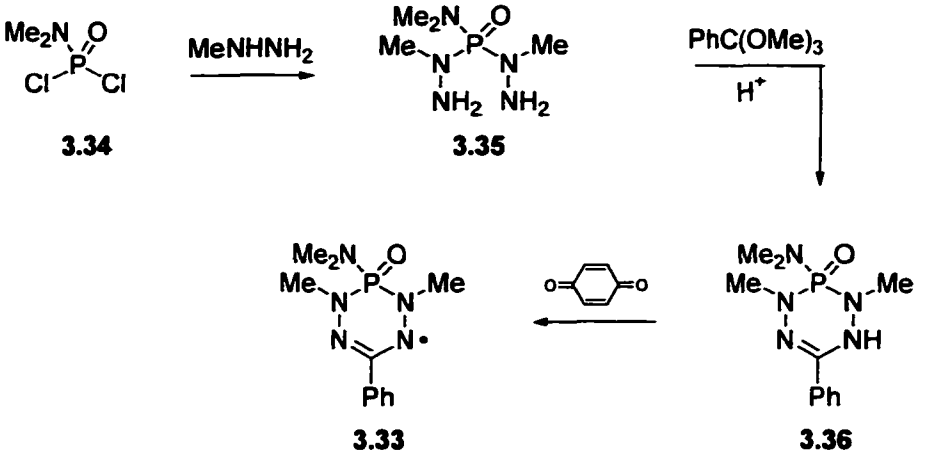

Scheme 3.14. Synthesis of (6-dimethylamino)-6-phosphaverdazyl **3.33**.

Dimethylamino phosphonic acid dichloride **3.34** was prepared as per Walsh and Toy.[116] Reaction of **3.34** with excess methylhydrazine gave bis(hydrazide) **3.35** as a white viscous oil which was used without further purification. A refluxing solution of **3.35** and trimethylorthobenzoate with a catalytic amount of acetic acid afforded tetrazine **3.36**, which was purified by chromatography and recrystallized from CH_3CN. The ^1H NMR spectrum of bis(hydrazide) **3.35** gave rise to the anticipated signals; a doublet at 2.88 ppm

(J_{PH} = 8.1 Hz) and broad singlet at 4.35 ppm for the N-Me and NH_2 groups respectively. The exocyclic N-Me protons appear as a doublet at 2.67 ppm (J_{PH} = 9.6 Hz). The ^1H NMR of tetrazine **3.36** also gave the anticipated signals. Two distinct doublets are observed for the N-Me groups at 2.74 and 3.15 ppm (J_{PH} = 9.6 and 5.9 Hz respectively) and one doublet at 7.01 ppm (J_{PH} = 8.8 Hz) is observed for the NH proton. The exocyclic N-Me protons of **3.36** appear as a doublet at 2.64 ppm (J_{PH} = 9.6 Hz). The ^{31}P $\{^1H\}$ NMR spectra of bis(hydrazide) **3.35** and tetrazine **3.36** gave sharp singlets at 25.3 and 7.1 ppm respectively.

Phosphaverdazyl **3.33** was generated using benzoquinone. The synthesis of **3.33** is virtually identical to that of **3.25** with the exception of benzoquinone used as oxidant. Phosphaverdazyl **3.33** is red in solution and decomposes after 1 to 2 days.[117]

The experimental and simulated EPR spectra of phosphaverdazyl **3.33** are shown in Figure 3.7. The best simulation of the EPR spectrum of **3.33** included hyperfine coupling to two 2-coordinate nitrogens, two 3-coordinate nitrogens, and six N-Me protons (6.5, 4.3, and 4.6 G respectively), in addition to one exocyclic nitrogen atom (4.6 G) and six protons (4.5 G). Coupling to phosphorus was 0 G.

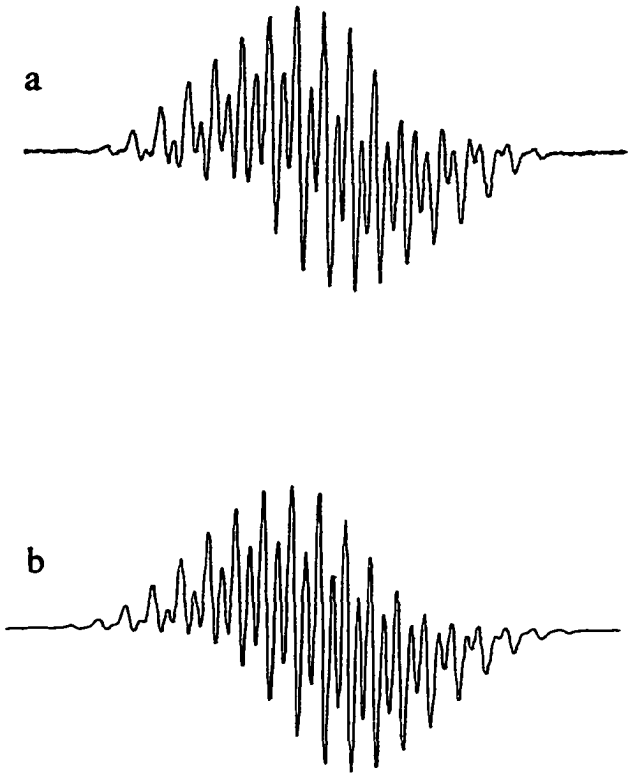

Figure 3.7. Experimental (a) and simulated (b) EPR spectra of phosphaverdazyl **3.33**. Sweep width of the experimental spectrum is 100 G.

The corresponding anion of phosphaverdazyl **3.33** was also generated. Deprotonation of tetrazine **3.36** with NaH generated solutions of the yellow anion **3.37**. The anion is extremely oxygen sensitive, forming radical **3.33** immediately on exposure to air. The anion was alkylated with MeI to form the 2-*N*-methylated tetrazine **3.38** (Scheme 3.15).

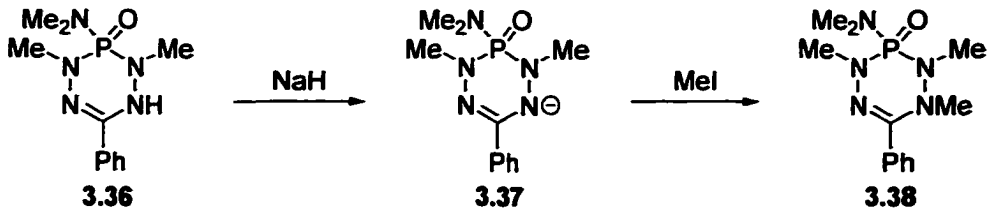

3.36 **3.37** **3.38**

Scheme 3.15. Synthesis of anion **3.37** and N-methyltetrazine **3.38**.

The ^{1}H NMR spectrum of **3.38** is nearly identical to that of tetrazine **3.36**. In addition to the peaks arising from the methyl groups at N1 and N5 and the exocyclic Me_2N group, a doublet at 2.90 ppm (J_{PH} = 1.5 Hz) was observed for the new methyl group introduced at nitrogen in position 2. A sharp singlet at 6.4 ppm was observed in the ^{31}P NMR spectrum.

A more elaborate functionalization of the 6-phosphaverdazyl skeleton is represented by radical **3.39**. The synthesis of this derivative is outlined in Scheme 3.16. Hexachlorocyclotriphosphazene **3.40** was treated with two equivalents of 2,2′-biphenol in the presence of triethylamine to afford **3.41**. Reaction of this intermediate with methylhydrazine afforded bis(hydrazide) **3.42** as a white solid which was purified by column chromatography. Cyclization with trimethylorthobenzoate afforded tetrazine **3.43** as a pink oil. Purification by column chromatography followed by crystallization from ether gave **3.43** as pink crystals. Radical **3.39** was generated using benzoquinone. Similar to verdazyl **3.33**, verdazyl **3.39** is red in solution and decomposes after several days.

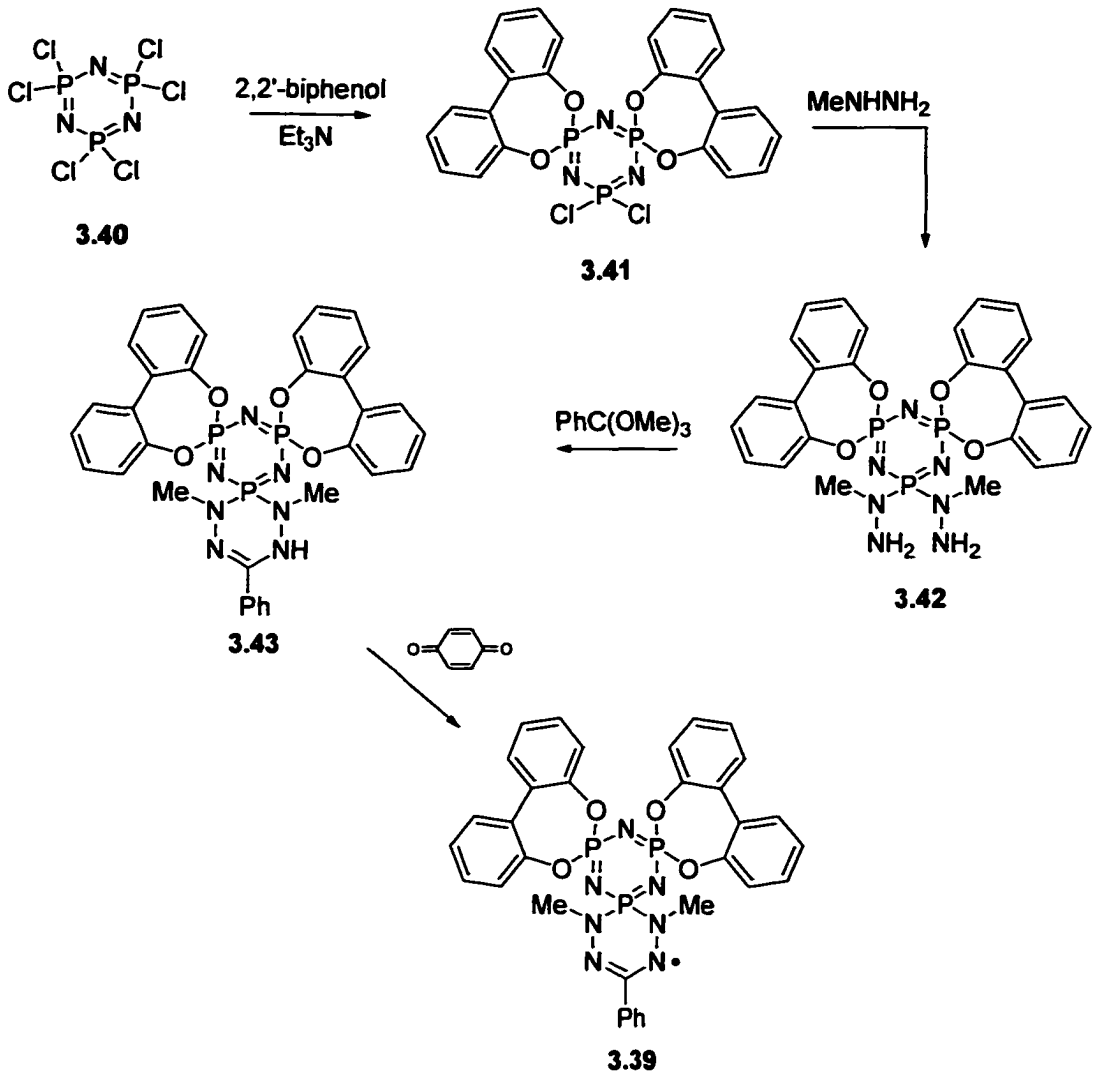

Scheme 3.16. Synthesis of 6-phosphaverdazyl **3.39**.

The ^{1}H NMR spectra of **3.42** and **3.43** are consistent with the other bis(hydrazides) and tetrazines. The former has (in addition to the aromatic resonances) the expected resonances for the N-Me protons (2.94 ppm, J_{PH} = 11.0 Hz) and the NH_2 protons (3.61 ppm) and the latter has spectroscopic features associated with the N-Me (3.30, J_{PH} = 8.8 Hz; 2.90 ppm, J_{PH} = 11.0 Hz) and NH protons (6.17 ppm, J_{PH} = 5.9 Hz) analogous to tetrazines **3.30** and **3.36**.

The ^{31}P $\{^1H\}$ NMR spectrum of **3.42** does not give the expected doublet and triplet from an AX_2 system; there are what appear to be two sets of complex multiplets. This may arise from second order effects. In contrast, the ^{31}P $\{^1H\}$ spectrum for tetrazine **3.43** gives the expected doublet and triplet of an AX_2 system.

The X-ray crystal structure of tetrazine **3.43** is presented in Figure 3.8 and the relevant bond lengths and bond angles are presented in Table 3.2.

Table 3.2. Selected bond lengths (Å) and bond angles (°) for the structure of tetrazine **3.43**.

Atoms	Distance	Atoms	Distance
P(1)-N(2)	1.573(4)	P(3)-N(7)	1.648(5)
P(1)-N(1)	1.584(4)	P(3)-N(4)	1.679(4)
P(1)-O(1)	1.587(4)	N(4)-N(5)	1.422(5)
P(1)-O(2)	1.590(4)	N(4)-C(411)	1.481(6)
P(2)-N(3)	1.561(4)	N(5)-C(1)	1.386(7)
P(2)-N(1)	1.574(4)	N(6)-C(1)	1.286(7)
P(2)-O(4)	1.577(4)	N(6)-N(7)	1.407(5)
P(2)-O(3)	1.589(4)	N(7)-C(711)	1.440(6)
P(3)-N(3)	1.588(4)	C(1)-C(111)	1.497(7)
P(3)-N(2)	1.597(4)		

Atoms	Angle	Atoms	Angle
N(2)-P(1)-N(1)	118.9(2)	N(2)-P(3)-N(4)	109.4(2)
N(2)-P(1)-O(1)	106.4(2)	N(7)-P(3)-N(4)	99.9(2)
N(1)-P(1)-O(1)	112.3(2)	P(2)-N(1)-P(1)	120.1(3)
N(2)-P(1)-O(2)	111.0(2)	P(1)-N(2)-P(3)	120.9(3)
N(1)-P(1)-O(2)	104.9(2)	P(2)-N(3)-P(3)	123.0(3)
O(1)-P(1)-O(2)	102.19(19)	N(5)-N(4)-C(411)	112.3(4)
N(3)-P(2)-N(1)	118.7(2)	N(5)-N(4)-P(3)	106.1(3)
N(3)-P(2)-O(4)	110.6(2)	C(411)-N(4)-P(3)	116.5(4)
N(1)-P(2)-O(4)	106.6(2)	C(1)-N(5)-N(4)	117.2(4)
N(3)-P(2)-O(3)	105.2(2)	C(1)-N(6)-N(7)	118.0(5)
N(1)-P(2)-O(3)	111.5(2)	N(6)-N(7)-C(711)	113.0(5)
O(4)-P(2)-O(3)	103.21(19)	N(6)-N(7)-P(3)	123.6(4)
N(3)-P(3)-N(2)	115.9(2)	C(711)-N(7)-P(3)	122.9(4)
N(3)-P(3)-N(7)	108.4(3)	N(6)-C(1)-N(5)	124.2(5)
N(2)-P(3)-N(7)	112.4(3)	N(6)-C(1)-C(111)	117.8(6)
N(3)-P(3)-N(4)	109.6(2)	N(5)-C(1)-C(111)	117.9(5)

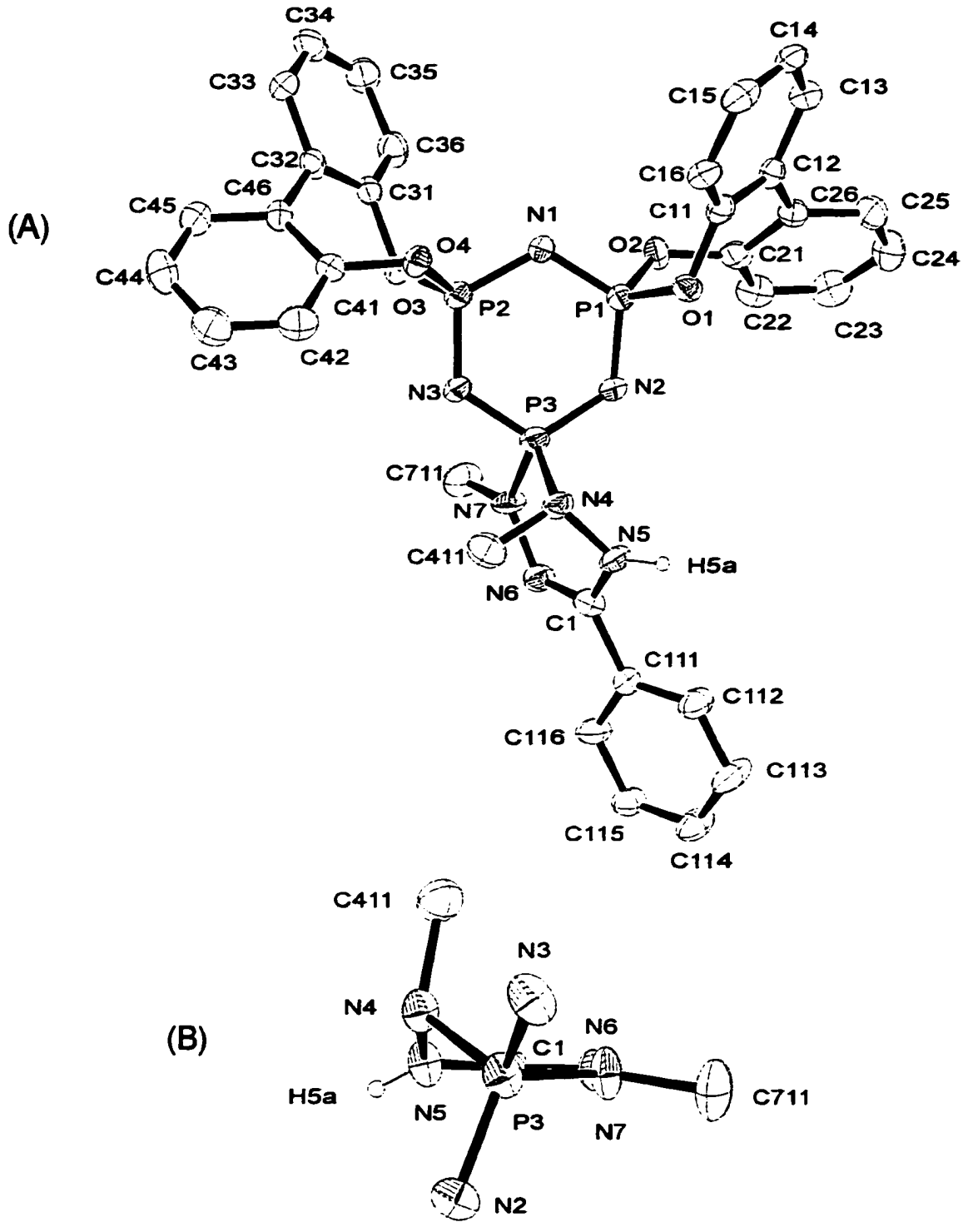

Figure 3.8. X-ray crystal structure of tetrazine **3.43** (A) and edge-on view looking down the P3 atom (B). Hydrogen atoms removed for clarity.

The phosphazene ring is planar and, as expected, is connected to the tetrazine ring in a spirocyclic manner. Similar to structure **3.30** (Figure 3.4), the tetrazine ring of **3.43** is non planar with one N-Me group (N7 and C711) lying essentially in the plane of the ring (defined by atoms N7, N6, C1, and N5) and the second N-Me group (N4 and C411) lying almost perpendicular to this plane.

The experimental and simulated EPR spectra of radical **3.39** are presented in Figure 3.9. The hyperfine coupling constants for the simulated spectrum were not obtained by the usual spectral simulation method because the broad featureless lines in the experimental spectrum precluded such an analysis. We therefore resorted to an ENDOR (Electron Nuclear DOuble Resonance) experiment performed by Dr. Andrew Ichimura of Michigan State University. ENDOR is an EPR technique which yields hyperfine coupling constants in a "decoupled" way. The couplings are not multiplicative so each coupling constant a(X) produces a set of peaks independent of the other couplings. The ENDOR spectrum for radical **3.39** is presented in Figure 3.10.

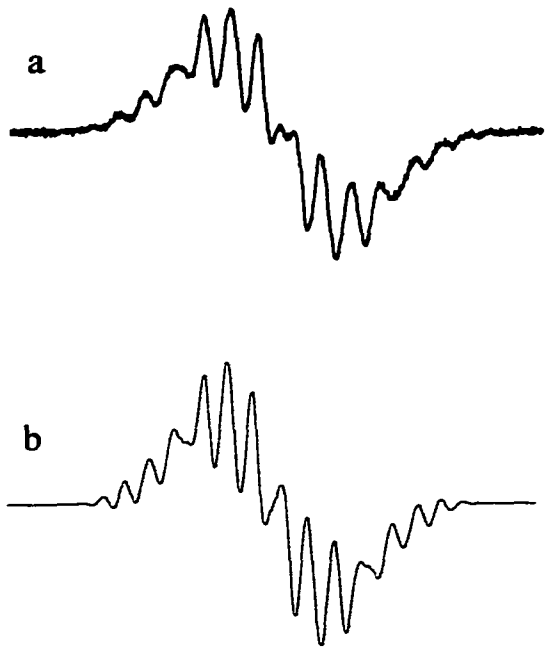

Figure 3.9. Experimental (a) and simulated (b) EPR spectra of radical **3.39**. Sweep width of the experimental spectrum is 100 G.

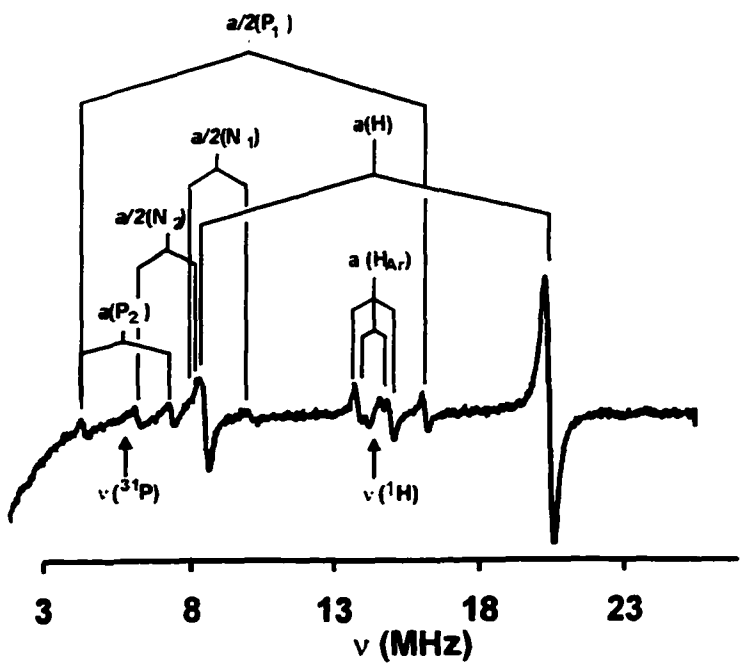

Figure 3.10. ENDOR spectrum of radical **3.39**.

The hyperfine coupling constants extracted from the ENDOR experiment were used directly in the EPR simulation of radical **3.39**, giving a reasonable fit, although there are some minor discrepancies between the simulated and experimental spectra. The couplings to the 2- and 3-coordinate nitrogens (6.45 and 5.18 G, respectively) and the N-Me protons (4.24 G) are consistent with those of the previous 6-phosphaverdazyl derivatives. Similar to radical **3.25**, there is a relatively large coupling to the spirocyclic phosphorus atom (7.29 G) as well as smaller hyperfine coupling constants to the other phosphorus atoms (1.06 G). Hyperfine coupling to the P_3N_3 ring nitrogen atoms was not observed. This may be because the couplings were too small or perhaps they were masked by the "shoulder" at the low frequency end of the spectrum.

3.5 Discussion

Table 3.3 summarizes the EPR parameters found for phosphaverdazyl radicals **3.11a**, **3.25**, **3.31**, **3.33** and **3.39**. The hyperfine coupling constants for the divalent nitrogens ($N_{2,4}$), trivalent nitrogens ($N_{1,5}$), and the N-Me protons are similar to one another and also similar to those of a parent 6-oxoverdazyl **3.11a**. As was found for the "parent" verdazyls, hyperfine coupling to the 2-coordinate nitrogens is slightly higher than that of the 3-coordinate nitrogens in the phosphaverdazyls. Upon closer inspection of Table 3.3, some interesting features emerge. The hyperfine couplings to phosphorus for radicals **3.25**, **3.31**, **3.33** and **3.39** vary substantially. Another curious observation concerns **3.33**: there is a relatively large hyperfine coupling to the *exocyclic* dimethylamino group while the coupling to phosphorus is zero. The following discussion attempts to provide a rationale for these observations.

Table 3.3. EPR parameters for selected verdazyl and phosphaverdazyl radicals.[a]

	3.11a	**3.25**	**3.31**	**3.33**	**3.39**
G	2.0037	2.0038	2.0038	2.0037	2.0036
$a(N_{2,4})$	6.5	6.4	6.4	6.5	6.45
$a(N_{1,5})$	5.3	4.4	5.3	4.3	5.18
$a(CH_3)$	5.3	4.6	5.4	4.6	4.24
a(P)		5.2	0.2	0	7.29
a(N′)				4.6	
$a(CH_3')$				4.5	

[a] Hyperfine coupling constants are in G. $N_{2,4}$ refers to the two-coordinate nitrogens, $N_{1,5}$ to the three coordinate nitrogens, N′ and CH_3' to the exocyclic nitrogen and methyl group in **3.33**.

The geometric and electronic structures of the parent verdazyls (**3.3** and **3.11**) provide some insights. As discussed earlier, verdazyl derivatives of type **3.11** are known to be essentially planar.[45] Both extended Hückel and high-level DFT calculations indicate that the unpaired electron of verdazyl **3.11** resides in a π–molecular orbital with no contribution from the p-orbitals at positions 3 and 6 (Figure 3.11a).[106,110] The qualitative similarities between $a(N_{1,5})$, $a(N_{2,4})$, and $a(CH_3)$ in all the phophaverdazyls suggest a similar basic electronic structure. Therefore, by analogy, the SOMOs of radicals **3.31** and **3.33** (Figure 3.11b and c respectively) would suggest a planar geometry with essentially zero coupling to phosphorus due to the node passing through positions 3 and 6.

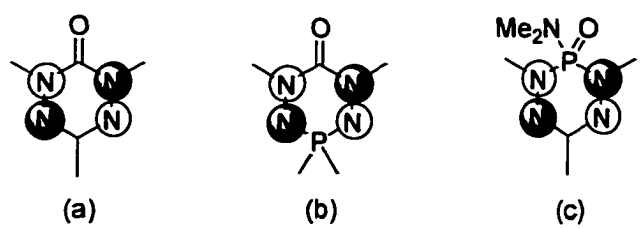

Figure 3.11. The π-SOMOs of radical **3.11** (a), **3.31** (b), and **3.33** (c). The SOMOs contain two nodes; one of which passes through positions 3 and 6.

Why then, do radicals **3.25** and **3.39** have a relatively large spin density at phosphorus? Recall that verdazyls of type **3.3** are puckered at the 6 position (Figure 3.12a). We propose that the relatively large a(P) suggests a puckered geometry for radicals **3.25** and **3.39** (Figure 3.12b). The non-planar geometry permits σ–π orbital mixing which therefore permits spin leakage onto the phosphorus atom. It is worth noting that coupling to a(P) is much more sensitive than a(N)[118] and therefore the amount of spin found at phosphorus likely does not constitute more than a few percent.

(a) (b)

Figure 3.12. Schematic representation of the puckered geometry of radicals **3.3** (a) and radicals **3.25** and **3.39** (b).

The lack of long-term stability of the phosphaverdazyls has prevented X-ray analysis to determine the geometric structure. To gain a better understanding of the skeletal atom and substituent effects on the structures and spin distributions of the phosphaverdazyls, Dr. Lars Öhrström (Chalmers Institute of Technology, Göteberg, Sweden) performed high level DFT calculations on several verdazyl derivatives in collaboration with our group. The results of these calculations by Dr. Öhrström will be included here to aid in understanding the experimental studies.

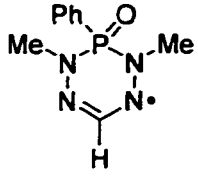

3.25a

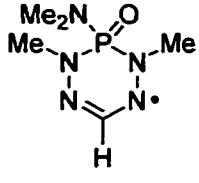

3.33a

DFT calculations were performed on simplified model compounds **3.25a** and **3.33a**. For **3.25a**, three local minima were found (referred to as **3.25a'**, **3.25a''**, and **3.25a'''**) and are shown in Figure 3.13. The spin populations for the three conformers of **3.25a** are summarized in Table 3.4

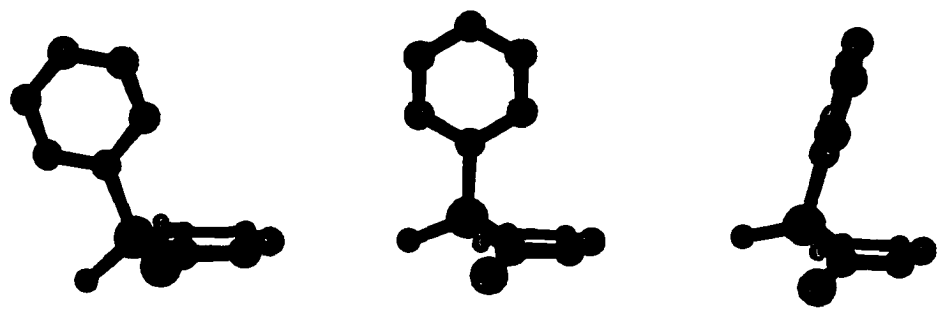

3.25' **3.25''** **3.25'''**

Figure 3.13. Three DFT optimized structures for **3.25a**.

Table 3.4. DFT spin populations analyses for the optimized structures of **3.25a**.

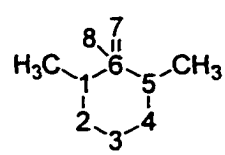

	3.25a'	**3.25a''**	**3.25a'''**
$N_{1,5}$	0.178	0.182	0.180
$N_{2,4}$	0.327	0.306	0.328
C_3	-0.089	-0.074	-0.079
P_6	0.013	0.027	0.031
O_7	-0.004	-0.006	-0.003
8	(C) –0.009	-0.009	0.000
1,5-CH_3	0.009	0.009	0.009

The six membered ring of conformer **3.25a'** is nearly flat: the N1-P6-N5 plane forms a dihedral angle of 6° with the plane of the rest of the ring. In conformers **3.25a''** and **3.25a'''**, the phosphorus atom is bent out of the plane of the ring, producing half-boat conformations with dihedral angles of 30° and 38° respectively. The relative energies for the three structures are relatively close (**3.25a'**, 0; **3.25a''**, +1.2; and **3.25a'''**, 3.2 kcal mol^{-1}). This suggests that molecule **3.25a** may not have a strong preference for a planar or bent geometry. The phosphorus spin populations are larger for the bent structures, 0.027 and 0.030 for **3.25a''** and **3.25a'''** versus 0.013 for **3.25a'**. The EPR spectrum of this radical would seem to suggest that in solution the conformation of the ring is somewhat bent, although the quantitative aspects of the geometry cannot be determined from the EPR spectrum alone. Also, as seen in Figure 3.13, the plane containing the phenyl group of structures **3.25a'** and **3.25a''** is essentially parallel with the P=O bond whereas in **3.25a'''**, the phenyl group is rotated by 90°.

The DFT calculations performed on model compound **3.33a** also produced three local minima (referred to as **3.33a'**, **3.33a''**, and **3.33a'''**). The optimized structures are shown in shown in Figure 3.14, and spin density populations for the three conformers are summarized in Table 3.5.

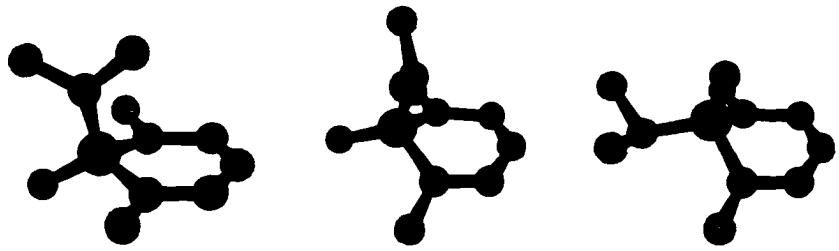

3.33a' 3.33a'' 3.33a'''

Figure 3.14. Three DFT optimized structures for **3.33a**.

Table 3.5. DFT spin population analyses for the optimized geometries of **3.33a**.[a]

	3.33a'	**3.33a''**	**3.33a'''**
$N_{1,5}$	0.179, 0.201	0.179, 0.185	0.201
$N_{2,4}$	0.320	0.331	0.316
C_3	-0.087	-0.081	-0.078
P_6	-0.014	-0.024	0.015
O_7	-0.001	-0.005	0.034
N_8	0.044	-0.003	-0.001
1,5-CH_3	0.009	0.01	0.007

[a]See Table 3.4 for atom position definitions

The lowest energy structure **3.33a'** is almost planar with the N-P-N moiety bent out of the plane of the ring by 17°. The other conformers, **3.33a''** (2.4 kcal higher than **3.33a'**) and **3.33a'''** (19.4 kcal) are significantly more bent with dihedral angles of the N-P-N moiety of 35° and 50° respectively. Based on the $a(^{31}P)$ values of **3.33a**, the near planarity of conformer **3.33a'** appears to be consistent with our previous argument concerning radical **3.11**. Indeed, the calculated spin population at phosphorus is small for **3.33** (Table 3.5).

The most striking feature of **3.33a** is the orientation of the dimethylamino group (Figure 3.15). In conformers **3.33a'** and **3.33a''**, the Me_2N groups are in pseudo-axial positions. The group in **3.33a''** is rotated by 90° with respect to **3.33a'**. The orientation

of the Me_2N group in **3.33a'** positions the nitrogen p orbital over the verdazyl π SOMO. This p orbital has the correct symmetry to overlap with the π SOMO of the verdazyl ring and thus provides a mechanism for spin leakage onto the exocyclic nitrogen observed in the EPR spectrum (Table 3.3) and DFT calculations (Table 3.5).

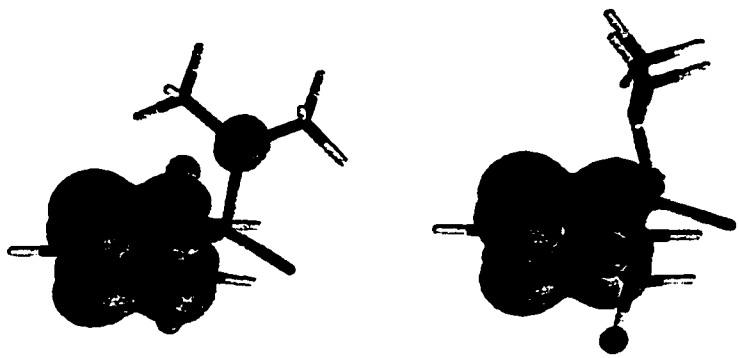

3.33a' **3.33a"**

Figure 3.15. Spin density plots of conformers **3.33a'** and **3.33a"**.

This general arrangement of p orbitals is known as spiroconjugation[119,120] and is shown schematically in **3.44** as viewed down the end of the molecule. Spiroconjugation provides an alternative method for spin propagation or spin coupling from the conventional spin delocalization mechanisms in π conjugated systems.

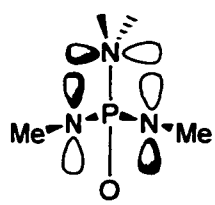

3.44

The barrier to rotation about the P-N (exocyclic) bond is relatively small at 6 ± 2 kcal/mol and suggests that the observed hyperfine coupling constants are most likely due to a weighted average of the various conformers. This also suggests that if the π orbitals

could be geometrically constrained in the proper orientation (i.e the orientation depicted in **3.44**), the strength of spiroconjugation may be enhanced further. This was in fact the main reason behind the preparation of the phosphazene based phosphaverdazyl **3.39**. The phosphazene ring and phosphaverdazyl ring are linked at one phosphorus atom, forcing the two rings to be orientated perpendicular to one another.

At first glance the large a(P) and small a(N) for **3.39** may seem inconsistent with the coupling constants of phosphaverdazyl **3.33**. Although the exocyclic nitrogens in radical **3.39** are now constrained in a conformation which maximizes spiroconjugation, the electronic nature of the nitrogen atoms must be considered when comparing radicals **3.33** and **3.39**. The exocyclic nitrogen of radical **3.33** can be considered as a π donor with respect to phosphorus. The lone pair on the exocyclic nitrogen can donate to phosphorus as depicted in **3.45-3.45a**.

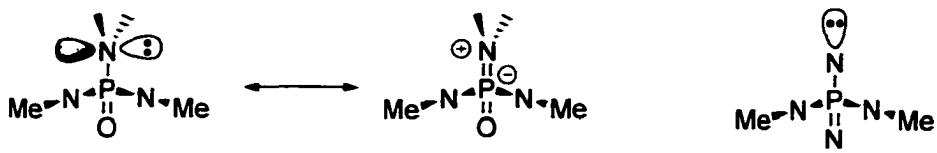

3.45 **3.45a** **3.46**

This would result in a shorter P-N bond, and a flattened geometry at the Me_2N group. The DFT calculations support this hypothesis: the P-N bond calculated for conformer **3.33a'** is shortened relative to the other two conformers, and the sum of the bond angles at the dimethylamino nitrogen is 357°. In the other conformers, **3.33a''** and **3.33a'''**, the P-N bond lengths are longer, and the dimethylamino nitrogen atoms are more pyramidal with the sum of the bond angles at 350° and 333° respectively. In the case of radical **3.39**, the lone pair of the exocyclic phosphazene nitrogen is in the plane of the

phosphazene ring; as shown in **3.46**, this lone pair has the wrong symmetry to spiroconjugate with the verdazyl π SOMO.

Thus, the nature of the substituent on phosphorus appears to be an important factor in determining the geometry of the verdazyl ring. We believe the π donation is responsible for stabilizing the more planar conformer of radical **3.33**. The lack of such π donating capabilities in radical **3.39** would suggest a non-planar verdazyl ring, and the EPR results (*a*(P) of 7.29 G) seem to be consistent with this.

3.6 Summary/Conclusions

The synthesis, characterization, and properties of some new phosphaverdazyl radicals have been described. We found that reaction of the appropriate bis(hydrazide) with an orthoester was an effective method in the preparation of the tetrazines. The tetrazines were purified by chromatography and could be isolated as crystalline solids. Benzoquinone was the oxidant of choice in generating the verdazyl radicals. We also found that deprotonation with NaH followed by oxidation (O_2, I_2 etc) was effective.

The EPR characterization of a variety of phosphaverdazyls suggested that the electronic environment at phosphorus is sensitive to the nature of the substituent at phosphorus. Unfortunately, the phosphaverdazyls do not appear to be as stable as the parent methylene or carbonyl bridged verdazyls. No phosphorus-containing verdazyl has been characterized crystallographically. This necessitated theoretical calculations that could provide insight into the molecular structure of these radicals. Experimental EPR results and DFT calculations have revealed a few interesting features. A qualitative relationship was proposed between *a*(P) and the geometry of the ring. When *a*(P) is zero (or < 1G), the verdazyl ring is planar, and when *a*(P) is relatively large (> 4 G), the

verdazyl ring is non-planar. The geometry of the verdazyl rings are also highly sensitive to the nature of the R group attached to phosphorus. The specific reasons behind this effect are not clear at this time. It is worth noting that in many diamagnetic cyclophosphazene systems, the substituents on phosphorus have a large effect on the ring conformations.[121] These subtle effects are similar to the observed sensitivity of the phosphaverdazyls to the nature of the substituent on phosphorus.

Perhaps the most intriguing feature of the phosphaverdazyls is the *exocyclic* spin density and the spiroconjugation mechanism by which it occurs. The phenomena of spiroconjugation in radical systems has been proposed in a few instances.[54,122-124] The consequences of this spin leakage could be important in the context of conducting and magnetic materials. For example, the synthetic methodology to phosphaverdazyl **3.39** can readily be adapted to prepare spirocyclic diradical **3.47** and triradical **3.48**. Since these two molecules have two or more unpaired electrons, the question of spin-spin communication can be tackled – how does a PN π system mediate spin exchange? Although the study of the electronic properties of these diradicals is outside the scope of this thesis, the synthesis of diradical **3.47** was started as a side project.

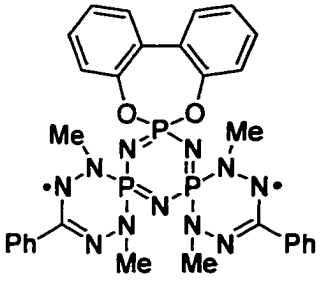

3.47

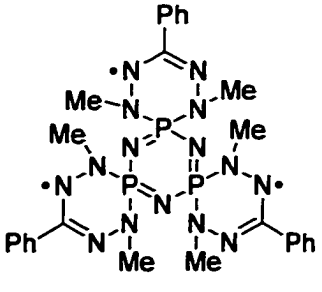

3.48

As shown in Scheme 3.17, hexachlorocyclotriphosphazene **3.40** was reacted with one equivalent of 2,2'-biphenol to give **3.49**. Subsequent reaction with methyhydrazine

afforded tetrakis(hydrazide) **3.50** as a white solid. The high polarity of **3.50** precluded purification by column chromatography. Trituration with a $CHCl_3$/Pet ether mixture gave almost pure **3.50**. Cyclization with trimethylorthobenzoate yielded bis(tetrazine) **3.51** as a pink oil. Chromatography followed by crystallization from ether yielded tetrazine **3.51** as pink crystals. Oxidation to diradical **3.47** has not yet been accomplished.

In the ^1H NMR, tetrakis(hydrazide) **3.50** has (in addition to the aromatic signals) the expected signal for the NH_2 protons (3.8 ppm) and the N-Me protons (2.8-2.9 ppm). However, the N-Me protons are not split into the expected doublets, but into a multiplet which we believe is due to second order effects. Similar to bis(hydrazide) **3.42**, the $^{31}P\{^1H\}$ NMR does not give the expected doublet and triplet for an AX_2 system; there are two sets of multiplets which may be complicated from second order effects. The ^1H NMR of bis(tetrazine) **3.51** has the expected resonances for the two N-Me protons and the NH proton. However, coupling to phosphorus is not observed (all peaks appear as broad singlets) and there is twice as many peaks than necessary. We believe this is due to a mixture of diastereomers in solution. This is corroborated in the $^{31}P\{^1H\}$ NMR spectrum, two pairs of a doublet and triplet are observed – one for each diastereomer. In addition, mass spectrometry and elemental analysis are both fully consistent with the proposed structure for **3.51**.

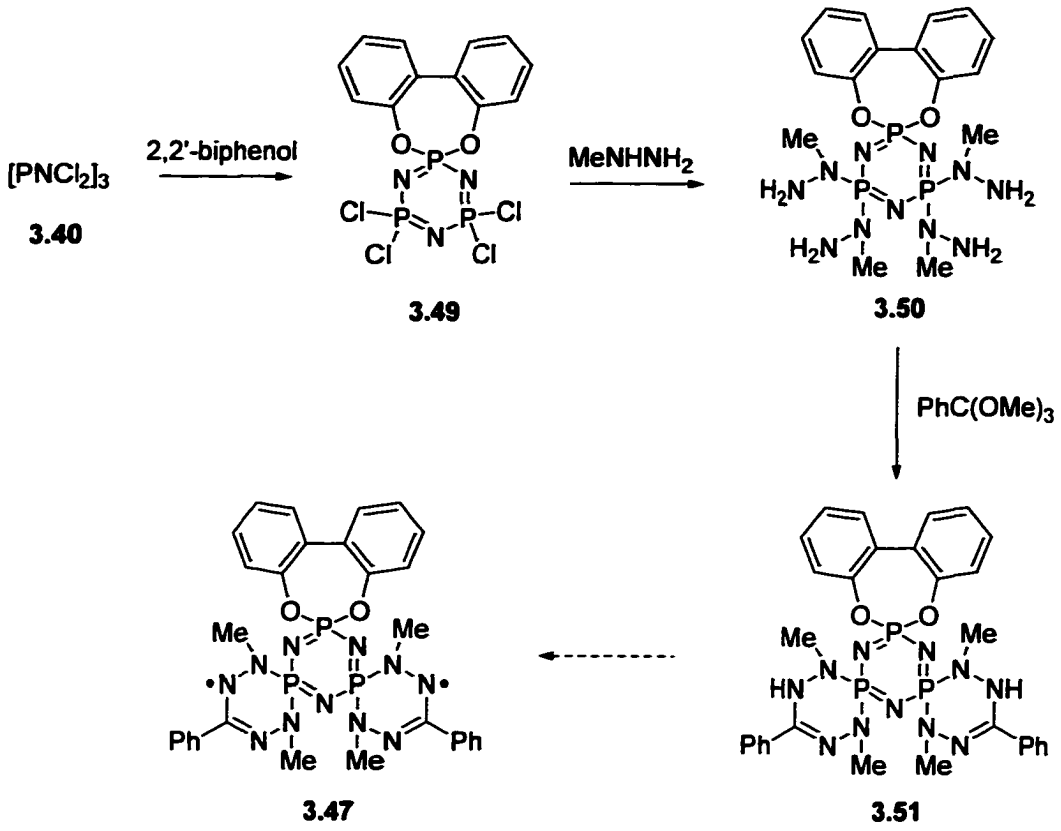

Scheme 3.17. Synthesis of bis(tetrazine) **3.51**.

In principle, the same methodology could be applied in the synthesis of triradical **3.48**. The synthesis of this compound would require hexakis(hydrazide) **3.52**, which has been described in the literature.[125]

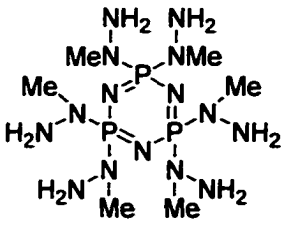

3.52

One possible further extension to this approach would be to link a large number verdazyl radicals on a polyphosphazene backbone as shown in **3.53**. This type of compound

would have a macroscopic number of spins, which could communicate via the P-N backbone to give new polymeric magnetic materials.

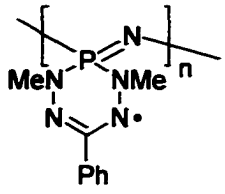

3.53

3.7 Experimental

Synthesis of 1,5-Dimethyl-6-oxo-3,6-diphenyl-6-phosphaverdazyl (3.25)

A solution of tetrazine **3.30** (302 mg, 1.00 mol) in THF (25 mL) was added to a slurry of NaH (~30 mg, ~1.25 mmol) in 20 mL of THF. The solution immediately turned bright yellow/orange, with the evolution of hydrogen gas. After 15 min of stirring at room temperature, a solution of $Bu_4N^+IO_4^-$ (450 mg, 1.03 mmol) in 30 mL of THF was added. The solution immediately turned deep red. The reaction mixture was stirred for 1 h and then concentrated under reduced pressure. Benzene was added, and the insoluble byproducts were filtered, giving a clear red filtrate of **3.25**, which was evaporated to give a red-brown solid.

Synthesis of Phenylphosphonic acid bis(1-methylhydrazide) (3.28)

A solution of $PhP(O)Cl_2$ **3.27** (2.008 g, 10.3 mmol) in 10 mL toluene was added dropwise to a solution of $MeNHNH_2$ (2.30 mL, 43.4 mmol) in 20 mL CH_2Cl_2 at – 42 °C. The solution was allowed to stir for 16 h while slowly warming to room temperature. The white precipitate was filtered in vacuo and the filtrated concentrated to a white solid.

The product was used without further purification. ^{1}H NMR ($CDCl_3$): δ 7.9-7.8 (m, 2H), 7.6-7.4 (m, 3H), 3.60 (br s, 4H), 2.88 ppm (d, 6H, J = 8.8 Hz). ^{31}P NMR ($CDCl_3$): δ 30.68 ppm.

Synthesis of 1,2,5,6-Tetrahydro-1,5-dimethyl-3,6-diphenyl-1,2,4,5,6-tetrazaphosphorine-6-oxide (3.30)

A solution of **3.28** (1.33g, 6.21 mmol), trimethyl orthobenzoate (1.15 mL, 6.48 mmol) and acetic acid (5 drops) was stirred for 16 h in 50 mL of CH_2Cl_2. The solvent was then removed under reduced pressure and the residue chromatographed (SiO_2, 1:1 CH_2Cl_2: CH_3CN) to give **3.30**, yield 0.931 g (50%). ^{1}H NMR ($CDCl_3$): δ 7.3-7.7 (m, 10H), 6.3 (d, 1H, J = 8.7 Hz), 3.23 (d, 3H, J = 6.0 Hz), 2.87 ppm (d, 3H, J = 10.3 Hz). ^{13}C NMR ($CDCl_3$): δ 140.1 (d, J = 9.3 Hz),132.3 (d, J = 3 Hz), 132.0, 131.2 (d, J = 10 Hz), 130.0, 128.5, 128.3,126.3, 37.2 (d, J = 4.5 Hz), 37.0 ppm (d, J = 4 Hz). ^{31}P NMR ($CDCl_3$): δ 12.8 ppm. Anal. Calcd for $C_{15}H_{17}N_4OP$: C, 60.00; H, 5.71; N, 18.66. Found: C, 59.85; H, 5.65; N, 18.40.

Synthesis of 1,5-Dimethyl-6-(*N*,*N*-dimethylamino)-6-oxo-3-phenyl-6-phosphaverdazyl (3.33)

Benzoquinone (23 mg, 0.213 mmol) was added to a solution of **3.36** (102 mg, 0.382 mmol) in 10 mL benzene. The solution immediately turned intense red. The solution was stirred for 30 min. under argon after which the solvent was removed under reduced pressure to leave a red semi-solid. The residue was chromatographed on an

alumina column (activity II-III) using CH_2Cl_2 as an eluant. The product was recovered as a red oil. UV-vis (CH_2Cl_2): λ_{max} 538, 295 nm.

_N,N_-Dimethylaminophosphonic acid bis(1-methylhydrazide) (3.35)

A solution of **3.34**[116] (9.010 g, 55.6 mmol) in 25 mL CH_2Cl_2 was added dropwise to a solution of methylhydrazine (12 mL, 226 mmol) in 40 mL CH_2Cl_2 at -42 °C (dry ice/ acetonitrile bath). The reaction mixture was stirred for 16 h and then the white precipitate of methylhydrazine hydrochloride was filtered in vacuo. The filtrate was evaporated in vacuo to give the product as a hygroscopic oil. The oil was used without further purification. The oil can be partially solidified if stirred in hexanes overnight. ^{1}H NMR (CD_2Cl_2): δ 4.35 (br s, 4H), 2.88 (d, 6H, J = 8.1 Hz), 2.67 ppm (d, 6H, J = 9.6 Hz). ^{31}P NMR ($CDCl_3$): δ 25.33 ppm. IR (CH_2Cl_2): (NH) 3338 (m), 3254 (m), 3170 (m), 1608 (m), 1460 (m), 1300 (s), (P=O) 1194 (s), 995 (s) cm^{-1}.

Synthesis of 1,2,5,6-Tetrahydro-1,5-dimethyl-6-(_N,N_-dimethylamino)-3-phenyl-1,2,4,5,6-tetrazaphosphorine-6-oxide (3.36)

A solution of **3.35** (4.128 g, 22.8 mmol), trimethylorthobenzoate (4.0 mL, 23.3 mmol) and acetic acid (10 drops) was refluxed for 16 h in 80 mL CH_2Cl_2. The solvent was then removed and the residue chromatographed on silica gel (1:1, CH_3CN:CH_2Cl_2) to give the product as a pink oil which solidified on standing. The solid residue was recrystallized from CH_3CN to give the product as clear prisms, yield 2.56 g (42%). ^{1}H NMR (CD_2Cl_2): δ 7.7-7.6 (m, 2H), 7.4-7.3 (m, 3H), 7.01 (d, 1H, J = 8.8 Hz), 3.15 (d, 3H, J = 5.9 Hz), 2.74 (d, 3H, J = 9.6 Hz), 2.64 ppm (d, 6H, J = 9.6 Hz). ^{13}C NMR (CD_2Cl_2):

δ 141.4 (d, J = 9.0 Hz), 132.8, 130.0, 128.8, 126.7, 39.2 (d, J = 5.7 Hz), 37.0 (d, J = 4.5 Hz), 36.6 ppm (d, J = 7.9 Hz). ^{31}P NMR (CD_2Cl_2): δ 7.11 ppm. IR (KBr): ν(NH) 3187 (s), 1606 (s), 1570 (m), 1515 (s), 1489 (s), 1462 (s), 1445 (s), 1325 (m), 1304 (s), 1255 (s), 1224 (s), 1200 (s) 1185 (s), 1144 (s), 1124 (s), 1083 (m), 1068 (m), 1029 (w), 995 (s), 959 (s), 931 (s), 773 (s), 764 (s), 749 (s), 691 (s), 633 (w), 621 (w), 595 (w), 523 (s), 497 (m), 467 (m), 406 (m) cm^{-1}. UV-vis (CH_2Cl_2): λ_{max} = 296 nm. Mp: 151-153 °C. Anal. Calcd for $C_{11}H_{18}N_5OP$: C, 49.43; H, 6.79; N, 26.20; P, 11.59. Found: C, 49.45; H, 6.62; N, 25.92; P, 10.93. MS (CI methane): m/z 268 (M + 1, 100%), 296 (M + 29, 12%).

Synthesis of 1,2,5,6-Tetrahydro-1,2,5-trimethyl-6-(N,N-dimethylamino)-3-phenyl-1,2,4,5,6-tetrazaphosphorine-6-oxide (3.38)

A solution of **3.36** (200 mg, 0.744 mmol) in THF (5 mL) was added dropwise via syringe to a suspension of NaH (38 mg, 1.50 mmol) in 5 mL THF. The solution quickly turned orange then bright yellow. The colour change was accompanied by hydrogen evolution. After 30 min, MeI (0.11 mL, 1.77 mmol) was added via syringe. The solution turned pale yellow. After 1.5 h the solvent was removed under reduced pressure to give a yellow waxy solid. The solid was dissolved in CH_2Cl_2 and the NaI salt was filtered off. The crude product was chromatographed on silica gel using CH_3CN:$CHCl_3$ (1:1) as an eluant. The product was recovered as a white crystalline solid, yield 111 mg (53%). ^{1}H NMR ($CDCl_3$): δ 7.5-7.3 (m, 5H), 3.20 (d, 3H, J = 5.9 Hz), 2.90 (d, 3H, J = 1.5 Hz), 2.76 (d, 3H, J = 9.6 Hz), 2.68 ppm (d, 6H, J = 9.6 Hz). ^{13}C NMR ($CDCl_3$): δ 143.7 (d, J = 11.3 Hz), 132.8, 129.6, 128.4, 128.1, 39.9, 36.6 (d, J = 4.5 Hz), 36.3 (d, J = 9.0 Hz), 35.4 ppm (d, J = 6.8 Hz). ^{31}P NMR ($CDCl_3$): δ 6.4 ppm. IR (KBr): 2970 (m), 1593 (m),

1569 (m), 1476 (m), 1444 (m), 1419 (w), 1364 (m), 1306 (m), 1271 (w), 1244 (s), 1193 (s), 1152 (m), 1078 (w), 1049 (m), 1024 (w), 996 (s), 970 (m), 941 (s), 796 (s), 779 (s), 751 (s), 732 (w), 703 (m), 683 (w) cm^{-1}. Mp: 90-92 °C. Anal Calcd. for $C_{12}H_{20}N_5OP$: C, 51.24; H, 7.17; N, 24.90; P, 11.01. Found: C, 50.88; H, 7.01; N, 24.63; P, 10.62. MS (CI methane): m/z 282 (M + 1, 100%), 310 (M + 29, 14%), 323 (M + 41, 2%).

Synthesis of 6-[2,2,4,4-bis(2,2'-dioxy-1,1'-biphenyl)-2,4,6,1,3,5-cyclotriphosphazen-6-yl]-1,5-dimethyl-3-phenyl-6-phosphaverdazyl (3.39)

Benzoquinone (~8 mg) was added to a solution of **3.43** (99 mg, 0.146 mmol) in 5 mL THF. The solution turned an intense cherry red. The solution was concentrated in vacuo to give a red oil. The crude product was chromatographed on alumina (CH_2Cl_2) to give **3.39** as a red oil. UV-vis (THF): λ_{max} = 540 nm. ($t_{½}$ = 2.1 days at $1.5x10^{-3}$ Mol/L).

Synthesis of 1,1-Dichloro-3,3,5,5-bis[spiro(2',2''-dioxy-1',1''-biphenyl)]-1,3,5,2,4,6-cyclotriphosphazene (3.41)

A solution of 2,2'-biphenol (0.595g, 3.2 mmol) in 15 mL THF was added dropwise to a solution of **3.49** (1.429g, 3.1 mmol) and triethylamine (1.1 mL, 7.93 mmol) in 40 mL THF. The solution was allowed to stir for 12 h. During the course of the reaction a fine white precipitate formed. The solution was filtered and the filtrate concentrated to an off white solid. The crude solid was chromatographed on silica gel (3/7, CH_2Cl_2/hexane) to give the product as while solid, yield 1.279g (71%). ^1H NMR (CD_2Cl_2): δ 7.6-7.3 (m, 16H). ^{13}C NMR (CD_2Cl_2): δ 148.0 (m), 130.4, 130.2, 128.8, 127.0, 122.0 ppm. ^{31}P NMR (CD_2Cl_2): δ 29.3 (t, J = 80 Hz), 19.8 ppm (d, J = 80 Hz).

Mp: 290-292 °C. Anal. Calcd for $C_{24}H_{16}N_3O_4P_3Cl_2$: C, 50.20; H, 2.81; N, 7.32; P, 16.18. Found: C, 49.86; H, 2.86; N, 7.17; P, 16.46. MS (CI methane): m/z 575 (M + 1, 100%), 603 (M + 29, 25%), 615 (M + 41, 1%).

Synthesis of 1,1,3,3-bis[spiro(2',2''-dioxy-1',1''-biphenyl)]-5,5-bis(1-methylhydrazide)-1,3,5,2,4,6-cyclotriphosphazene (3.42)

A solution of **3.41** (1.045g, 1.81 mmol) in 35 mL CH_2Cl_2 was added dropwise to a solution of $MeNHNH_2$ (0.44 mL, 8.3 mmol) in 30 mL CH_2Cl_2 at 0° C. A white precipitate formed during the addition. The reaction mixture was stirred for 12 h. The solution was filtered in vacuo and the filtrate concentrated to a white solid. The crude solid was chromatographed on silica gel (3/1, $CHCl_3/CH_3CN$) to give the product as a white solid, yield 1.045g (97%). ^1H NMR (CD_2Cl_2): δ 7.6-7.3 (m, 16H), 3.61 (br s, 4H), 2.94 ppm (d, 6H, J = 11.0 Hz). ^{13}C NMR (CD_2Cl_2): δ 148.7 (t, J = 3.4 Hz), 130.1, 130.0, 129.3, 126.3, 122.1, 40.2 ppm (d, J = 7.91 Hz). ^{31}P NMR ($CDCl_3$): δ 31.3-30.5 (m), 29.0-28.5 ppm (m). IR (KBr): 3327 (w), 3259 (w), 3185 (w), 2786 (w), 1609 (m), 1568 (w), 1500 (s), 1476 (s), 1438 (s), 1264 (s), 1230 (s), 1197 (s), 1173 (s), 1093 (s), 1037 (m), 1016 (m), 982 (m), 959 (s), 945 (s), 919 (s), 866 (s), 812 (m), 783 (s), 754 (s), 735 (s), 719 (s), 685 (m), 624 (s), 609 (s), 588 (w), 569 (w), 533 (s), 523 (m), 497 (m), 477 (m) cm^{-1}. Mp: 245-246 °C. Anal. Calcd for $C_{26}H_{26}N_7O_4P_3$: C, 52.62; H, 4.42; N, 16.52; P, 15.66. Found: C, 52.71; H, 4.44; N, 16.48; P, 16.57. MS (CI methane): m/z 594 (M + 1, 100%), 622 (M + 29, 21%).

Synthesis of 6-[2,2,4,4-bis(2,2'-dioxy-1,1'-biphenyl)-2,4,6,1,3,5-cyclotriphosphazen-6-yl]-1,2,5,6-tetrahydro-1,5-dimethyl-3-phenyl-1,2,4,5,6-tetrazaphosphorine (3.43)

A solution of **3.42** (410 mg, 0.691 mmol), trimethylorthobenzoate (0.24 mL, 1.40 mmol) and ~10 drops acetic acid in 110 mL MeOH was gently refluxed for five days during which a white precipitate formed. The solution was cooled in an ice bath and the solution was gravity filtered to afford crude **3.43**. The product is purified by chromatography on silica gel (benzene) to give the product as a clear oil. The oil was crystallized from ether to give the product as pink rectangles, yield 273 mg (58.1%). ^{1}H NMR ($CDCl_3$): δ 7.7-7.3 (m, 21H), 6.17 (d, 1H, J = 5.88 Hz), 3.30 (d, 3H, J = 8.82 Hz), 2.90 ppm (d, 3H, J = 11.04 Hz). ^{13}C NMR ($CDCl_3$): δ 148.3 (t, J = 4.52 Hz), 141.0 (d, J = 15.8 Hz), 132.5, 129.7, 129.6, 129.5, 128.9 (d, J = 7.91 Hz), 128.4, 126.5, 125.9, 121.8 (d, J = 12.4 Hz), 38.9 (d, J = 4.52 Hz), 36.6 ppm (d, J = 7.91 Hz). ^{31}P NMR ($CDCl_3$): δ 28.5 (d, J = 68 Hz), 10.72 ppm (t, J = 68 Hz). IR (KBr): 3333(w), 1501 (w), 1476 (w), 1438 (w), 1264 (m), 1228 (s), 1192 (sh), 1168 (s), 1117 (w), 1093 (s), 1044 (w), 1014 (w), 962 (m), 946 (w), 926 (w), 908 (m), 874 (m), 818 (w), 785 (w), 754 (w), 741 (w), 719 (w), 711 (w), 693 (w), 624 (w), 610 (m), 584 (w), 534 (w), 521 (w), 476 (w) cm^{-1}. Mp: 251-253 °C. Anal. Calcd for $C_{33}H_{28}N_7O_4P_3$: C, 58.33; H, 4.15; N, 14.43; P, 13.67. Found: C, 58.13; H, 4.07; N, 14.27; P, 13.83. MS (EI): m/z 680 (M + 1).

Synthesis of 1,1,3,3-Tetrachloro-5,5-(spiro-2',2''-dioxy-1',1''-biphenyl)-1,3,5,2,4,6-cyclotriphosphazene (3.49)

A solution of 2,2'-biphenol (2.183g, 11.7 mmol) in 30 mL THF was added dropwise over a 1.5 h period to a solution of hexachlorocyclotriphosphazene **3.40**

(4.068g, 11.7 mmol) and triethylamine (4.2 mL, 30.0 mmol) in 90 mL THF. During the course of the addition a fine white precipitate formed. The solution was allowed to stir overnight. The solution was filtered and triethylammonium chloride salt was washed with 10 mL THF. The filtrate was concentrated to a white solid. The crude solid was purified on silica gel (3/7, CH_2Cl_2/hexane) to give the product as a white crystalline solid, yield 4.643g (86%). ^{1}H NMR (CD_2Cl_2): δ 7.6-7.3 (m, 8H). ^{13}C NMR (CD_2Cl_2): δ 147.6 (d, J = 9.05 Hz), 130.6, 130.3, 128.6, 127.4 (d, J = 2.26 Hz), 121.9 ppm (d, J = 4.52 Hz) ^{31}P NMR (CD_2Cl_2): δ 25.0 (d, *J* = 72 Hz), 13.18 ppm (t, *J* = 72 Hz). Mp: 180-181 °C. Anal. Calcd for $C_{12}H_8N_3O_2P_3Cl_4$: C, 31.27; H, 1.75; N, 9.12; P, 20.16. Found: C, 31.28; H, 1.74; N, 9.19; P, 20.69. MS (CI methane): m/z 462 (M + 1, 100%), 490 (M + 29, 20%), 502 (M + 41, 1%).

Synthesis of 1,1-(Spiro-2',2''-dioxy-1',1''-biphenyl)-3,3,5,5-tetrakis(1-methylhydrazide)-1,3,5,2,4,6-cyclotriphosphazene (3.50)

A solution of **3.49** (4.264 g, 9.25 mmol) in 50 mL CH_2Cl_2 was added dropwise over a 2 h period to a solution of $MeNHNH_2$ (4.0 mL, 75.1 mmol) in 60 mL CH_2Cl_2. The solution was allowed to stir for 15 h during which a white precipitate formed. The solution was filtered in vacuo and the filtrate was concentrated to a white solid. Trituration twice with petroleum ether/$CHCl_3$ (3/1) gave the product as a white solid. Yield 3.791 g (82% crude). ^{1}H NMR (CD_2Cl_2): δ 7.6-7.2 (m, 8H), 3.80 (br s, 8H), 2.9-2.8 ppm (m, 12H). ^{13}C NMR (CD_2Cl_2): δ 148.9, 129.9, 129.4, 126.0, 122.0, 40.2 ppm. ^{31}P NMR (CD_2Cl_2): δ 30.0-29.6 (m), 27.9-27.2 ppm (m). IR (KBr): 3310 (m), 3183 (w), 2784 (w), 1614 (m), 1499 (m), 1477 (s), 1438 (s), 1218 (s), 1169 (s), 1096 (s), 1013 (s),

960 (s), 905 (s), 862 (s), 805 (m), 782 (s), 768 (s), 740 (s), 718 (s), 691 (s), 664 (s), 615 (s), 585 (m), 560 (m), 531(s) cm^{-1}. MS (FAB, mNBA): m/z 500.1 (M + 1). Exact Mass (EI): Actual, 499.1648. Found, 499.1640.

Synthesis of 6,4-[2,2(spiro-2,2'-dioxy-1,1'-biphenyl)-2,4,6,1,3,5-cyclotriphosphazen-4,6-yl]-bis(1,2,5,6-tetrahydro-1,5-dimethyl-3-phenyl-1,2,4,5,6-tetrazaphosphorine) (3.51)

To a refluxing solution of **3.50** (506 mg, 1.01 mmol) and acetic acid (~10 drops) in 20 mL CH_3CN was added dropwise a solution of $PhC(OMe)_3$ (0.42 mL, 2.45 mmol) in 60 mL CH_3CN. The slightly pink solution was refluxed for five days. The solution was cooled to room temperature after which the solvent was removed in vacuo to give a pink oil. The crude oil was chromatographed on silica gel (CH_2Cl_2/CH_3CN) to give the product as a pink oil which partially solidified under reduced pressure. The product was recrystallized from ether to give the product as pale pink clusters, yield, 483 mg (71%). ^1H NMR (CD_2Cl_2, 360 MHz): δ 7.74-7.06 (m, 18H), 6.32 (br s, 2H), 3.19 (s, 3H), 3.07 (br s, 3H), 2.87 (s, 3H), 2.65 ppm (br s, 3H). Tentative assignment of the ^{13}C NMR (CD_2Cl_2): Major isomer: δ 148.8 (apparent d, J = 10.2 Hz), 139.8 (apparent t, J = 7.14 and 6.80 Hz), 133.6, 130.2–130.0 (m) superimposed on 130.2–130.0 (m), 129.6, 129.3 (apparent d, J = 9.2 Hz), 128.7, 126.6–126.3 (m) superimposed on 126.5 (s), 122.2–122.0 (m), 38.1, 36.3 ppm. Minor isomer: δ 148.5 (apparent d, J = 9.58 Hz), 141.0 (apparent t, J = 7.83), 133.1, the aromatic carbons of the minor isomer appear to be overlapped by those of the major isomer, 39.2, 36.7 ppm. ^{31}P NMR (CD_2Cl_2): δ 28.07 (t, J = 65 Hz), 27.28 (t, J = 66 Hz), 8.84 (d, J = 66 Hz), 8.68 ppm (d, J = 65 Hz). IR (KBr): 3344 (w),

3247 (w), 2797 (w), 1607 (w), 1573 (w), 1501 (m), 1477 (m), 1439 (s), 1318 (w), 1261 (m), 1215 (s), 1174 (s), 120 (s), 1096 (s), 1066 (m), 1044 (w), 1014 (w), 962 (s), 918 (s), 906 (s), 860 (s), 821 (m), 783 (s), 771 (s), 744 (s), 714 (s), 693 (s), 650 (w), 614 (s), 584 (w), 563 (w), 532 (m), 514 (m) cm^{-1}. Mp: 183-184 °C. Anal. Calcd for $C_{32}H_{37}N_{11}O_{2.5}P_3$: C, 54.24; H, 5.26; N, 21.74 (hemi-etherate). Found: C, 53.97; H, 5.01; N, 22.04. MS (EI): m/z 672.1 (M + 1).

Chapter 4

Synthetic Efforts Toward Dioxadiazinyl Radicals

4.1 Introduction

In Chapter 3, a brief description was given on the parent verdazyl systems followed by the synthesis and characterization of some phosphaverdazyls in which perturbation of the verdazyl template was carried out at the carbon atoms in positions 3 and 6; the four nitrogen atoms of the verdazyl framework were kept in order to maintain radical stability. The idea that the nitrogen atoms help stabilize the verdazyls is an empirical assumption based on observation which raises an intriguing question; is it possible to prepare "heteroverdazyls" in which some of the *nitrogen* atoms are replaced by other heteroatoms?

Although the phosphaverdazyls demonstrated some interesting properties, there are still some inherent "problems" with these radicals. Their EPR spectra consist of coupling to two different pairs of nitrogen atoms and six protons; couplings are all in the range of 4-6 G. This gives rise to many overlapping peaks and produces extremely complicated spectra, which can render spectral simulation very difficult as was evident in Chapter 3 with some of the phosphaverdazyls that were examined. These spectra were further complicated when coupling to phosphorus was observed.

The coordination chemistry of verdazyls is also being pursued by other members of the Hicks group. Pyridine substituted verdazyls (**4.1**) offer a chelating environment similar to that of 2,2'-bipyridine (**4.2**).[126-128] However, the steric requirements of the N-Me groups provide some limits to complexation. For example, coworkers in the Hicks

group have yet to prepare M(**4.1**)$_3$ complexes. It is believed that the N-Me groups provide a steric barrier to the simultaneous coordination of three verdazyl radicals around a metal ion. This observation is consistent with the coordination chemistry of 2,2'-bipyridine derivatives: although M(**4.2**)$_3$ complexes are common, there are no known examples of analogous ML_3 complexes with methylated bipyridines **4.3** and **4.4**.

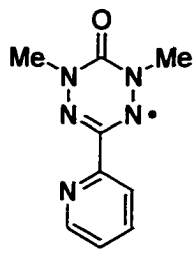

4.1

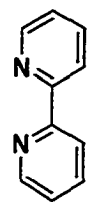

4.2

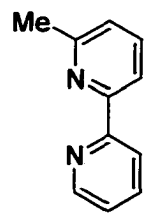

4.3

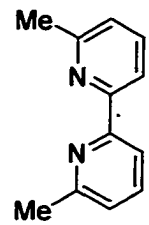

4.4

In light of these "problems" associated with verdazyls, one possible solution would be to substitute the verdazyl N-R groups with smaller, EPR silent groups. Therefore, we chose to substitute the verdazyl N-R groups (**4.5**) with oxygen atoms, which leads to 1,5,2,4-dioxadiazinyl radicals **4.6** as shown in Figure 4.1.

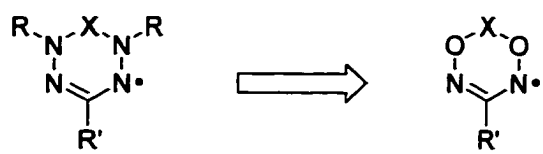

4.5 **4.6**

Figure 4.1. Substitution of the verdazyl N-R groups with oxygen.

The absence of the N-R groups in **4.6** may enhance the coordination chemistry possibilities. For example, pyridine substituted dioxadiazinyl radicals (**4.7**) also have a bipyridine-like chelating environment. Without any methyl groups to hinder complexation (as in **4.1**), ML_3 complexes analogous to M(**4.2**)$_3$ should be attainable.

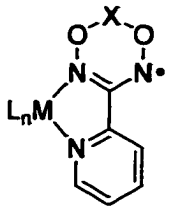

4.7

In addition, replacement of two nitrogen atoms and six protons (all spin active nuclei) by two oxygen atoms (whose predominant isotope is not spin active) would greatly simplify the EPR spectra in these radicals. Shown in Figure 4.2 are the simulated EPR spectra of radicals **4.5** and **4.6** (X = C=O, R = Me). The coupling constants used for **4.5** are taken from the literature.[115] For **4.6**, the coupling constant to the two-coordinate nitrogen atoms used is the same for the two-coordinate nitrogen atoms for **4.5**. For this example, coupling to the R' group is ignored. For radical **4.5**, the unpaired electron is coupled to two different pairs of nitrogen atoms, and six protons from the N-Me groups. Because the hyperfine coupling constants are similar in value, the spectrum is quite complicated (Figure 4.2a). As described in Chapter 3, when these spectra also contain other nuclei to which the unpaired electron couples, extracting the coupling constants can be difficult. In comparison, the EPR spectrum of radical **4.6** is reduced to a simple 1:2:3:2:1 five line pattern arising from coupling to the two equivalent nitrogen atoms (Figure 4.2b).

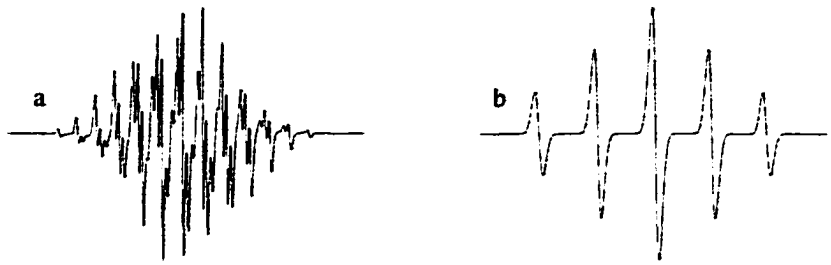

Figure 4.2. Simulated EPR spectra for radicals **4.5** and **4.6** (a and b, respectively).

Clearly, the issue of stability for the proposed radicals is of paramount importance. Because there are no known derivatives of radical **4.6**, it is difficult to predict what their stability will be. However, the "lone-pair-richness" of the ring system of **4.6** is maintained, and EHMO calculations suggest that the electronic structure of **4.6** is not unlike that of the verdazyls (Figure 4.3). Both radicals can be described as 7π electron systems and both have a π–SOMO constrained on the four heteroatoms of the ring. These factors make dioxadiazyls feasible targets as a new family of stable radicals.

This chapter describes exploratory synthetic efforts directed toward the 1,5,2,4-dioxadiazinyl radicals.

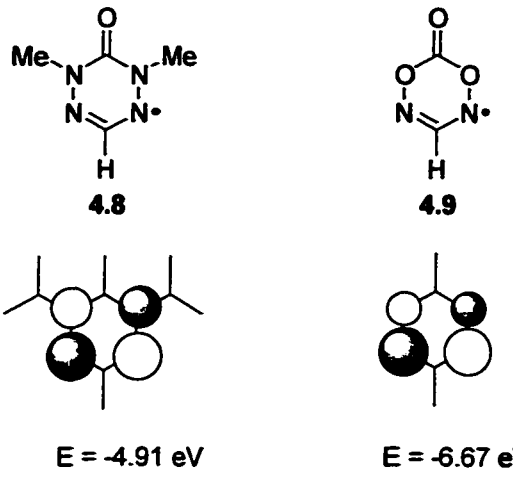

Figure 4.3. Representation of the SOMOs of verdazyl **4.8** and dioxadiazinyl **4.9**.

4.2 Synthetic strategies

The 1,5,2,4-dioxadiazine $C_2N_2O_2$ ring system of **4.6** is unknown (radical or otherwise). This necessitated the development of new heterocyclic synthetic strategies. By analogy with the verdazyls and phosphaverdazyls, we envisioned that the dioxadiazinyl radicals could be made by oxidation of a dioxadiazane (**4.10**) or dioxadiazine (**4.11**) precursor.

A synthetic route to the dioxadiazinyls can be envisaged based on chemistry directly analogous to the synthesis of the 6-oxoverdazyls described in Chapter 3 (Scheme 4.1). In this proposed route, reaction of phosgene **4.12** with two equivalents of hydroxylamine in the presence of base would give intermediate **4.13** (an analogue of the "bis-hydrazide" reagent **3.12**), which could then react with an aldehyde or an orthoester

to give the corresponding dioxadiazane **4.10** or dioxadiazine **4.11** respectively. Oxidation of **4.10** or **4.11** should give the dioxadiazinyl radical **4.14**.

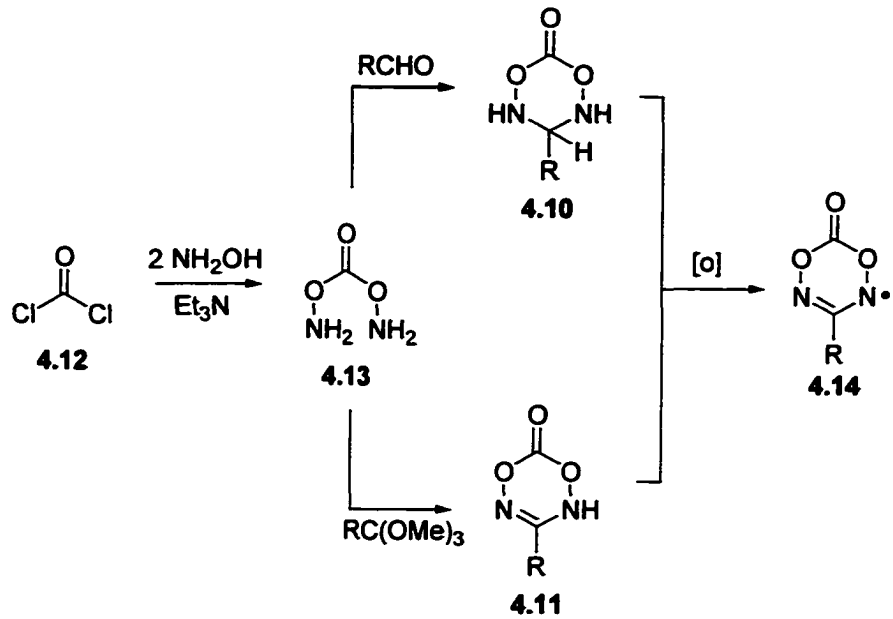

Scheme 4.1. Proposed synthesis of dioxadiazinyl **4.14**.

Although at first glance the reaction outlined in Scheme 4.1 seems reasonable, there is a serious flaw. Hydroxylamine is commonly known to react as a nucleophile with nitrogen rather than oxygen. Therefore, reaction of phosgene with hydroxylamine would likely form intermediate **4.15** rather than **4.13**. Consequently, this method was not pursued.

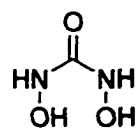

4.15

An alternative proposal for dioxadiazinyl radical synthesis was developed (Scheme 4.2). In principle, the dioxadiazine ring system could be obtained by a condensation reaction between phosgene and hydroxyamidoxime intermediate **4.16**.

Fortunately, there have been a few reports of derivatives of this (rather unusual) functional group and their synthesis comprises the rest of Scheme 4.2.[129-132] Chlorination of an oxime **4.17** (easily made from an aldehyde and hydroxylamine) gives hydroxyimidoyl chloride **4.18** which, upon treatment with excess hydroxylamine, is reported to yield hydroxyamidoxime **4.16**.

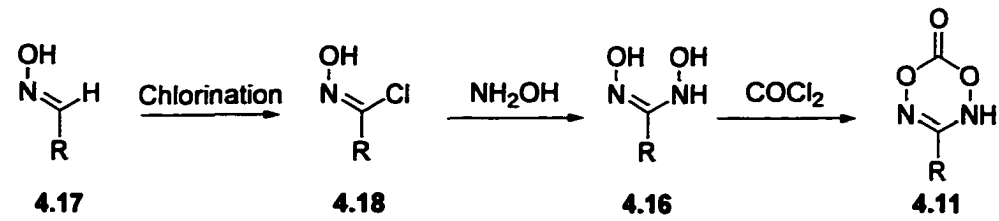

4.17 **4.18** **4.16** **4.11**

Scheme 4.2. Alternative synthesis of dioxadiazine **4.11**.

In addition to the significant advantage of synthetic feasibility over the previously described method, this proposed route is attractive for another reason: hydroxyamidoxime **4.16** is amenable to reaction with a variety of electrophiles, as shown in Figure 4.4. The large range of available electrophiles could potentially open up a rather large new family of heterocyclic radicals.

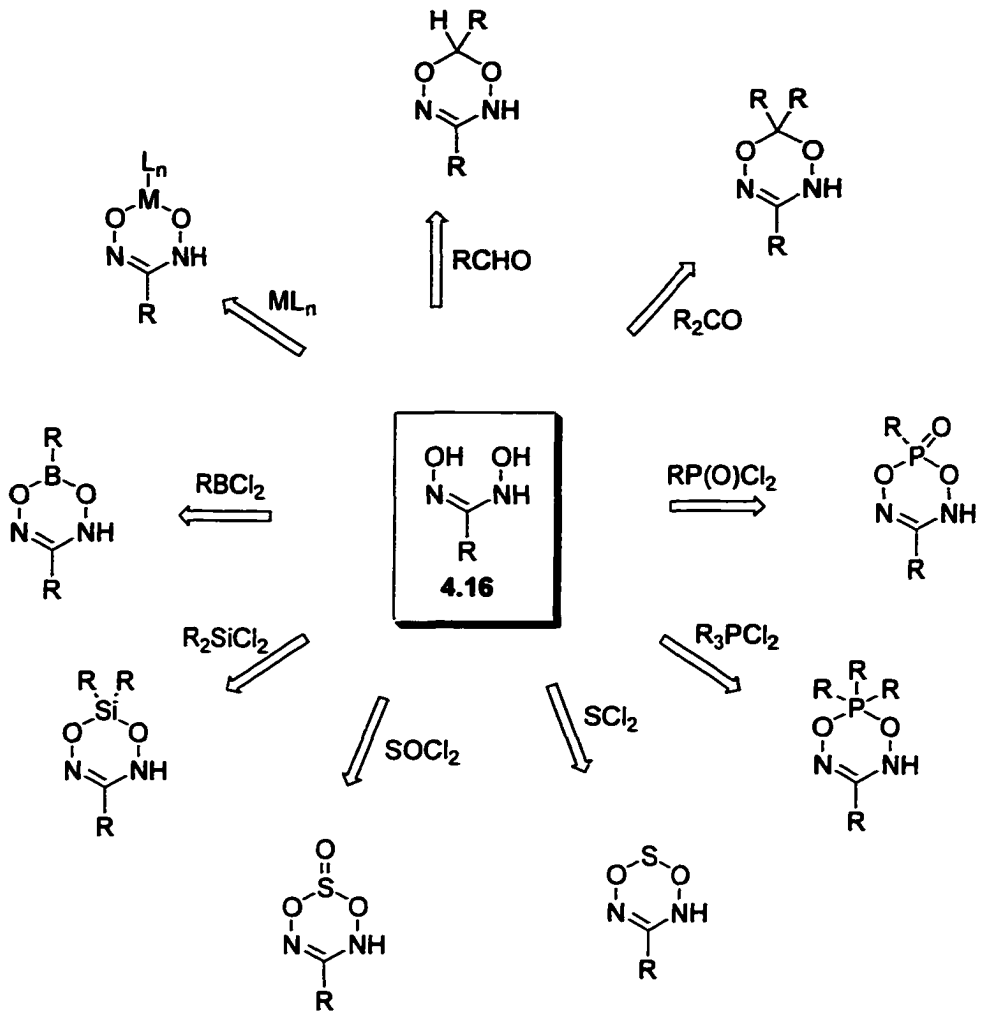

Figure 4.4. Possible transformations of hydroxyamidoxime **4.16**.

4.3 Synthesis of Hydroxyamidoxime 4.16

As described in the previous section, the key intermediate in the proposed synthesis of radicals **4.14** is hydroxyamidoxime **4.16**. The literature synthesis of hydroxyamidoxime **4.16** is outlined in Scheme 4.3.[129,131] Thus, chlorination of a methanol solution of benzaldoxime **4.17a** with excess chlorine gas gave hydroxyimidoyl chloride **4.18a** as a white solid. Treatment of **4.18a** with two equivalents of hydroxylamine yielded **4.16a** in low and irreproducible yields (0-30%), also as a white solid.

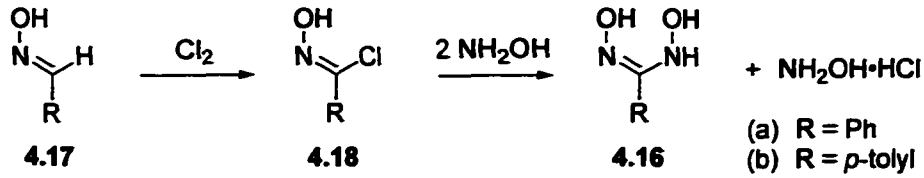

4.17 **4.18** **4.16**

Scheme 4.3. Literature synthesis of hydroxyamidoxime **4.16**.

The major product from the reaction of **4.18** with hydroxylamine is furoxan **4.19a**. This can be understood by considering the mechanism of the reaction between the hydroxyimidoyl chloride and hydroxylamine (Scheme 4.4). The first equivalent of hydroxylamine dehydrochlorinates hydroxyimidoyl chloride **4.18a** to generate nitrile oxide **4.20a**. The nitrile oxide can then react with another molecule of hydroxylamine to form the desired product **4.16a**, or dimerize to give furoxan **4.19a**. The stability of nitrile oxides is well known to be highly dependent on the nature of R;[133] the phenyl derivative **4.20a** is sufficiently unstable that dimerization occurs preferentially to hydroxylamine addition.

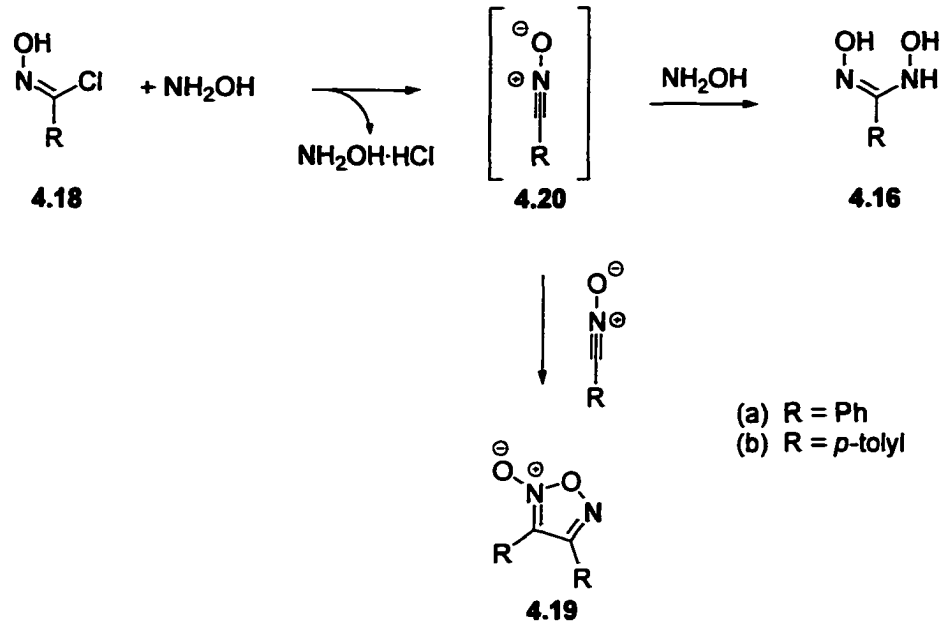

Scheme 4.4. Reaction pathways of nitrile oxide **4.20**.

Closer examination of this two-step reaction resulted in several significant modifications to the literature preparation of hydroxyamidoximes. The first modification concerns the nature of the hydroxylamine employed in these reactions. Commercial hydroxylamine comes as a hydrochloride salt and can be dehydrochlorinated to give free hydroxylamine in aqueous media. However, this process is inefficient in organic solvents due to the poor solubility of $NH_2OH{\cdot}HCl$. Originally, we generated free hydroxylamine by stirring a slurry of hydroxylamine hydrochloride and excess triethylamine in THF overnight. The triethylammonium chloride salt was filtered off and the filtrate solution of free hydroxylamine was then used in subsequent reactions. This method is inefficient and does not proceed to completion unless a large excess of triethylamine is added; the presence of excess triethylamine with hydroxylamine causes problems in subsequent chemistry. Although there is a protocol for the isolation of pure hydroxylamine, this material is known to decompose at room temperature, and explode violently at higher

temperatures;[134] this idea was therefore quickly abandoned. We eventually found that dehydrochlorination of hydroxylamine hydrochloride can be effectively carried out with triethylamine as the base and DMF as the solvent. The Et_3N•HCl salt is insoluble and is easily filtered off leaving a solution of free hydroxylamine for reaction with hydroxyimidoyl chloride.

The synthesis of hydroxyimidoyl chloride **4.18a** was also modified. Chlorine gas is poisonous, difficult to add stoichiometrically, and can chlorinate other parts of the molecule (particularly aromatic rings). Fortunately, chlorinating agents other than Cl_2 can be employed. *N*-chlorosuccinimide (NCS) is known to cleanly, effectively, and safely chlorinate oximes in DMF.[135] For example, the preparation of 2-methoxybenzohydroxyimidoyl chloride using Cl_2 gas was unsuccessful; only ring chlorinated products were obtained. When oxidized with NCS in DMF, 2-methoxybenzohydroximoyl chloride was obtained in 92 % yield with no detectable ring chlorination. Therefore, NCS in DMF was employed to chlorinate oxime **4.17** to hydroxyimidoyl chloride **4.18**.

At this point, the potential allergenic properties of these compounds need to be mentioned. While working on the synthesis of compound **4.16a**, two members of our lab contracted severe itching blisters. It is not clear which compounds caused the allergenic reaction (**4.18a**, **4.19a**, **4.20a**, or **4.16a**). There is evidence in the literature of nitrile oxides and furoxans exhibiting these properties.[133,136] We suspect it was hydroxyimidoyl **4.18a** and for these reasons other derivatives were pursued.

Fortunately, the *p*-tolyl substituted derivatives (**4.18b-4.20b**) did not appear to be allergenic. More importantly, the rate of dimerization of the *p*-tolyl substituted nitrile

oxide is much slower (5-7 days) than the phenyl substituted nitrile oxide (30-60 min).[133] It is recommended that proper precaution be used when working with these compounds.

In the synthesis of **4.16b** (Scheme 4.4), the order in which the reagents are added was found to be important. Thus, a freshly generated solution of hydroxyimidoyl chloride **4.18b** is added to a cold solution of hydroxylamine. Nitrile oxide **4.20b** is generated *in situ* in the presence of excess hydroxylamine which forms hydroxyamidoxime **4.16b** and minimizes the formation of the furoxan by-product **4.19b**. Hydoxyamidoxime **4.16b** is obtained from CH_2Cl_2 as a white crystalline solid in 25-45% yield. The ^1H NMR in d_6-DMSO is shown in Figure 4.5. Sharp singlets at 10.2, 8.3 and 8.1 ppm characterize the NH and the two OH groups. The two doublets at 7.4 and 7.1 ppm are due to the aromatic protons and the singlet at 2.3 ppm is assigned to the methyl group. Mass spectrometry gives the expected M + 1 peak (167 m/z). Both elemental analysis and IR spectroscopy give results consistent with the proposed structure. The product can be stored for several months in the solid state without decomposition. After long term storage (> 3 months), **4.16b** decomposes to furoxan **4.19b** and other unidentifiable products.

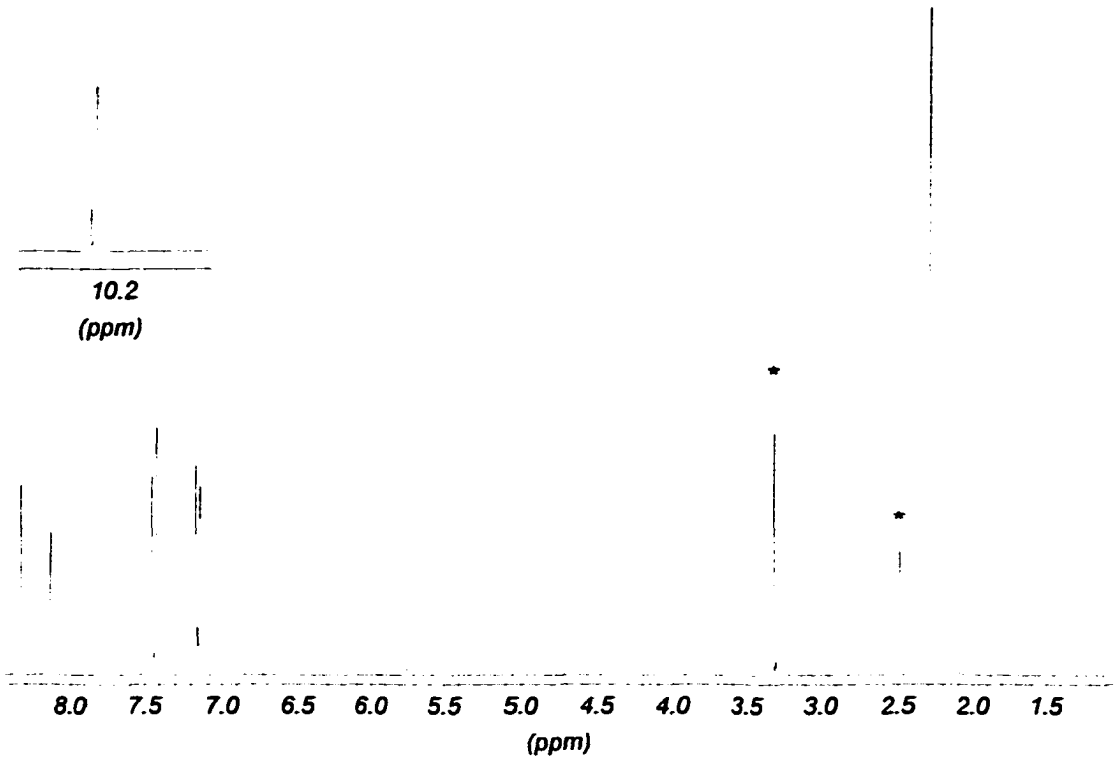

Figure 4.5. ^{1}H NMR spectrum of hydroxyamidoxime **4.16b** in d_6-DMSO. The peaks with asterisks at 2.5 and 3.3 ppm are due to DMSO and water respectively.

Although the reaction is performed identically each time, the yield of the reaction fluctuates. The reasons for this capricious behaviour are not yet understood, however, the synthetic modifications are an improvement over the literature procedures.

4.4 Cyclization reactions of hydroxyamidoxime 4.16b

Hydroxyamidoxime **4.16b** can be regarded as a 1,3-diol and therefore the cyclization reactions can be viewed as a "protection" of the diol moiety. Based on a literature procedure converting 1,3 diols to cyclic carbonates, we first attempted to cyclize **4.16b** using triphosgene.[137] A solution of triphosgene was slowly added to a cold

solution of **4.16b** in the presence of an external base (Scheme 4.5). TLC analysis of the crude reaction mixture suggested several products. The ^{1}H NMR spectrum of the crude reaction mixture was very complicated, also suggesting the production of multiple products. A wide range of reaction conditions were varied, (including solvent, temperature, and base) and in each case the desired product was not isolated.

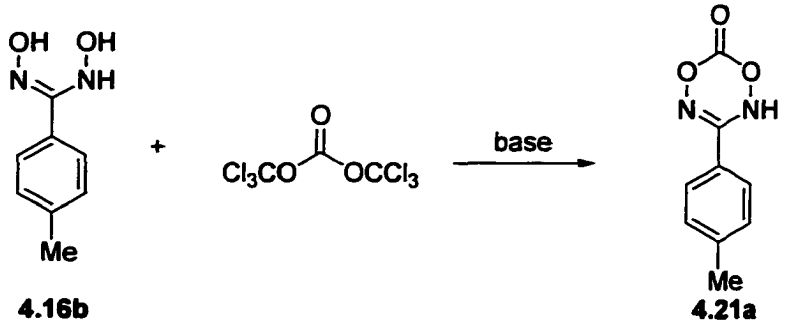

Scheme 4.5. Attempted synthesis of dioxadiazine **4.21a**.

Cyclization reactions of **4.16b** with a wide range of electrophiles were explored. This includes phosgene synthons such as carbonyl diimidazole, dimethyl carbonate, and carbon dioxide, as well as other main group electrophiles with reactive P-Cl and Si-Cl groups (Scheme 4.6). Unfortunately, none of these reactions proceeded as desired. In each case many unidentifiable products were formed.

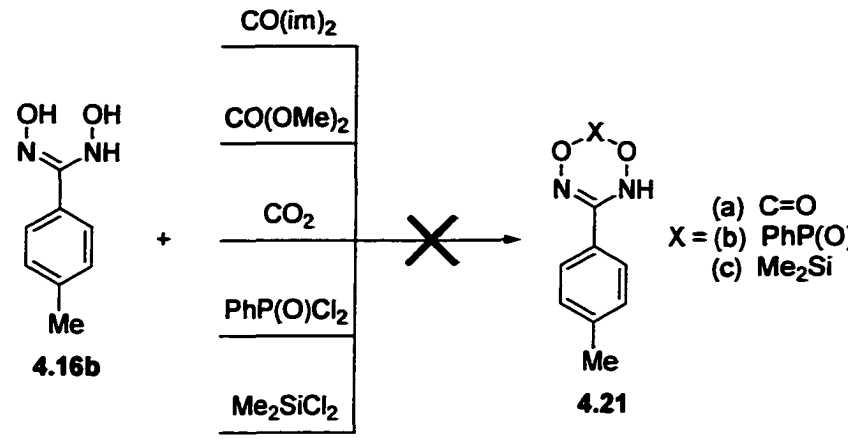

Scheme 4.6. Attempted synthesis of **4.21** using various electrophiles.

The next attempted synthesis of **4.21** employed electrophiles with two different leaving groups with substantially different activity (Scheme 4.7). Thus, reaction of **4.16a** with ethyl chloroformate should give **4.22** as an isolable intermediate. Nucleophilic attack of the hydroxy group under more forcing conditions may then afford the desired product **4.21a**. However, when hydroxyamidoxime **4.16a** was reacted with ethyl chloroformate, only product **4.23** was isolated. Clearly, the loss of the OH functionality in **4.23** prevents any possibility of isolating dioxadiazine **4.21a**. Compound **4.23** may provide some insight into the possible pathways for reactions in Scheme 4.5 and Scheme 4.6. In the case of the reactions in Scheme 4.5 and Scheme 4.6, loss of the OH functionality could then be followed by more decomposition reactions giving rise to the myriad of products observed. Despite many reactions with a variety of electrophiles and different reaction conditions, the desired dioxadiazine product was never isolated. It appears that reaction of hydroxyamidoxime with strong electrophiles proceeds in an uncontrolled fashion.

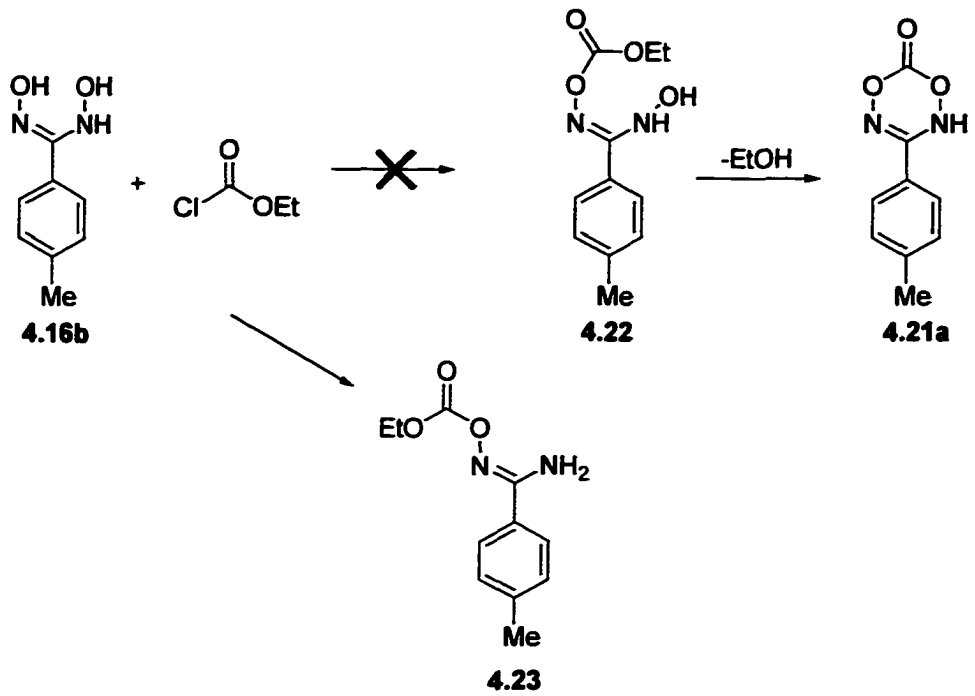

Scheme 4.7. Reaction pathway of **4.16b** with ethyl chloroformate.

We then turned to the reaction of **4.16b** with milder electrophiles, namely aldehydes and ketones. The initial reaction between hydroxyamidoxime **4.16b** and propionaldehyde under acid catalyzed conditions gave dioxadiazine **4.24a** (Scheme 4.8).

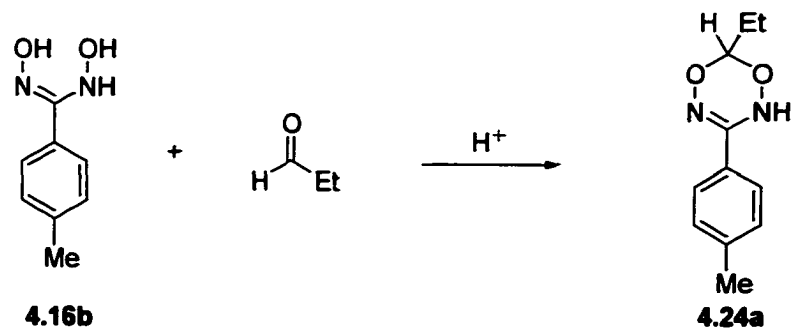

Scheme 4.8. Cyclization of **4.16b** with propionaldehyde.

Dioxadiazine **4.24a** was purified by flash chromatography on silica gel to give a white solid in 88% yield. The product slowly decomposes in solution and in the solid state.

The characterization data are fully consistent with the proposed structure. In the ^{1}H NMR spectrum (Figure 4.6), the NH proton appears as a singlet at 6.3 ppm. The methine proton gives a triplet at 5.3 ppm. The methylene and methyl protons of the ethyl group appear as a multiplet and a triplet at 1.8 and 1.0 ppm respectively. Finally, the pair of doublets at 7.7 and 7.2 ppm are due to the four aromatic protons. When the ^{1}H NMR of **4.24a** is run in d_6-DMSO, the singlet at 6.3 ppm is shifted to 9.9 ppm which is consistent with the general solvent dependence of NH protons.

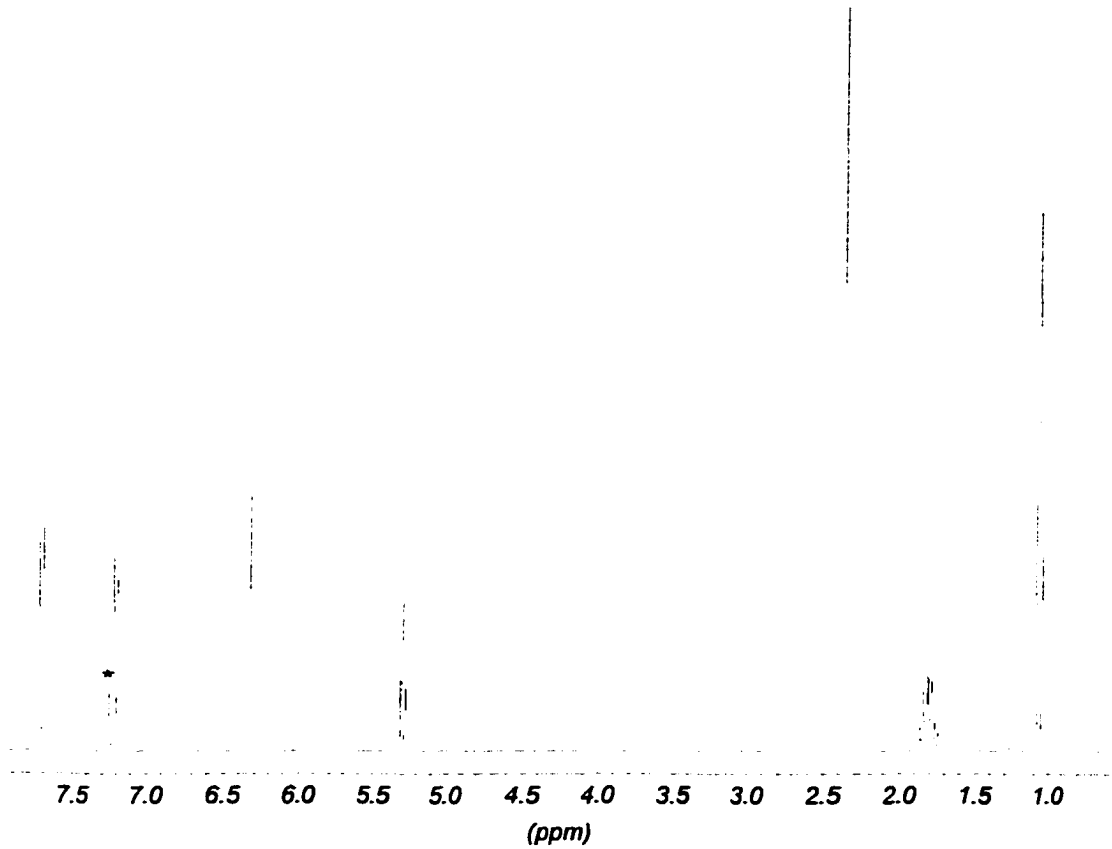

Figure 4.6. The ^{1}H NMR spectrum of compound **4.24a** in $CDCl_3$. The asterisk denotes the residual $CHCl_3$ peak.

The ^{13}C NMR gives the expected nine resonances. A strong band at 3276 cm^{-1} (νNH) is observed in the IR spectrum. Mass spectrometry gives the correct molecular ion (m/z = 207, M + 1) and the elemental analysis agrees with the calculated values within the allowable limits.

Although the data for compound **4.24a** are encouraging, they are not unambiguous. An alternative structure for the product of Scheme 4.8 can be envisioned – **4.24b** – which would also be entirely consistent with the available data. Examination of the mechanism provides some insight into how **4.24a** and **4.24b** could form. As shown in Scheme 4.9, ring closure of presumed intermediate **4.25** can proceed by attack by either the OH or NH group, accompanied by loss of water. Attack by the OH group would give the desired product **4.24a**. Attack by the NH group would give the five membered *N*-hydroxy-1,2,4-oxadiazolidine **4.24b**.

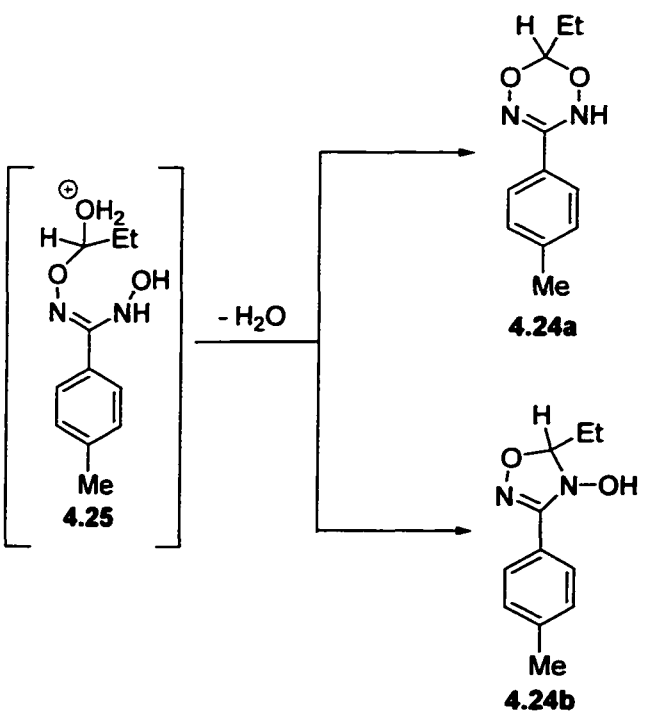

Scheme 4.9. Possible cyclization pathways of intermediate **4.25**.

It is not immediately obvious which pathway is favoured. The possible resonance structures for **4.25** in which the nitrogen lone pair is delocalized would lower the nucleophilicity of nitrogen and therefore favour the OH group as the nucleophile (Figure 4.7). However, in general five-membered ring formation is favoured over six-membered ring formation in cyclization reactions and this argument would favour NH attack.

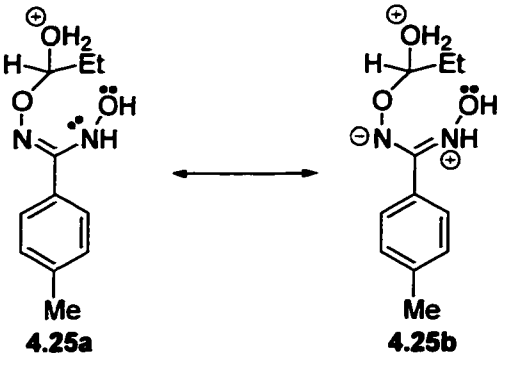

Figure 4.7. Resonance contributors for intermediate **4.25**.

The ways in which **4.24a** and **4.24b** can be distinguished from each other are limited. A lack of precedent for either kind of molecule means that there are no reference compounds to aid in the assignments of the ^{1}H and ^{13}C NMR spectra. Elemental analysis and mass spectrometry are not helpful because both compounds have the same molecular formula. The differences in the ^{13}C spectra would be expected to be small. Similar problems could be expected in the ^{1}H spectra. The only potential diagnostic peaks between **4.24a** and **4.24b** are the NH and OH protons. Both NH and OH resonances can be found over a large ppm range and both are susceptible to exchange with the solvent protons. The same problem can also occur in IR spectroscopy; the distinction between NH and OH stretches is not always obvious. In the case of **4.24**, the shape of the strong, somewhat broad peak at 3276 cm^{-1} does not allow distinction between an NH and an OH stretch, although the broadness of the peak is more characteristic of OH stretches. An X-

ray crystal structure would allow for definitive assignment of the molecular structure, however, we were not able to grow crystals of suitable quality.

The synthesis of other dioxadiazine derivatives was explored. Compounds **4.26** and **4.27** were synthesized according to Scheme 4.10 using *p*-tolualdehyde and acetone respectively.

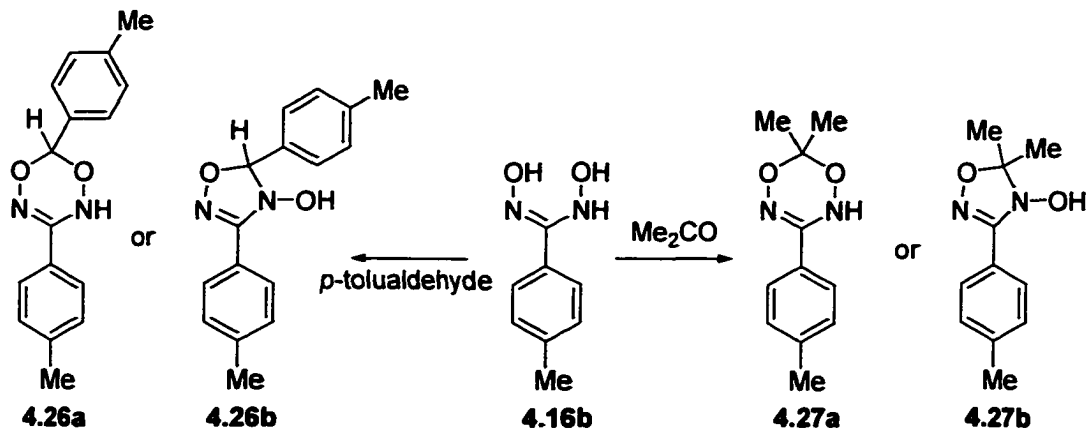

Scheme 4.10. Synthesis of **4.26** and **4.27**.

Product **4.26** was purified by flash chromatography on silica gel to give a white solid in 31% yield. Unlike **4.24**, **4.26** is indefinitely stable in solution and in the solid state. Unfortunately, spectroscopic characterization of **4.26** was also inconclusive. Similar to **4.24**, the data are fully consistent with both the six-membered ring **4.26a** and the five-membered ring **4.26b**. However, the IR, ^{1}H, and ^{13}C NMR spectra for compound **4.26** were almost identical to those of compound **4.24**. This may suggest that **4.24** and **4.26** have analogous structures.

Reaction of **4.16b** with acetone gave compound **4.27** as a white solid which was purified by flash chromatography on silica gel in 54% yield. The purified product slowly oxidized in air to a red solid. Compound **4.27** was fully characterized and also gave nearly identical peaks to **4.24** and **4.26** in the IR, ^{1}H and ^{13}C NMR spectra.

Unfortunately, we were not able to grow crystals suitable for X-ray analysis for compounds **4.26** and **4.27**.

An alternative method to unambiguously assign the structure of compounds **4.24**, **4.26**, and **4.27** would be to examine the EPR spectra of the corresponding radicals. The EPR spectra of the six-membered ring and the five-membered ring radicals should be different because the unpaired electrons are in different environments. The structures of the corresponding radicals **4.24a** and **4.24b** that would result from oxidation are shown in **4.28** and **4.29**. In the case of radical **4.28**, the EPR spectrum should consist of a predominant 1:2:3:2:1 five line pattern, consistent with the unpaired electron coupled to two equivalent nitrogen atoms (ignoring coupling to other nuclei) as indicated in Figure 4.2. In the case of radical **4.29**, the chemical inequivalency of the two nitrogen atoms should produce two different *a*(N) values and subsequently give a predominant nine line pattern consisting of a triplet of triplets.

Attempts to oxidize **4.24** or **4.26** were unsuccessful. The standard oxidants to prepare verdazyls (benzoquinone, DDQ, and PbO_2) failed to react. Deprotonation to the anion followed by oxidation to the radical was also unsuccessful using NaH. A stronger base, *n*BuLi, was tried which produced yellow solutions initially believed to be the anion. However, attempts to oxidize these yellow solutions (O_2, I_2) did not produce the radicals. It would seem unlikely that the yellow solutions were due to the anion as they would likely react with O_2 or I_2 to produce the desired radicals.

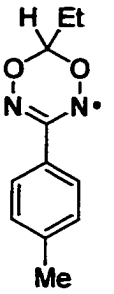

4.28

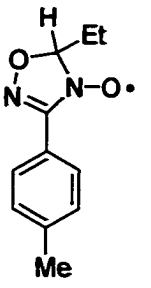

4.29

It was expected that it would be more difficult to prepare the dioxadiazinyls by oxidation than the corresponding oxidation reaction of the tetrazanes to verdazyls, because two nitrogen atoms were replaced with more electronegative oxygen atoms. This is corroborated by the semi-emperical calculations (Figure 4.3) which indicated that the SOMO of **4.9** was lower in energy than **4.8**. However, even considering these factors, it is still surprising that **4.24** and **4.26** could not be oxidized.

In contrast to **4.24** and **4.26**, a CH_2Cl_2 solution of **4.27** was oxidized with benzoquinone to give a cherry red solution. Solutions of the radical decomposed within 24 hours preventing isolation of this species. The experimental and simulated EPR spectra of this solution are shown in Figure 4.8. The nine line pattern is consistent with the unpaired electron coupling to two *inequivalent* nitrogen atoms (8.5 G and 5.65 G). We are left to conclude that the radical generated was most likely nitroxide **4.30** and not dioxadiazinyl **4.31**.

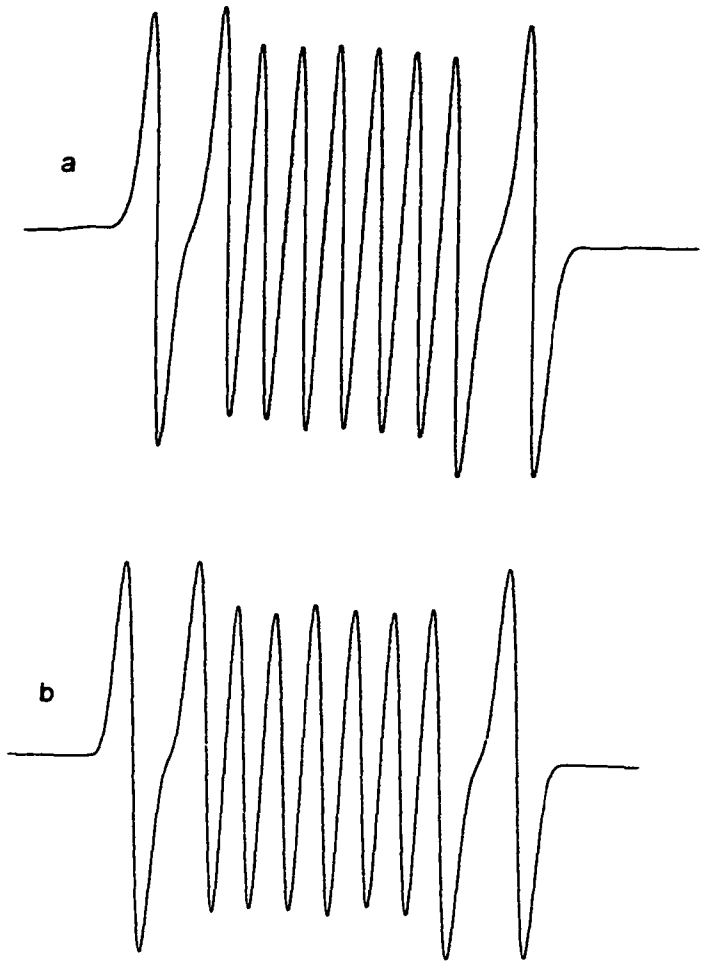

Figure 4.8. Experimental (a) and simulated (b) EPR spectra of **4.30**. The sweep width of the experimental spectrum is 100 G.

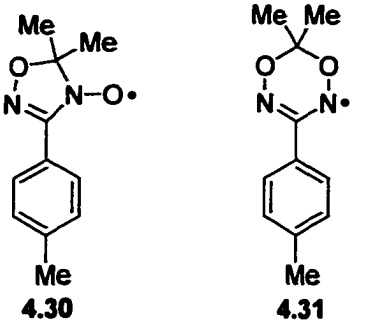

4.30 **4.31**

The differences in chemical reactivity between **4.24/4.26** and **4.27** can be interpreted in one of two ways. If we assume that compounds **4.24** and **4.26** are the desired six-membered dioxadiazines, this would suggest that the cyclization reactions of **4.16b** are substrate dependent; aldehydes give the six-membered dioxadiazines and the ketone gives the five-membered oxadiazolidine **4.27b**. Alternatively, assuming the five membered rings **4.24b** and **4.26b** were made in each case, the observed differences in chemical reactivity may be due to more subtle factors. One feature that distinguishes **4.27** and **4.24/4.26** is that the former has a methine proton α to the hydroxylamine nitrogen atom. Hydroxylamines with protons attached to the α-carbon are known to decompose to nitrones when oxidized.[14] Therefore, we may have been forming the radicals but the presence of the methine proton could have led to rapid decomposition to nitrone **4.33** (Scheme 4.11). However, nitrone formation was not observed and colour changes (indicative of the radical) were also not observed. These are only qualitative observations and therefore the structure of compounds **4.24** and **4.26** are still open to debate.

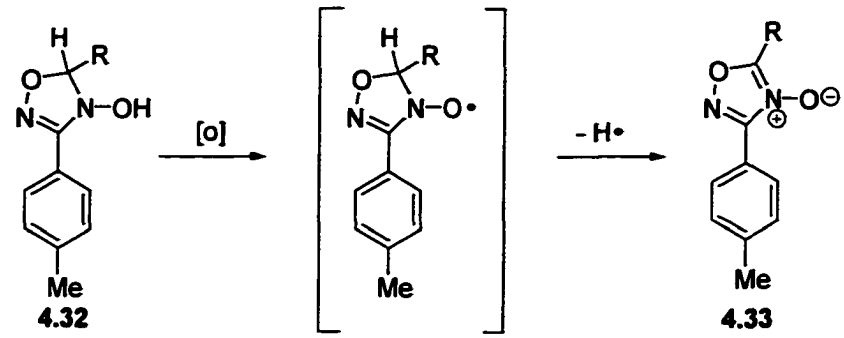

Scheme 4.11. Formation of nitrone **4.33** from hydroxylamine **4.32.**

4.5 Conclusions

This chapter describes our efforts to prepare a new class of radicals, the dioxadiazinyls. An intermediate, hydroxyamidoxime **4.16b**, was prepared and fully characterized. This compound undergoes cyclization reactions with propionaldehyde, *p*-tolualdehyde, and acetone. However, the products from the cyclization reactions could not be unambiguously assigned. The characterization data for each compound are fully consistent with the six-membered dioxadiazines (**4.24a** and **4.26a**) or with the five membered hydroxylamines (**4.24b** and **4.26b**). Attempts to oxidize **4.24** and **4.26** have failed and thus the structure of these two compounds is still open to debate.

The reaction of **4.16b** with acetone produced hydroxylamine **4.27b** and not the desired dioxadiazine **4.27a**. This conclusion was based on the EPR spectrum of the species we oxidized (**4.27**) which we assigned as radical **4.30**. The similarities of the spectroscopic characteristics between **4.27b** and **4.24/4.26** would suggest that the structure of compounds **4.24** and **4.26** are the five-membered oxadiazolidines. Despite the spectroscopic similarities, there are still differences in their reactivity, which precludes definitive assignments for **4.24**, **4.26**, and **4.27**.

If the five-membered hydroxylamines are the products, a different synthetic approach will be needed to access the dioxadiazinyl targets. Two similar possibilities are outlined in Scheme 4.12. The reaction of ethyl chloroformate with oxime **4.17b** should give **4.34** as an isolable intermediate. Chlorination of **4.34** with NCS could then give compound **4.35**. Reaction of **4.35** with hydroxylamine under forcing conditions could then cyclize to give dioxadiazine **4.21**. Alternatively, reaction of **4.34** with hydroxylamine could give dioxadiazane **4.36**. The synthetic approaches outlined in Scheme 4.12 are similar to Neugebauer's alternative synthesis of the 6-oxo and 6-thioxoverdazyls described in Scheme 3.6 from Chapter 3.[106]

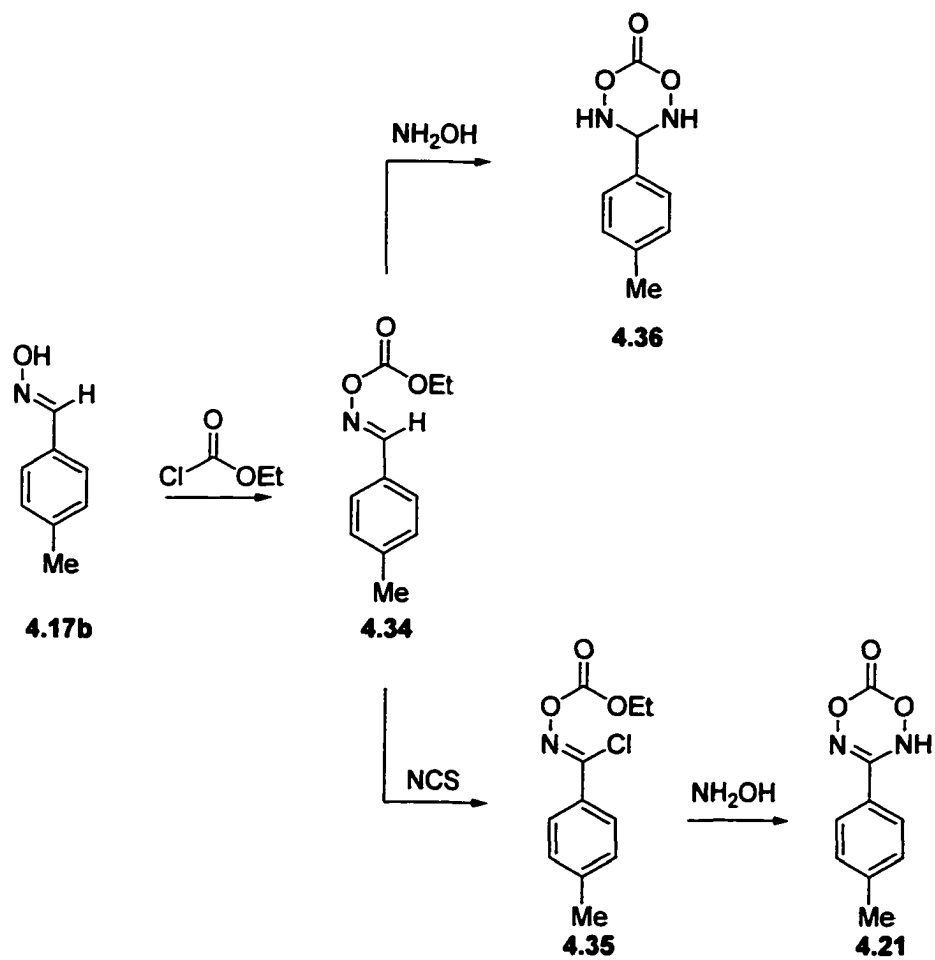

Scheme 4.12. Alternative synthesis of dioxadiazine **4.21**.

4.6 Experimental

Attempted synthesis of N-Hydroxybenzamidoxime (4.16a)

A slurry of hydroxylamine hydrochloride (465 mg, 6.69 mmol) and ethylenediamine (404 mg, 6.72 mmol) in 8 mL CH_2Cl_2 was vigorously stirred to produce a biphasic system. To this slurry was added a solution of **4.18a** (1.03 g, 6.62 mmol) in 5 mL CH_2Cl_2. The white precipitate, which immediately formed was filtered and the filtrate concentrated to an off-white waxy solid, yield 329 mg (32.6%). The product was crystallized from EtOAc to give yellow crystals. ^{1}H NMR and mass spectrometry confirm that the product isolated was furoxan **4.19a** and not **4.16a**. ^{1}H NMR ($CDCl_3$): δ 8.66 (d, 2H, J = 7.4 Hz), 8.46 (d, 2H, J = 7.4 Hz), 7.66-7.35 ppm (m, 6H). MS (FAB, *m*NBA): m/z 239 (M + 1).

Synthesis of N-Hydroxy-*p*-toluamidoxime (4.16b)

Triethylamine (5.0 mL, 36.1 mmol) was added via syringe to a solution of hydroxylamine hydrochloride (2.150 g, 31.0 mmol) in 35 mL DMF. A white precipitate immediately formed. After stirring for 2 h, the solution was filtered and the filtrate cooled in an ice bath. To this cold solution was added a solution of **4.18b** (2.54 g, 15.0 mmol) in 15 mL DMF via syringe. A white precipitate quickly formed. After stirring for 16 h the solution was poured onto 200 ml water. The aqueous solution was extracted 2x with 200 mL ether. The combined organics were washed 2x 200 mL water and 1x 200 mL brine. The organic layer was dried over Na_2SO_4, gravity filtered, and concentrated under vacuo to a green oil. Upon addition of CH_2Cl_2, the product precipitates as a white

microcrystalline solid, 896 mg (36%). ^{1}H NMR (DMSO): δ 10.25 (s, 1H), 8.34 (d, 1H, J = 1.5 Hz), 8.14 (d, 1H, J = 1.5 Hz), 7.44 (d, 2H, J = 8.1 Hz), 7.16 (d, 2H, J = 8.1 Hz), 2.30 ppm (s, 3H). ^{13}C NMR (DMSO): δ 156.9, 138.2, 129.3, 128.4, 127.7, 20.9 ppm. IR (KBr): 3350 (s), 3322 (s), 3075 (m), 2784 (s, broad), 1623 (s), 1523 (m), 1481 (m), 1382 (w), 1372 (sh), 1341 (m), 1285 (w), 1215 (w), 1185 (w), 1125 (w), 1114 (w), 1057 (w), 1034 (w), 961 (w), 946 (s), 823 (s), 775 (m), 756 (w), 726 (w), 672 (w), 635 (w), 602 (w), 524 (w), 483 (m) cm^{-1}. Mp: 88-89 °C. Anal Calcd. for $C_8H_{10}N_2O_2$: C, 57.82; H, 6.07; N, 16.86. Found: C, 57.85; H, 5.96; N, 16.83. MS (CI methane): m/z 167 (M + 1), 195 (M + 29), 207 (M + 41).

Synthesis of Benzaldehyde chloroxime (4.18a)

Chlorine gas was bubbled through a solution of **4.17a** (261 mg, 2.16 mmol) in 10 mL MeOH at 0 °C until the blue colour no longer persisted. The solution was diluted with 10 mL of water and extracted with 15 mL ether. The organic layer was washed with 10 ml of water and dried over Na_2SO_4. The solution was concentrated to an off white solid. The product was used without further purification. ^{1}H NMR (DMSO): δ 12.24 (s, 1H), 7.82-7.79 (m, 2H), 7.49-7.40 (m, 3H).

Synthesis of *p*-Tolualdehyde chloroxime (4.18b)[135]

NCS (2.006 g, 15.0 mmol) was added in small portions to a stirring solution of *p*-tolualdehyde oxime (2.025 g, 15.0 mmol) in 15 mL DMF. Each portion was added once the orange colour had dissipated and the reaction solution has cooled. Once the addition was completed the yellowish solution was poured onto 70 mL water. The aqueous layer

was extracted 2x 70 mL ether. The organic layer was washed 2x 70 mL water and once with 70 mL brine. The organic layer was dried over Na_2SO_4, filtered, and concentrated in vacuo to a white solid. The solid was used without further purification. ^1H NMR ($CDCl_3$): δ 7.84 (s, 1H), 7.71 (d, 2H, J = 8.1 Hz), 7.20 (d, 2H, J = 8.1 Hz), 2.37 ppm (s, 3H).

General reaction for the attempted synthesis of (4.21a)

A solution of triphosgene (74 mg, 0.25 mmol) in 1 mL CH_2Cl_2 was added dropwise to a solution of **4.16b** (83 mg, 0.50 mmol) and pyridine (0.25 mL, 3.1 mmol) in 1.5 mL CH_2Cl_2 at –78 °C. A white precipitate immediately formed and the solution turned green. Once the addition was complete, the solution was allowed to slowly warm to room temperature and stir at room temperature for 10 h. The resultant yellow solution was quenched with 10 mL saturated NH_4Cl. The aqueous layer was extracted with 10 mL CH_2Cl_2, and then the combined organic layers were washed with 10 mL 1M HCl, saturated $NaHCO_3$, and brine. The organic layer was dried over $NaSO_4$, gravity filtered and concentrated to a yellow semi-solid. The crude solid was chromatographed on silica gel. No isolable product was obtained.

General reaction for the attempted synthesis of (4.21b)

A solution a $Me_2NP(O)Cl_2$ (203 mg, 1.25 mmol) in 40 mL THF was added dropwise over a 2 h period to a solution of **4.16b** (202 mg, 1.22 mmol) and Et_3N (0.35 mL, 2.52 mmol) in 20 mL THF at –42 °C. During the addition a white precipitate formed. Once the addition was complete, the solution was allowed to slowly warm to

room temperature and stir for 10 h. The resultant yellow solution was filtered and concentrated to a yellow oil. The oil was chromatographed on silica gel. No isolable product was obtained.

General reaction for the attempted synthesis of (4.21c)

A solution of Me_2SiCl_2 (0.15 mL, 1.23 mmol) in 5 mL CH_2Cl_2 was added dropwise to a solution of **4.16b** (206 mg, 1.20 mmol) and Et_3N (0.33 mL, 2.38 mmol) in 15 mL CH_2Cl_2. The solution was allowed to stir at room temperature for 10 h. The reaction mixture was concentrated to a white solid. The solid was dissolved in ether (50 mL) and water (50 mL). The layers were separated and the organic layer was washed with another 50 mL portion of water. The organic layer was dried over $MgSO_4$, gravity filtered, and concentrated to a white oil. The oil was solidified with the addition of $CHCl_3$. The crude solid was chromatographed on silica gel. No isolable product was obtained.

Reaction of ethyl chloroformate with 4.16b (4.23)

A solution of ethyl chloroformate (0.12 mL, 1.26 mmol) in 10 mL THF was added dropwise to a solution of **4.16b** (201 mg, 1.21 mmol) and 2,4,6-trimethylpyridine (0.155 mL, 1.17 mmol) in 50 mL THF at –78 °C. The solution was allowed to stir for 16 h during which a white precipitate formed. The solution was gravity filtered and concentrated in vacuo to a white gummy solid. The solid was chromatographed on silica gel (hexanes/CH_2Cl_2, 1/1) and recrystallized from hexanes/EtOAc (4/1) to give a white solid, yield 56 mg (20%). ^{1}H NMR ($CDCl_3$): δ 7.53 (d, 2H, J = 8.1 Hz), 7.15 (d, 2H, J =

8.1 Hz), 5.11 (s, 2H), 4.27 (q, 2H, J = 7.4 Hz), 2.32 (s, 3H), 1.31 ppm (t, 3H, J = 7.4 Hz). ^{13}C NMR ($CDCl_3$): δ 156.3, 153.8, 141.1, 129.3, 127.9, 126.5, 64.4, 21.3, 14.2 ppm. IR (KBr): 3490 (s), 3350 (s), 2980 (m), 2913 (w), 1751 (s), 1622 (s), 1583 (s), 1564 (m), 1520 (w), 1476 (m), 1449 (w), 1406 (s), 1367 (s), 1250 (s), 1183 (m), 1116 (m), 1071 (w), 1006 (m), 928 (m), 855 (m), 827 (s), 780 (m), 727 (w), 685 (w), 651 (w), 604 (w), 540 (w), 492 (m) 429 (w) cm^{-1}. MS (EI): m/z 222 (M^+).

Synthesis of 6-ethyl-3-*p*-tolyl-1,5,2,4-dioxadiazine (4.24a)/

5-ethyl-4-hydroxy-3-*p*-tolyl-1,2,4-oxadiazolidine (4.24b)

To a stirring solution of **4.16b** (201 mg, 1.21 mmol) in 10 mL 100% EtOH was added propionaldehyde (0.1 mL, 1.4 mmol) followed by *p*-toluenesulfonic acid monohydrate (~7-8 mg). The reaction was monitored by TLC. After 2.5 h, the reaction mixture was concentrated in vacuo to a white solid. The solid residue was chromatographed on silica gel (EtOAc/hexanes, 1/9) to give the product as a white fluffy solid, yield 220 mg (88%). ^{1}H NMR ($CDCl_3$): δ 7.70 (d, 2H, J = 8.09 Hz), 7.19 (d, 2H, J = 8.09 Hz), 6.31 (s, 1H), 5.28 (t, 1H, J = 5.88 Hz), 2.36 (s, 3H), 1.89-1-72 (m, 2H), 1.05 ppm (t, 3H, J = 7.36 Hz). ^{13}C NMR ($CDCl_3$): δ 159.2, 141.1, 129.4, 127.5, 122.8, 102.1, 25.0, 21.5, 8.5 ppm. IR (KBr): 3276 (s), 2968 (m), 2923 (m), 2877 (m), 2849 (w), 1609 (w), 1597 (m), 1567 (w), 1512 (m), 1461 (m), 1426 (m), 1382 (w), 1363 (w), 1345 (s), 1322 (w), 1307 (w), 1285 (w), 1262 (w), 1183 (w), 1134 (s), 1116 (w), 1076 (w), 1053 (w), 1020 (w), 980 (s), 919 (m), 907 (s), 878 (m), 824 (s), 796 (w), 771 (w), 749 (w), 720 (w), 699 (w), 679 (w), 637 (w), 605 (w), 510 (w), 494 (w), 481 (w) cm^{-1}. Mp: 105-106

°C. Anal Calcd. for $C_{11}H_{14}N_2O_2$: C, 64.06; H, 6.84; N, 13.58. Found: C, 64.26; H, 6.96; N, 13.61. MS (FAB, *m*NBA): m/z 207.1 (M + 1).

Synthesis of 3,6-Di-*p*-tolyl-1,5,2,4-dioxadiazine (4.26a)/ 4-hydroxy-3,5-di-*p*-tolyl-1,2,4-oxadiazolidine (4.26b)

To a solution of **4.16b** (200 mg, 1.20 mmol) in 10 mL 100% EtOH was added *p*-tolualdehyde (147 mg, 1.22 mmol) followed by *p*-toluenesulfonic acid monohydrate (~8 mg). The solution was refluxed for 8.5 h then stirred at room temp for an additional 16 h. The solution was concentrated in vacuo to a white solid. The solid residue was chromatographed on silica gel (EtOAc/hexanes, 1/19) to give the solid as a white solid, yield 101 mg (31%). ^{1}H NMR (DMSO): δ 9.93 (s, 1H), 7.70 (d, 2H, J = 8.09 Hz), 7.40 (d, 2H, J = 8.09 Hz), 7.30 (d, 2H, J = 8.09 Hz), 7.25 (d, 2H, J = 8.09 Hz), 6.11 (s, 1H), 2.35 (s, 3H), 2.32 ppm (s, 3H). ^{13}C NMR (DMSO): δ 159.6, 140.7, 138.9, 133.2, 129.3, 129.0, 127.3, 127.2, 122.4, 100.5, 21.0, 20.8 ppm. IR (KBr): 3213 (s, br), 2860 (m), 1566 (m), 1559 (w), 1507 (m), 1445 (m), 1411 (m), 1382 (w), 1362 (w), 1338 (s), 1304 (m), 1289 (m), 1264 (w), 1206 (w), 1182 (m), 1106 (s), 1019 (m), 1005 (w), 950 (w), 922 (m), 905 (s), 882 (w), 814 (s), 777 (m), 724 (m), 677 (w), 637 (w), 612 (w), 567 (w), 547 (m), 499 (m) cm^{-1}. Mp: 99-100 °C. MS (FAB, *m*NBA): m/z 269.1 (M + 1). Exact Mass (FAB): Actual, 268.1211. Found, 268.1286.

Synthesis of 5,5-Dimethyl-4-hydroxy-3-*p*-tolyl-1,2,4-oxadiazolidine (4.27b)

p-Toluenesulfonic acid monohydrate (~8 mg) was added to a solution of **4.16b** (197 mg, 1.19 mmol) in 10 mL acetone. The solution was gently refluxed for 30 min

after which the solution was concentrated in vacuo to a white solid. The solid residue was chromatographed on silica gel (EtOAc/hexanes, 1/9) to give the product as a white crystalline solid, yield 132 mg (54%). Upon exposure to air, the solid slowly oxidizes to a red solid. ^{1}H NMR (DMSO): δ 9.30 (s, 1H), 7.66 (d, 2H, J = 8.83 Hz), 7.27 (d, 2H, J = 8.09 Hz), 2.34 (s, 3H), 1.42 ppm (s, 6H). ^{13}C NMR (DMSO): δ 158.8, 140.2, 129.1, 127.0, 123.6, 100.8, 22.2, 21.0 ppm. IR (KBr): 3225 (s, br), 3014 (w), 2985 (w), 2854 (w), 1618 (w), 1593 (w), 1560 (w), 1511 (w), 1450 (s), 1385 (m), 1370 (m), 1349 (w), 1305 (w), 1269 (w), 1219 (w), 1181 (w), 1151 (w), 1115 (w), 1085 (w), 1040 (w), 1019 (w), 967 (w), 926 (s), 903 (w), 831 (w), 815 (s), 796 (w), 722 (m), 688 (w), 656 (w), 589 (w), 546 (w), 496 (m) cm^{-1}. Mp: dec 120 °C. MS (FAB, *m*NBA): m/z 207 (M + 1). Exact Mass (FAB): Actual, 206.1055. Found, 206.1130.

Synthesis of nitroxide (4.30)

Benzoquinone (35 mg, 0.32 mmol) was added to a solution of **4.27b** (132 mg, 0.640 mmol) in 20 ml CH_2Cl_2. The solution quickly turned an intense red. UV-vis (CH_2Cl_2): λ_{max} = 547, 508 (sh), 590 nm (sh).

Chapter 5

Conclusions

5.1 Conclusions and General Remarks

The goal of this thesis was the targeted synthesis of new stable radicals. As evident with the many difficulties encountered throughout this thesis, the design of stable radicals is not trivial. This was most evident in Chapter 2, in which the thioaminyls targeted can at best be described as persistent. We were unsuccessful at preparing any thioaminyl diradicals and therefore were unable to test our hypothesis that thioaminyls **2.10** should be stable, high–spin molecules. Even though bis(sulfenamide) **2.18** is a direct extension of sulfenamide **2.23b**, the former could not be oxidized. This underlines an important point regarding radicals, that is, the synthesis of simple systems does not necessarily translate to more complex ones.

The synthesis of new heteroverdazyls was accomplished. The insertion of phosphorus at the 6–position in the verdazyl core affects the electronic nature of the radical. The geometry of the verdazyl ring (flat versus puckered) appears to be sensitive to the nature of the substituents attached to phosphorus. For example, the small structural difference at phosphorus between phosphaverdazyls **3.25** and **3.33** (phenyl and dimethylamino respectively) is enough to alter the shape from a puckered geometry to a flat geometry respectively. There appears to be a correlation between the geometry of the verdazyl ring and the spin density found at phosphorus. When the spin at phosphorus is zero (as found by EPR spectroscopy) the verdazyl ring is predicted to be flat because at

the HMO level, a node passes through the 3 and 6 positions. This is corroborated by the results of high level DFT calculations.

Exocyclic spin–leakage was observed for phosphaverdazyl **3.33**. This was rationalized from a mechanism involving spiroconjugation. This is also corroborated by DFT calculations. Spiroconjugation is interesting because it provides an alternative mechanism for spin propagation from the conventional π conjugated systems.

We synthesized and fully characterized the hydroxyamidoxime intermediate **4.16b**. Cyclization of **4.16b** was accomplished with aldehydes and a ketone. The reaction of **4.16b** with acetone yields the five membered oxadiazolidine **4.27b**. Oxidation with benzoquinone gives nitroxide **4.30** as confirmed by EPR spectroscopy. Reactions of **4.16b** with *p*-tolualdehyde and propionaldehyde yield products which have yet to be identified. Spectral data cannot unambiguously determine whether the cyclization products are the desired six membered dioxadiazines or the five membered oxadiazolidines. Without clear identification of the radical precursors it is difficult to assess whether the dioxadiazinyls are feasible. As discussed in Chapter 4, these radicals are attractive for several reasons. Their simplified EPR spectra would render them easier to characterize and low–level calculations predict them to have superior stability compared with the verdazyls. Perhaps the most attractive feature is their potential as ligands in transition metal complexes. The reduced steric requirements of the dioxadiazinyl system offer two advantages over the verdazyls. Unlike the verdazyls, which can only coordinate two chelates around the metal center, the dioxadiazinyls should be able to coordinate three chelates around a metal. Also, the less sterically demanding dioxadiazinyl chelate should form stronger ligand–metal interactions. These

stronger interactions could have magnetic consequences. For these reasons the dioxadiazinyls merit further research (see below).

5.2 Future Directions

Of the systems discussed, there are still many avenues worth exploring. For example, the synthesis and characterization of diradical **3.47** and triradical **3.48** should provide an indication of the strength of interaction between the two unpaired electrons in these systems. This could also help assess the effectiveness of a P-N ring system to mediate spin-spin coupling.

As discussed above, the dioxadiazinyls still warrant more study. In light of the difficulties with our synthetic approach, it may be necessary to consider alternatives. As mentioned in Chapter 4, the synthetic route to the dioxadiazinyls based on the chemistry directly analogous to the verdazyls was not considered (see Scheme 4.1). We concluded that hydroxylamine would react with phosgene to give intermediate **4.15** and not **4.13**. However, if an oxophilic reagent was used in place of phosgene, such as R_2SiCl_2, compound **5.1** should be feasible. This is an analogue of the bis(hydrazide) reagent **3.12a**. If this intermediate could be synthesized, application of the standard verdazyl chemistry may provide a route to the elusive dioxadiazinyl ring system.

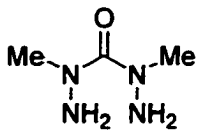

3.12a

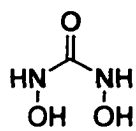

4.15

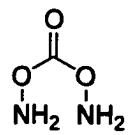

4.13

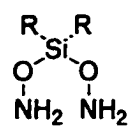

5.1

Appendix

X-ray Crystallographic Data

Table I. Summary of crystallographic data for bis(sulfenamide) **2.18**.

empirical formula	$C_{21}H_{20}N_4O_4S_2$
formula weight	456.53
space group	$Pmn2_1$
a (Å)	34.638(10)
b (Å)	4.3724(12)
c (Å)	6.9026(19)
V (Å^3)	1045.4(5)
Z	2
ρ (calcd) (g cm^{-3})	1.45
μ (mm^{-1})	0.29
radiation	MoKα, graphite monochromated
λ (Å)	0.71073
temperature (K)	293
2θ range (deg)	4-50
no. of observed reflections	5046
no. of unique reflections	1735
no. of parameters	145
R^a	0.046
$R_w{}^b$	0.102

$^a R = \Sigma(|F_o| - |F_c|) / \Sigma |F_o|$ $^b R_w = [\Sigma_w(|F_o| - |F_c|)^2 / \Sigma_w (|F_o|)^2]^{1/2}$

Table II. Bond lengths (Å) and bond angles (°) for bis(sulfenamide) **2.18**.[a]

Atoms	Distance	Atoms	Distance
S(1)-N(2)	1.683(4)	C(3)-C(4)	1.363(7)
S(1)-C(6)	1.772(4)	C(4)-C(5)	1.384(6)
O(1)-N(1)	1.214(5)	C(5)-C(6)	1.370(6)
O(2)-N(1)	1.223(5)	C(7)-C(8)	1.378(6)
N(1)-C(1)	1.429(6)	C(7)-C(10)	1.400(5)
N(2)-C(7)	1.439(5)	C(8)-C(9)	1.371(5)
C(1)-C(2)	1.382(6)	C(8)-C(12)	1.502(6)
C(1)-C(6)	1.395(6)	C(10)-C(11)	1.490(8)
C(2)-C(3)	1.354(7)		

Atoms	Angle	Atom	Angle
N(2)-S(1)-C(6)	101.2(2)	C(5)-C(6)-C(1)	116.5(4)
O(1)-N(1)-O(2)	121.8(5)	C(5)-C(6)-S(1)	121.3(3)
O(1)-N(1)-C(1)	118.8(4)	C(1)-C(6)-S(1)	122.2(3)
O(2)-N(1)-C(1)	119.5(4)	C(8)-C(7)-C(10)	121.7(4)
C(7)-N(2)-S(1)	117.3(3)	C(8)-C(7)-N(2)	119.1(4)
C(2)-C(1)-C(6)	121.8(5)	C(10)-C(7)-N(2)	119.1(4)
C(2)-C(1)-N(1)	117.6(4)	C(9)-C(8)-C(7)	117.6(4)
C(6)-C(1)-N(1)	120.5(4)	C(9)-C(8)-C(12)	119.6(5)
C(3)-C(2)-C(1)	120.2(5)	C(7)-C(8)-C(12)	122.8(4)
C(2)-C(3)-C(4)	119.2(5)	C(8)-C(9)-C(8)	123.6(4)
C(3)-C(4)-C(5)	120.9(5)	C(7)-C(10)-C(7)	117.5(6)
C(6)-C(5)-C(4)	121.4(5)	C(7)-C(10)-C(11)	121.3(3)

[a] Estimated standard deviations are given in parentheses.

Table III. Bond lengths (Å) and bond angles (°) for tetrazine **3.30**.[a]

Atoms	Distance	Atoms	Distance
C(1)-N(3)	1.294(3)	C(10)-C(15)	1.388(4)
C(1)-N(2)	1.378(4)	C(10)-P	1.789(3)
C(1)-C(2)	1.476(4)	C(11)-C(12)	1.383(4)
C(2)-C(7)	1.379(4)	C(12)-C(13)	1.365(5)
C(2)-C(3)	1.389(4)	C(13)-C(14)	1.375(5)
C(3)-C(4)	1.380(4)	C(14)-C(15)	1.375(5)
C(4)-C(5)	1.362(5)	P-O	1.480(2)
C(5)-C(6)	1.385(5)	P-N(4)	1.654(2)
C(6)-C(7)	1.376(5)	P-N(1)	1.671(2)
C(8)-N(1)	1.458(4)	N(1)-N(2)	1.424(3)
C(9)-N(4)	1.460(3)	N(3)-N(4)	1.401(3)
C(10)-C(11)	1.377(4)		

Atoms	Angle	Atom	Angle
N(3)-C(1)-N(2)	122.0(3)	C(13)-C(14)-C(15)	120.4(3)
N(3)-C(1)-C(2)	117.3(3)	C(14)-C(15)-C(10)	119.8(3)
N(2)-C(1)-C(2)	120.7(3)	O-P-N(4)	115.4(1)
C(7)-C(2)-C(3)	118.9(3)	O-P-N(1)	112.8(1)
C(7)-C(2)-C(1)	120.0(3)	O-P-C(10)	111.0(1)
C(3)-C(2)-C(1)	121.1(3)	N(4)-P-N(1)	101.4(1)
C(4)-C(3)-C(2)	120.3(3)	N(4)-P-C(10)	107.4(1)
C(5)-C(4)-C(3)	120.5(4)	N(1)-P-C(10)	108.2(1)
C(4)-C(5)-C(6)	119.7(4)	N(2)-N(1)-C(8)	114.9(2)
C(7)-C(6)-C(5)	120.2(4)	N(2)-N(1)-P	108.1(2)
C(6)-C(7)-C(2)	120.5(4)	C(8)-N(1)-P	118.8(2)
C(11)-C(10)-C(15)	119.3(3)	C(1)-N(2)-N(1)	116.8(2)
C(11)-C(10)-P	122.0(2)	C(1)-N(3)-N(4)	116.3(2)
C(15)-C(10)-P	118.6(3)	N(3)-N(4)-C(9)	112.5(2)
C(10)-C(11)-C(12)	120.3(3)	N(3)-N(4)-P	125.8(2)
C(13)-C(12)-C(11)	120.1(4)	C(9)-N(4)-P	120.7(2)
C(12)-C(13)-C(14)	120.1(4)		

[a] Estimated standard deviations are given in parentheses.

Table IV. Summary of crystallographic data for bis(tetrazine) **3.43**.

empirical formula	$C_{37}H_{38}N_7O_5P_3$
formula weight	753.65
space group	P-1
a (Å)	11.806(2)
b (Å)	12.037(2)
c (Å)	14.155(3)
α (deg)	100.027(4)
β (deg)	91.835(5)
γ (deg)	110.325(4)
V (Å^3)	1848.1(7)
Z	2
ρ (calcd) (g cm^{-3})	1.35
μ (mm^{-1})	0.21
radiation	MoKα, graphite monochromated
λ (Å)	0.71073
temperature (K)	293
2θ range (deg)	4-50
no. of observed reflections	13920
no. of unique reflections	6474
no. of parameters	470
R^a	0.064
R_w^b	0.131

$^a R = \Sigma(|F_o|-|F_c|) / \Sigma |F_o|$ $^b R_w = [\Sigma_w(|F_o|-|F_c|)^2 / \Sigma_w (|F_o|)^2]^{1/2}$

Table V. Bond lengths (Å) and bond angles (°) for bis(tetrazine) **3.43**.[a]

Atoms	Distance	Atoms	Distance
P(1)-N(2)	1.573(4)	C(14)-C(15)	1.395(8)
P(1)-N(1)	1.584(4)	C(15)-C(16)	1.381(8)
P(1)-O(1)	1.587(4)	C(21)-C(22)	1.372(8)
P(1)-O(2)	1.590(4)	C(21)-C(26)	1.405(8)
P(2)-N(3)	1.561(4)	C(22)-C(23)	1.400(8)
P(2)-N(1)	1.574(4)	C(23)-C(24)	1.379(9)
P(2)-O(4)	1.577(4)	C(24)-C(25)	1.381(8)
P(2)-O(3)	1.589(4)	C(25)-C(26)	1.407(7)
P(3)-N(3)	1.588(4)	C(31)-C(32)	1.370(7)
P(3)-N(2)	1.597(4)	C(31)-C(36)	1.373(7)
P(3)-N(7)	1.648(5)	C(32)-C(33)	1.406(7)
P(3)-N(4)	1.679(4)	C(32)-C(46)	1.486(7)
N(4)-N(5)	1.422(5)	C(33)-C(34)	1.387(8)
N(4)-C(411)	1.481(6)	C(34)-C(35)	1.352(8)
N(5)-C(1)	1.386(7)	C(35)-C(36)	1.397(8)
N(6)-C(1)	1.286(7)	C(41)-C(42)	1.363(7)
N(6)-N(7)	1.407(5)	C(41)-C(46)	1.392(7)
N(7)-C(711)	1.440(6)	C(42)-C(43)	1.378(8)
O(1)-C(11)	1.407(6)	C(43)-C(44)	1.377(8)
O(2)-C(21)	1.387(6)	C(44)-C(45)	1.382(8)
O(3)-C(31)	1.422(6)	C(45)-C(46)	1.382(7)
O(4)-C(41)	1.410(6)	C(111)-C(112)	1.375(8)
C(1)-C(111)	1.497(7)	C(111)-C(116)	1.376(7)
C(11)-C(16)	1.362(7)	C(112)-C(113)	1.397(7)
C(11)-C(12)	1.380(7)	C(113)-C(114)	1.356(8)
C(12)-C(13)	1.420(7)	C(114)-C(115)	1.348(8)
C(12)-C(26)	1.459(8)	C(115)-C(116)	1.385(7)
C(13)-C(14)	1.355(8)		

Atoms	Angle	Atoms	Angle
N(2)-P(1)-N(1)	118.9(2)	C(14)-C(13)-C(12)	120.2(6)
N(2)-P(1)-O(1)	106.4(2)	C(13)-C(14)-C(15)	122.2(6)
N(1)-P(1)-O(1)	112.3(2)	C(16)-C(15)-C(14)	117.7(6)
N(2)-P(1)-O(2)	111.0(2)	C(11)-C(16)-C(15)	120.3(6)
N(1)-P(1)-O(2)	104.9(2)	C(22)-C(21)-O(2)	117.5(6)
O(1)-P(1)-O(2)	102.19(19)	C(22)-C(21)-C(26)	122.4(6)
N(3)-P(2)-N(1)	118.7(2)	O(2)-C(21)-C(26)	119.7(6)
N(3)-P(2)-O(4)	110.6(2)	C(21)-C(22)-C(23)	119.0(7)
N(1)-P(2)-O(4)	106.6(2)	C(24)-C(23)-C(22)	120.3(7)
N(3)-P(2)-O(3)	105.2(2)	C(23)-C(24)-C(25)	120.2(6)
N(1)-P(2)-O(3)	111.5(2)	C(24)-C(25)-C(26)	121.2(6)
O(4)-P(2)-O(3)	103.21(19)	C(21)-C(26)-C(25)	117.0(6)

N(3)-P(3)-N(2)	115.9(2)	C(21)-C(26)-C(12)	121.2(5)
N(3)-P(3)-N(7)	108.4(3)	C(25)-C(26)-C(12)	121.7(6)
N(2)-P(3)-N(7)	112.4(3)	C(32)-C(31)-C(36)	124.4(5)
N(3)-P(3)-N(4)	109.6(2)	C(32)-C(31)-O(3)	118.7(5)
N(2)-P(3)-N(4)	109.4(2)	C(36)-C(31)-O(3)	116.7(5)
N(7)-P(3)-N(4)	99.9(2)	C(31)-C(32)-C(33)	116.5(5)
P(2)-N(1)-P(1)	120.1(3)	C(31)-C(32)-C(46)	123.0(5)
P(1)-N(2)-P(3)	120.9(3)	C(33)-C(32)-C(46)	120.3(5)
P(2)-N(3)-P(3)	123.0(3)	C(34)-C(33)-C(32)	119.2(6)
N(5)-N(4)-C(411)	112.3(4)	C(35)-C(34)-C(33)	122.7(7)
N(5)-N(4)-P(3)	106.1(3)	C(34)-C(35)-C(36)	118.9(6)
C(411)-N(4)-P(3)	116.5(4)	C(31)-C(36)-C(35)	118.0(6)
C(1)-N(5)-N(4)	117.2(4)	C(42)-C(41)-C(46)	121.6(5)
C(1)-N(6)-N(7)	118.0(5)	C(42)-C(41)-O(4)	119.1(5)
N(6)-N(7)-C(711)	113.0(5)	C(46)-C(41)-O(4)	119.2(5)
N(6)-N(7)-P(3)	123.6(4)	C(41)-C(42)-C(43)	120.6(6)
C(711)-N(7)-P(3)	122.9(4)	C(44)-C(43)-C(42)	119.1(6)
C(11)-O(1)-P(1)	120.5(3)	C(43)-C(44)-C(45)	120.1(6)
C(21)-O(2)-P(1)	122.9(3)	C(44)-C(45)-C(46)	121.3(6)
C(31)-O(3)-P(2)	120.5(3)	C(45)-C(46)-C(41)	117.3(5)
C(41)-O(4)-P(2)	121.0(4)	C(45)-C(46)-C(32)	121.4(5)
N(6)-C(1)-N(5)	124.2(5)	C(41)-C(111)-C(116)	121.1(5)
N(6)-C(1)-C(111)	117.8(6)	C(112)-C(111)-C(116)	119.1(5)
N(5)-C(1)-C(111)	117.9(5)	C(112)-C(111)-C(1)	120.6(6)
C(16)-C(11)-C(12)	123.2(6)	C(116)-C(111)-C(1)	120.3(5)
C(16)-C(11)-O(1)	118.1(5)	C(111)-C(112)-C(113)	119.3(6)
C(12)-C(11)-O(1)	118.5(5)	C(114)-C(113)-C(112)	121.3(6)
C(11)-C(12)-C(13)	116.4(6)	C(115)-C(114-C(113)	119.1(6)
C(11)-C(12)-C(26)	123.2(5)	C(114)-C(115)-C(116)	121.3(6)
C(13)-C(12)-C(26)	120.4(5)	C(111)-C(116)-C(115)	120.0(6)

[a] Estimated standard deviations are given in parentheses.

References

1. Palmer, W. G. *Valency: classical and modern*; second ed.; University Press: Cambridge, 1963.

2. Russell, C. A. *The History of Valency*; Leicester University Press: Great Britain, 1971.

3. Lewis, G. N. *Journal of the American Chemical Society* **1916**, 762-785.

4. Griller, D.; Ingold, K. U. *Accounts of Chemical Research* **1976**, *9*, 13-19.

5. Andrews, W. L. S.; Pimentel, G. C. *Journal of Chemical Physics* **1966**, *44*, 2527-2528.

6. Kochi, J. K. *Free Radicals*; John Wiley & Sons: New York, 1973; Vol. 1.

7. Gomberg, M. *Journal of the American Chemical Society* **1900**, *22*, 757-771.

8. McBride, J. M. *Tetrahedron* **1974**, *30*, 2009-2022.

9. Goto, K.; Kubo, T.; Yamamoto, K.; Nakasuji, K.; Sato, K.; Shiomi, D.; Takui, T.; Kubota, M.; Kobayashi, T.; Yakusi, K.; Ouyang, J. *Journal of the American Chemical Society* **1999**, *121*, 1619-1620.

10. Rajca, A.; Utamapanya, S.; Thayumanavan, S. *Journal of the American Chemical Society* **1992**, *114*, 1884-1885.

11. Rajca, A.; Utamapanya, S. *Journal of the American Chemical Society* **1993**, *115*, 10688-10694.

12. Piloty, O.; Schwerin, B. G. *Berichte der Deutschen Chemischen Gesellschaft* **1901**, *34*, 1870-1887.

13. Piloty, O.; Schwerin, B. G. *Berichte der Deutschen Chemischen Gesellschaft* **1901**, *34*, 2354-2367.

14. Forrester, A. R.; Hay, J. M.; Thomson, R. H. *Organic Chemistry of Stable Free Radicals*; Academic Press: London, 1968.

15. Weiland, H.; Roth, K. *Berichte der Deutschen Chemischen Gesellschaft* **1920**, *53*, 210-221.

16. Weiland, H.; Kögel, F. *Berichte der Deutschen Chemischen Gesellschaft* **1922**, *55*, 1798-1803.

17. Meyer, K. H.; Bilbroth, H. G. *Berichte der Deutschen Chemischen Gesellschaft* **1919**, *52*, 1476-1489.

18. Meyer, K. H.; Reppe, W. *Berichte der Deutschen Chemischen Gesellschaft* **1921**, *54*, 327-331.

19. Rozantsev, E. G. *Free Nitroxyl Radicals*; Plenum: New York, 1970.

20. Keana, J. F. W. *Chemical Reviews* **1978**, *78*, 37-64.

21. Dupeyre, R.-M.; Rassat, A. *Journal of the American Chemical Society* **1966**, *88*, 3180-3181.

22. Osiecki, J. H.; Ullman, E. F. *Journal of the American Chemical Society* **1968**, *90*, 1078-1079.

23. Ullman, E. F.; Call, L.; Osiecki, J. H. *Journal of Organic Chemistry* **1970**, *35*, 3623-3631.

24. Caneschi, A.; Gatteschi, D.; Rey, P. *The Chemistry and Magnetic Properties of Metal Nitronyl Nitroxide Complexes*; Lippard, S. J., Ed.; John Wiley & Sons: New York, 1991; Vol. 39, pp 331-429.

25. Goldschmidt, S. *Berichte der Deutschen Chemischen Gesellschaft* **1920**, *53*, 44.

26. Goldschmidt, S.; Renn, K. *Berichte der Deutschen Chemischen Gesellschaft* **1922**, *55*, 628-647.

27. Goldschmidt, S.; Graef, F. *Berichte der Deutschen Chemischen Gesellschaft* **1928**, *61*, 1858-1869.

28. Singer, L. S.; Kikuchi, C. *Journal of Chemical Physics* **1955**, *23*, 1738-1739.

29. Lord, N. W.; Blinder, S. M. *Journal of Chemical Physics* **1961**, *34*, 1693-1708.

30. Reid, D. H. *Chemistry and Industry* **1956**, 1504-1505.

31. Reid, D. H. *Tetrahedron* **1958**, *3*, 339-352.

32. Koutentis, P. A.; Chen, Y.; Cao, Y.; Best, T. P.; Itkis, M. E.; Beer, L.; Oakley, R. T.; Cordes, A. W.; Brock, C. P.; Haddon, R. C. *Journal of the American Chemical Society* **2001**, *123*, 3864-3871.

33. Sogo, P. B.; Nakazaki, M.; Calvin, M. *Journal of Chemical Physics* **1957**, *26*, 1343-1345.

34. Burford, N.; Passmore, J.; Schriver, M. J. *Journal of the Chemical Society. Chemical Communications* **1986**, 140-142.

35. Awere, E. G.; Burford, N.; Mailer, C.; Passmore, J.; Schriver, M. J.; White, P. S.; Banister, A. J.; Oberhammer, H.; Sutcliffe, L. H. *Journal of the Chemical Society. Chemical Communications* **1987**, 66-69.

36. Preston, K. F. *Magnetic Resonance in Chemistry* **1990**, *28*, 189-204.

37. Mayer, R.; Domschke, G.; Bleisch, S. *Tetrahedron Letters* **1978**, *42*, 4003-4006.

38. Barclay, T. M.; Cordes, A. W.; Haddon, R. C.; Itkis, M. E.; Oakley, R. T.; Reed, R. W.; Zhang, H. *Journal of the American Chemical Society* **1999**, *121*, 969-976.

39. Cordes, A. W.; Mingie, J. R.; Oakley, R. T.; Reed, R. W.; Zhang, H. *Canadian Journal of Chemistry* **2001**, *79*, 1352-1359.

40. Cordes, A. W.; Haddon, R. C.; MacKinnon, C. D.; Oakley, R. T.; Patenaude, G. W.; Reed, R. W.; Rietveld, T.; Vajda, K. E. *Inorganic Chemistry* **1996**, *35*, 7626-7632.

41. Barclay, T. M.; Cordes, A. W.; Laat, R. H. d.; Goddard, J. D.; Haddon, R. C.; Jeter, D. Y.; Mawhinney, R. C.; Oakley, R. T.; Palstra, T. T. M.; Patenaude, G. W.; Reed, R. W.; Westwood, N. P. C. *Journal of the American Chemical Society* **1997**, *119*, 2633-2641.

42. Barclay, T. M.; Cordes, A. W.; George, N. A.; Haddon, R. C.; Itkis, M. E.; Mashuta, M. S.; Oakley, R. T.; Patenaude, G. W.; Reed, R. W.; Richardson, J. F.; Zhang, H. *Journal of the American Chemical Society* **1998**, *120*, 352-360.

43. Miura, Y.; Kinoshita, M. *Bulletin of the Chemical Society of Japan* **1977**, *50*, 1142-1146.

44. Kuhn, R.; Trischmann, H. *Angewandte Chemie, International Edition English* **1963**, *2*, 155.

45. Neugebauer, F. A.; Fischer, H. *Angewandte Chemie, International Edition English* **1980**, *19*, 724-725.

46. Weil, J.; Bolton, J. R.; Wertz, J. E. *Electron Paramagnetic Resonance. Elementary Theory and Practical Applications*; Wiley Interscience: New York, 1994.

47. Jux, N.; Holczer, K.; Rubin, Y. *Angewandte Chemie, International Edition English* **1996**, *35*, 1986-1990.

48. Loss, S.; Magistrato, A.; Cataldo, L.; Hoffmann, S.; Geoffroy, M.; Röthlisberger, U.; Grützmarcher, H. *Angewandte Chemie, International Edition English* **2001**, *40*, 723-726.

49. Kahn, O. *Molecular Magnetism*; VCH: New York, 1993.

50. Lahti, P. M. *Magnetic Properties of Organic Materials*; Marcel Dekker: New York, 1999.

51. Miller, J. S.; Eipstein, A. J. *Angewandte Chemie, International Edition English* **1994**, *33*, 385-415.

52. Miller, J. S. *Advanced Materials* **1994**, *6*, 322-324.

53. Haddon, R. C. *Nature* **1975**, *256*, 394-396.

54. Chi, X.; Itkis, M. E.; Patrick, B. O.; Barclay, T. M.; Reed, R. W.; Oakley, R. T.; Cordes, A. W.; Haddon, R. C. *Journal of the American Chemical Society* **1999**, *121*, 10395-10402.

55. Janzen, E. G.; Blackburn, B. J. *Journal of the American Chemical Society* **1969**, *91*, 4481-4490.

56. Rosenthal, I.; Mossoba, M. M.; Riesz, P. *Canadian Journal of Chemistry* **1982**, *60*, 1486-1492.

57. Swartz, H. M.; Bolton, J. R.; Borg, D. C. *Biological Applications of Electron Spin Resonance*; Wiley-Interscience: New York, 1972.

58. Georges, M. K.; Veregin, R. P. N.; Kazmaier, P. M.; Hamer, G. K. *Macromolecules* **1993**, *26*, 2987-2988.

59. Hawker, C. J. *Accounts of Chemical Research* **1997**, *30*, 373-382.

60. Patten, T. E.; Matyjaszewski, K. *Accounts of Chemical Research* **1999**, *32*, 895-903.

61. Borden, W. T.; Davidson, E. R. *Journal of the American Chemical Society* **1977**, *99*, 4587-4594.

62. Dowd, P. *Journal of the American Chemical Society* **1966**, *88*, 2587-2589.

63. Dixon, D. A.; Dunning, T. H. J.; Eades, R. A.; Kleier, D. A. *Journal of the American Chemical Society* **1981**, *103*, 2878-2880.

64. Rule, M.; Matlin, A. R.; Seeger, D. E.; Hilinski, E. F.; Dougherty, D. A.; Berson, J. A. *Tetrahedron* **1982**, *38*, 787-798.

65. Wright, B. B.; Platz, M. S. *Journal of the American Chemical Society* **1983**, *105*, 628-630.

66. Goodman, J. L.; Berson, J. A. *Journal of the American Chemical Society* **1985**, *107*, 5409-5424.

67. Kato, S.; Morokuma, K.; Feller, D.; Davidson, E. R.; Borden, W. T. *Journal of the American Chemical Society* **1983**, *105*, 1791-1795.

68. Fort, R. C. J.; Getty, S. J.; Hrovat, D. A.; Lahti, P. M.; Borden, W. T. *Journal of the American Chemical Society* **1992**, *114*, 7549-7552.

69. Dowd, P. *Journal of the American Chemical Society* **1970**, *92*, 1066-1068.

70. Nash, J. J.; Dowd, P.; Jordan, K. D. *Journal of the American Chemical Society* **1992**, *114*, 10071-10072.

71. Longuet-Higgins, H. C. *Journal of Chemical Physics* **1950**, *18*, 265-274.

72. Berson, J. A. *meta-Quinonoid Compounds*; Patai, S. and Rappoport, Z., Ed.; John Wiley & Sons: Toronto, 1988; Vol. 2, pp 455-536.

73. Dougherty, D. A. *Accounts of Chemical Research* **1991**, *24*, 88-94.

74. Kothe, G.; Denkel, K.-H.; Sümmermann, W. *Angewandte Chemie, International Edition English* **1970**, *11*, 906-907.

75. Ito, A.; Miyajima, H.; Yoshizawa, K.; Tanaka, K.; Yamabe, T. *Journal of Organic Chemistry* **1997**, *62*, 38-43.

76. Wienk, M. M.; Janssen, R. A. J.; Meijer, E. W. *Journal of Physical Chemistry* **1995**, *99*, 9331-9336.

77. Wienk, M. M.; Janssen, R. A. J. *Chemical Communications* **1996**, 1919-1920.

78. Wienk, M. M.; Janssen, R. A. J. *Journal of the American Chemical Society* **1997**, *119*, 5398-5403.

79. Okada, K.; Imakura, T.; Oda, M.; Murai, H. *Journal of the American Chemical Society* **1996**, *118*, 3047-3048.

80. Okada, K.; Imakura, T.; Oda, M.; Kajiwara, A.; Kamachi, M.; Yamaguchi, M. *Journal of the American Chemical Society* **1997**, *119*, 5740-5741.

81. Mukai, K.; Nagai, H.; Ishizu, K. *Bulletin of the Chemical Society of Japan* **1975**, *48*, 2381-2382.

82. Rajca, A. *Chemical Reviews* **1994**, *94*, 871-893.

83. Miura, Y.; Yamamoto, A.; Katsura, Y.; Kinoshita, M. *Journal of Organic Chemistry* **1982**, *47*, 2618-2622.

84. Miura, Y.; Kitagishi, Y.; Ueno, S. *Bulletin of the Chemical Society of Japan* **1994**, *67*, 3282-3288.

85. Miura, Y.; Momoki, M.; Nakatsuji, M. *Journal of Organic Chemistry* **1998**, *63*, 1555-1565.

86. Miura, Y.; Kurokawa, S.; Nakatsuji, M. *Journal of Organic Chemistry* **1998**, *63*, 8295-8303.

87. Miura, Y.; Ohana, T. *Journal of Organic Chemistry* **1988**, *53*, 5770-5772.

88. Patai, S. *The Chemistry of Sulphenic Acids and Their Derivatives*; John Wiley & Sons Ltd:, 1990.

89. Miura, Y.; Tanaka, A.; Hirotsu, K. *Journal of Organic Chemistry* **1991**, *56*, 6638-6643.

90. Davis, F. A.; Friedman, A. J.; Kluger, E. W.; Skibo, E. B.; Fretz, E. R.; Milicia, A. P.; LeMasters, W. C. *Journal of Organic Chemistry* **1977**, *42*, 967-972.

91. Bentley, M. D.; Douglass, I. B.; Lacadie, J. A.; Weaver, D. C.; Davis, F. A.; Eitelman, S. J. *Chemical Communications* **1971**, 1625-1626.

92. Miura, Y.; Katsura, Y.; Kinoshita, M. *Bulletin of the Chemical Society of Japan* **1979**, *52*, 1121-1125.

93. Miura, Y. *Journal of Physical Chemistry* **1983**, *87*, 3450-3455.

94. Miura, Y.; Asada, H.; Kinoshita, M. *Bulletin of the Chemical Society of Japan* **1977**, *50*, 1855-1877.

95. Miura, Y.; Yamamoto, A.; Katsura, Y.; Kinoshita, M. *Journal of Organic Chemistry* **1980**, *45*, 3875-3880.

96. Miura, Y.; Asada, H.; Kinoshita, M. *Bulletin of the Chemical Society of Japan* **1980**, *53*, 720-725.

97. Nakatsuji, M.; Miura, Y.; Teki, Y. *Journal of the Chemical Society. Perkin Transactions 2* **2001**, 738-744.

98. Miura, Y.; Oka, H.; Momoki, M. *Synthesis* **1995**, 1419-1422.

99. Chisholm, M. H.; Corning, J. F.; Huffman, J. C. *Inorganic Chemistry* **1984**, *23*, 754-757.

100. Bochmann, M.; Webb, K. J. *Inorganic Synthesis* **1997**, *31*, 158-160.

101. Kuhn, R. *Angewandte Chemie, International Edition English* **1964**, *3*, 762-763.

102. Kuhn, R.; Neugebauer, F. A.; Trischmann, H. *Angewandte Chemie, International Edition English* **1965**, *4*, 72.

103. Katritzky, A. R.; Belyakov, S. A. *Canadian Journal of Chemistry* **1994**, *72*, 1849-1856.

104. Raphaelian, L.; Hooks, H.; Ottmann, G. *Angewandte Chemie, International Edition English* **1967**, *6*, 363-364.

105. Neugebauer, F. A.; Fischer, H.; Siegel, R.; Krieger, C. *Chemische Berichte* **1983**. *116*, 3461-3481.

106. Neugebauer, F. A.; Fisher, H.; Krieger, C. *Journal of the Chemical Society. Perkin Transactions 2* **1993**, 535-544.

107. Neugebauer, F. A. *Angewandte Chemie, International Edition English* **1973**, *12*, 455-464.

108. Fischer, P. H. H. *Tetrahedron* **1967**, *23*, 1939-1952.

109. Williams, D. E. *Acta Crystallographica Section B* **1973**, *29*, 96-102.

110. Brook, D. J.; Fox, H. H.; Lynch, V.; Fox, M. A. *Journal of Physical Chemistry* **1996**, *100*, 2066-2071.

111. Neugebauer, F. A.; Otting, W.; Smith, H. O.; Trischmann, H. *Chemische Berichte* **1972**, *105*, 549-553.

112. Kornuta, P. P.; Bobkov, V. N.; Polumbrik, O. M.; Markovskii, L. N. *Zhurnal Obshchei Khimii* **1978**, *48*, 697-698.

113. Majoral, J. P.; Kraemer, R.; Navech, J.; Mathis, F. *Journal of the Chemical Society. Perkin Transaction 1* **1976**, 2093-2098.

114. Kornuta, P. P.; Bobkov, V. N.; Polumbrik, O. M.; Markovskii, L. N. *Zhurnal Obshchei Khimii* **1981**, *51*, 2449-2456.

115. Hicks, R.; Hooper, R. *Inorganic Chemistry* **1999**, *38*, 284-286.

116. Walsh, E. N.; Toy, A. D. F. *Inorganic Synthesis* **1963**, *7*, 69-71.

117. Hicks, R. G.; Öhrström, L.; Patenaude, G. W. *Inorganic Chemistry* **2001**, *40*, 1865-1870.

118. Roberts, B. P. *The Chemistry of Phosphoranyl Radicals*; Heyden: London, 1980; Vol. 6.

119. Simmons, H. E.; Fukunaga, T. *Journal of the American Chemical Society* **1967**, *89*, 5208-5215.

120. Dürr, H.; Gleiter, R. *Angewandte Chemie, International Edition English* **1978**, *17*, 559-569.

121. Allcock, H. R. *Chemical Reviews* **1972**, *72*, 315-356.

122. Haddon, R. C.; Mayo, S. L.; Chichester, S. V.; Marshall, J. H. *Journal of the American Chemical Society* **1985**, *107*, 7585-7591.

123. Haddon, R. C.; Chichester-Hicks, S. V.; Mayo, S. L. *Inorganic Chemistry* **1988**, *27*, 1911-1915.

124. Frank, N. L.; Clérac, R.; Sutter, J.-P.; Daro, N.; Kahn, O.; Coulon, C.; Green, M. T.; Golhen, S.; Ouahab, L. *Journal of the American Chemical Society* **2000**, *122*, 2053-2061.

125. Kraemer, R.; Galliot, C.; Mitjaville, J.; Caminade, A.-M.; Majoral, J. P. *Heteroatom Chemistry* **1996**, *7*, 149-154.

126. Barr, C. L.; Chase, P. A.; Hicks, R. G.; Lemaire, M. T.; Stevens, C. L. *Journal of Organic Chemistry* **1999**, *64*, 8893-8897.

127. Hicks, R. G.; Lemaire, M. T.; Thompson, L. K.; Barclay, T. M. *Journal of the American Chemical Society* **2000**, *122*, 8077-8078.

128. Barclay, T. M.; Hicks, R. G.; Lemaire, M. T.; Thompson, L. K. *Inorganic Chemistry* **2001**, *40*, 6521-6524.

129. Ley, H. *Berichte der Deutschen Chemischen Gesellschaft* **1898**, *31*, 2126-2129.

130. Malatesta, L.; Pizzotti, R. *Gazzetta Chimica Italiana* **1946**, *76*, 141-147.

131. Armand, J.; Minvielle, R.-M. *Comptes Rendus de L'Academie des Sciences. Serie II* **1965**, *260*, 2512-2515.

132. Huethers, C.; Cretsos, J. M.; Shackelford, J. M. *Journal of Chemical and Engineering Data* **1963**, *8*, 624-625.

133. Grundmann, C.; Grünanger, P. *The Nitrile Oxides. Versatile Tools of Theoretical and Preparative Chemistry*; Springer-Verlag: Berlin, 1971.

134. Hurd, C. D. *Inorganic Synthesis* **1939**, 87.

135. Liu, K.-C.; Shelton, B. R.; Howe, R. K. *Journal of Organic Chemistry* **1980**, *45*, 3916-3918.

136. Torssell, K. G. *Nitrile Oxides, Nitrones and Nitronates in Organic Synthesis. Novel Strategies in Synthesis*; VCH:, 1988.

137. Burk, R. M.; Roof, M. B. *Tetrahedron Letters* **1993**, *34*, 395-398.